MINERALOGICAL MAGAZINE

JOURNAL OF THE MINERALOGICAL SOCIETY

Vol. 32 March 1959 No. 244

Cornubite, a new mineral dimorphous with cornwallite.

By G. F. Claringbull, B.Sc., Ph.D., A.Inst.P., M. H. Hey, M.A., D.Sc. and R. J. Davis, M.A., D.Phil.

Dept. of Mineralogy, British Museum (Natural History).

[Read 7 November 1957.]

Summary. A new copper arsenate, dimorphous with cornwallite, has been found on specimens from five localities in Cornwall, one in Devon, and one in Cumberland. The name *cornubite* (from Cornubia, the medieval Latin name for Cornwall) is proposed for the new mineral. Chemical analyses of cornubite and cornwallite agree well with $Cu_5(AsO_4)_2(OH)_4$; sp. gr. cornubite 4·64, cornwallite 4·52. X-ray study suggests that the unit-cell of cornubite has a volume of 228 Å.^{3} or a simple multiple thereof. New X-ray data for cornwallite (a 17·33, b 5·82, c 4·60 Å., β 92° 13′) agree well with L. G. Berry's except for a. Powder data for both are given.

DURING an examination of some copper phosphates and arsenates from Cornwall in 1955, one specimen belonging to Sir Arthur Russell was found to give an X-ray powder pattern different from any known copper mineral; on further study this has proved to be a new mineral, dimorphous with cornwallite, for which we propose the name cornubite, from Cornubia, the Roman name for Cornwall. The specimens from Wheal Carpenter, Gwinear, Cornwall, carry well-crystallized quartz, coated with dark green fibrous cornwallite, on which there are apple-green patches of botryoidal fibrous cornubite. Subsequently we have found several further specimens of cornubite: one, B.M. 42818, from St. Day, Cornwall, was labelled chenevixite and carries light to dark green massive porcellaneous cornubite with crystals of olivenite; a second, B.M. 1956,460, carries massive light apple-green cornubite with crystals of liroconite, and according to Sir Arthur Russell must have come from Wheal Gorland, Gwennap, the only known Cornish locality for liroconite; one from Wheal Muttrell, Gwennap, B.M. 1958,771, carries green massive cornubite with olivenite, malachite, and an unidentified bright green mineral on rusty quartz; two come from Wheal Phoenix, Linkinhorne, Cornwall, one, B.M. 1958,778, with bright green glassy

botryoidal cornubite and pale green drusy cornwallite on quartz, the other, B.M. 1958,769, with green glassy and also porcellaneous cornubite, olivenite, and stained feldspar on rotten granite; one, B.M. 1958,767, from the Marquis shaft, Bedford United mines, Tavistock, Devon, has

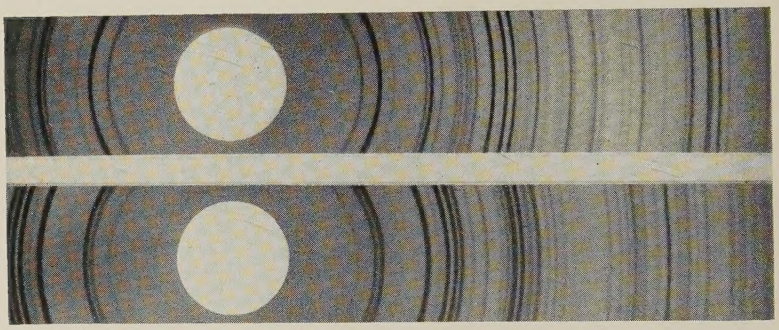

FIG. 1. X-ray powder photographs of cornubite (above) and cornwallite (below) from Wheal Carpenter.

green glassy botryoidal cornubite with olivenite, malachite, and cuprite; and two, B.M. 1958,122 and 779, from Potts Gill mine, Caldbeck, Cumberland, carry light and dark green botryoidal cornubite, with on the latter specimen a bluish skin of cornwallite. All the last six specimens were collected and presented by Mr. A. W. G. Kingsbury.

We have not been able to isolate single crystals of cornubite; one fibrous fragment from Sir Arthur Russell's type specimen gave a good fibre pattern, but was unfortunately lost and repeated attempts to find equally well-crystallized material on any of the above specimens failed. The fibre photograph showed a layer-line spacing of $9{\cdot}0 \pm 0{\cdot}2$ Å. with every third layer-line stronger than its neighbours. The zero layer-line of this pattern could readily be indexed to well within the experimental error of measurement on the basis of d_{100} 5·35 Å., d_{010} 4·72 Å., γ^* 88°, with very few absent diffractions, and from this data we can calculate an apparent cell-volume of 228 Å.^{3}; the true cell-volume must be an integral multiple of this. Attempts to index the non-zero layer-lines and so derive complete unit-cell data, using V. Vand's method,[1] indicate that the mineral is almost certainly anorthic, and that probably both d_{100} and d_{010} should have double the above values, although there are now many absences and still a few unindexable lines, so that the true cell may be even larger.

[1] Acta Cryst., 1948, vol. 1, p. 290.

TABLE I. X-ray powder data for cornubite (B.M. 1958,122, from Potts Gill, Caldbeck, Cumberland). Cu-$K\alpha$ radiation, camera diameter 11·46 cm. Third (l) index by comparison with a fibre photograph (layer-line spacing 9·0 Å.). B, broad.

d (meas.)	$I.$	$l.$	d (meas.)	$I.$	$l.$	d (meas.)	$I.$	$l.$
5·35	6	0	2·265	2	? 1	1·492	7	3
5·22	1	—	2·240	4	1, 3	1·467	5	3
4·88	1	—	2·180	2	0	1·457	1	—
4·72	10(1)	0	2·143	4	0, ? 3	1·442	2 B	0
4·53	1	—	2·090	6	3	1·408	2	? 0
4·31	4	2	2·071	5	3	1·392	1	? 0
3·93	2	2	2·027	1 B	—	1·373	6	0
3·59	6	0	1·973	4	3	1·353	1	—
3·49	8	0	1·957	6	3	1·340	4	0
3·42	1	? 3	1·919	4	3	1·321	1	—
3·33	6	2	1·899	1	—	1·308	4	—
3·10	6	2	1·853	1	—	1·300	5	0
3·05	6	2	1·829	4	—	1·281	2	—
2·98	6	1	1·797	4	0	1·269	1	—
2·932	6	2	1·747	6	0	1·241	1 B	—
2·868	7	1	1·720	2	3	1·227	2	—
2·688	9	0	1·696	1	—	1·217	2	—
2·616	2	? 2	1·662	4 B	3	1·203	4 B	? 0
2·562	10(2)	3	1·630	1	—	1·190	1	—
2·525	1	—	1·608	1	—	1·181	2	—
2·489	10(3)	3	1·593	5	3	1·172	2	—
2·443	4	? 2	1·575	7	0, 3	1·158	1	—
2·390	4	? 1	1·544	1	—	1·151	4	0
2·358	5	0	1·524	7	3			
2·303	7	0	1·515	6	3			

The X-ray powder pattern (table I) correlates well with the fibre pattern, and l indices can be assigned to most of the low-angle powder lines. Identical powder patterns were given by both the light green and the dark green crusts on Sir Arthur Russell's specimen, and also by material from the other Cornish specimens; material examined from one Cumberland specimen (B.M. 1958,122) included both light and dark green crusts and also a thin light green layer under the dark green—all yielded identical patterns.

A microchemical analysis on 6·6 mg. of cornubite from Sir Arthur Russell's specimen gave the results shown in table II, where they are compared with a new analysis of cornwallite from the same specimen and with the theoretical composition for $Cu_5(AsO_4)_2(OH)_4$; the densities and empirical unit-cell contents are also included in table II. The cited percentage of water in the cornubite is obtained by difference. The mineral only lost 2·8 % H_2O at 450° C., and was then still bright green;

in view of the small amount of material available, the sample was not further heated lest some arsenic might be volatilized. Despite this difficulty, there is clear evidence that cornubite is a polymorph of cornwallite, and that the structural unit of volume 228 Å.^{3} contains $Cu_5(AsO_4)_2(OH)_4$. The observed specific gravity is some 3 % lower than the calculated, but this is not an unduly great difference for cryptocrystalline material.

TABLE II. Chemical analyses and specific gravities of cornubite (A) and cornwallite (B) from Wheal Carpenter compared with the theoretical composition for $Cu_5(AsO_4)_2(OH)_4$ (calc.); together with the atomic contents of the unit cell or pseudo-cell of cornubite (volume 228 Å.^{3}) (A′) and of the unit cell of cornwallite (B′), and the calculated densities for the ideal formula.

		A.	*B.*	*Calc.*		*A′.*	*B′.*
CuO ...	...	59·86	60·29	59·94	Cu	4·8	9·70
As_2O_5	...	35·07	33·97	34·63	As	1·95	3·82
H_2O ...	...	[5·07]	5·80	5·43	O	7·9	15·12
Insol.	...	—	0·82	—	OH	3·6	8·24
Total	...	[100·00]	100·88	100·00			
					O+OH	11·5	23·36
$D_{4°}^{20°}$ ...	...	4·64	4·52				
$D_{4°}^{20°}$ calc.	...	4·8	4·645				

A new analysis of cornwallite was also made (table II), and an X-ray powder study (table III) of material from the same specimen. The powder photographs agree excellently with one another and with L. G. Berry's data,[1] and were readily indexed; the new data are somewhat fuller than Berry's and are therefore listed (table III). Berry's cell-dimensions were confirmed, except for the *a*-dimension, for which we find a value of 17·33 Å., appreciably lower than Berry's value of 17·61 Å. (see table III). The new analysis confirms the formula $Cu_5(AsO_4)_2(OH)_4$; it seems probable that, as Berry suggests, the high water content shown in many analyses of cornwallite is due to non-crystalline impurities, and that our material was purer than most. We have been able to obtain a new specific gravity for cornwallite, and while still appreciably lower than the calculated value the discrepancy is not serious considering that the mineral is finely fibrous. It is interesting that, despite these discrepancies, the observed densities in table II are in the order predicted from the X-ray unit-cell volumes.

[1] Amer. Min., 1951, vol. 36, p. 490.

TABLE III. X-ray powder data for cornwallite from Sir Arthur Russell's specimen of cornubite (Wheal Carpenter, Gwinear, Cornwall). Cu-$K\alpha$ radiation, camera diameter 11·46 cm. Indices and d calc. based on a cell with a 17·33, b 5·82, c 4·60 Å., β 92° 13′. [L. G. Berry found a 17·61, b 5·81, c 4·60 Å., β 92° 15′.] B, broad; D, doublet; T, triplet.

d (meas.)	I.	hkl.	d (calc.)
8·76	4	200	8·673
5·47	5½	110	5·506
4·82	7	210	4·827
4·60	8 B	001	4·598
4·35	1	400	4·336
4·11	2	$\bar{2}01$	4·134
		310	4·097
—	—	201	3·996
3·91	1	—	—
—	—	011	3·606
3·53	9 T	$\bar{1}11$	3·552
		111	3·508
		410	3·475
3·36	2 ?D	$\bar{2}11$	3·368
—	—	211	3·293
3·22	10	$\bar{4}01$	3·218
3·10	9 D	401	3·121
		$\bar{3}11$	3·101
3·02	8 ?D	311	3·019
2·974	2	510	2·978
—	—	020	2·905
2·890	5	600	2·891
—	—	120	2·865
2·817	1	$\bar{4}11$	2·815
2·740	6	220	2·755
		411	2·750
2·590	4	320	2·596
		610	2·589
2·539	5	$\bar{5}11$	2·539
2·478	8 B	$\bar{6}01$	2·492
	?T	511	2·462
		021	2·458
—	—	$\bar{1}21$	2·439
—	—	121	2·424
2·414	9 D	420	2·414
		601	2·405
—	—	$\bar{2}21$	2·377
2·350	6 D	221	2·350

d (meas.)	I.	hkl.	d (calc.)
2·292	7B	002	2·298
		$\bar{6}11$	2·290
		710	2·280
		$\bar{3}21$	2·277
—	—	321	2·244
—	—	$\bar{2}02$	2·243
2·223	5	520	2·229
		611	2·222
—	—	202	2·201
2·177	6	800	2·168
—	—	$\bar{4}21$	2·156
2·141	1		
2·112	4		
2·064	2		
2·001	1 BD		
1·880	5		
1·831	5		
1·798	4½		
1·772	6		
1·753	2		
1·729	5		
1·700	1		
1·683	4		
1·646	6		
1·612	4		
1·598	1		
1·580	5		
1·555	5		
1·523	5 B		
1·506	2		
1·490	2		
1·456	5 D		
1·437	4		
1·425	5		
1·407	4		
1·398	4		
1·380	4		
1·369	5		
1·346	6		
1·333	4		

Delhayelite, a new silicate from the Belgian Congo.

By Th. G. Sahama and Kai Hytönen, M.A.

Institute of Geology, University of Helsinki, Finland.

[Taken as read 6 November 1958.]

Summary. The complex kalsilite-bearing melilite-nephelinite from Mt. Shaheru in the Belgian Congo with götzenite, combeite, and kirschsteinite contains yet another new silicate for which the name *delhayelite* is proposed.

Delhayelite is orthorhombic with a 6·53, b 24·65, c 7·04 Å. Possible space-groups $Pmn2_1$ and $Pmmn$. Weak super-cell with doubled a-axis. Distinct cleavage parallel to (010). Birefringence weak. $\alpha \approx \beta \approx \gamma = 1{\cdot}532$. $2V_\alpha = 83°$. Optical orientation: $a = \alpha$, $b = \gamma$, $c = \beta$. Sp. gr. 2·60. Chemical composition corresponds to the tentative formula $(Na,K)_4Ca_5Al_6Si_{32}O_{80}.18H_2O.3(Na_2,K_2)(Cl_2,F_2,SO_4)$.

FROM a complex kalsilite-bearing melilite-nephelinite lava from Mt. Shaheru, Nyiragongo area, North Kivu in the Belgian Congo, three new silicates have been described by Sahama and Hytönen (1957 *a* and *b*), viz götzenite, combeite, and kirschsteinite. Further petrographic data for the rock have been given by Sahama and Meyer (1958). The same rock specimen, numbered S. 80, still contained a constituent the microscopic identification of which could not be made. This mineral, which occurs in the rock in very minute amounts, was studied by optical and X-ray methods as well as chemically. The data obtained were not consistent with those for any known species. For that reason the mineral was temporarily put aside.

Recently, however, Mountain (1957) and Gard and Taylor (1957) published descriptions of a new mineral from the Bultfontein mine, Kimberley, which they named rhodesite. A comparison of the data for rhodesite with those for the Shaheru mineral discloses the fact that, though representing distinctly different species, the two minerals are closely related to each other. It therefore seems pertinent to give a description of the Shaheru mineral, for which the name delhayelite is proposed. This name is after the Belgian geologist F. Delhaye, a pioneer in the geological exploration of the North Kivu area.

Delhayelite occurs in the rock as elongated crystals the shape of which is not fibrous but platy as is schematically indicated in fig. 1. The axis of elongation was taken as the c-axis. Rotation and Weissenberg photographs about all three crystallographic axes proved the mineral to be

orthorhombic with a primitive cell. The following conditions limiting possible reflections were found: $h00$, $h0l$, and $hk0$ with no restrictions; $0k0$ with $k = 2n$; $00l$ with $l = 2n$; $0kl$ with $k+l = 2n$. Possible space-groups are $Pmn2_1$ and $Pmmn$. Unit-cell dimensions are: a 6·53±0·03 Å.; b 24·65±0·2 Å.; c 7·04±0·03 Å. This cell is, however, only a sub-cell. The a-axis rotation photograph shows extremely weak layer-lines that correspond to a doubled a-axis, viz a 13·05±0·06 Å. A doubling of the c-axis could not be seen but is possible. The true cell might be non-primitive as found for rhodesite by Gard and Taylor (op. cit.). The extra reflections defining this larger true cell are too weak for establishing the true space-group. An electron microscope not being available to the authors, the electron diffraction method could not be used for closer characterization of the superlattice.

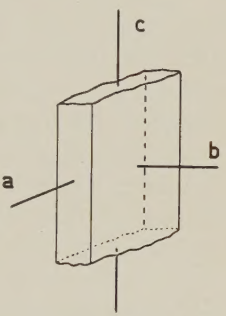

FIG. 1. Schematical shape of the delhayelite crystals.

The powder data of delhayelite, recorded with the Philips Norelco diffractometer, are reproduced in table I. The indexing was based on the dimensions of the super-cell given above.

TABLE I. Powder data of delhayelite. Filtered copper radiation.

hkl.	*I.*	2Θ.	*d.*	$Q_{obs.}$	$Q_{calc.}$
020	35	7·18	12·301	0·0066	0·0066
040	25	14·37	6·1584	0·0264	0·0264
300	1	20·395	4·3506	0·0528	0·0528
260	10	25·56	3·4820	0·0825	0·0828
102	3	26·13	3·4074	0·0861	0·0865
400	3	27·32	3·2616	0·0940	0·0939
080	100	28·985	3·0779	0·1056	0·1056
401	5	30·16	2·9606	0·1141	0·1141
280	5	32·08	2·7876	0·1287	0·1290
004 0.14.0	5	51·915	1·7597	0·3229	0·3227 0·3234
024	3	52·47	1·7424	0·3294	0·3293
0.16.0	5	60·015	1·5401	0·4216	0·4224

The mineral is colourless. In thin section it shows a somewhat wavy extinction with very low interference colours, abnormally bluish grey in sections perpendicular to the b-axis. Birefringence 0·002–0·003. $\alpha \approx \beta \approx \gamma = 1{\cdot}532 \pm 0{\cdot}002$. Optically negative. $2V_\alpha = 83° \pm 3°$. The optical orientation was determined with the Berek compensator on a

crystal mounted on the goniometer head of the Weissenberg camera. Comparison of optical tests and rotation photographs results in the following relationship between the axes of the unit-cell and of the optical indicatrix: $a = \alpha$, $b = \gamma$, $c = \beta$. Very distinct cleavage parallel to (010).

The separation of the mineral for chemical analysis was rather difficult. In the course of the heavy liquid separation the specific gravity of delhayelite proved to be $2{\cdot}60 \pm 0{\cdot}03$. This value is virtually identical with the specific gravity of kalsilite and only slightly lower than that of nepheline. Both these minerals are present in the rock in amounts greatly exceeding that of the delhayelite. By repeated centrifuging in bromoform and in Clerici solution the main part of the nepheline could be removed. Kalsilite and delhayelite, on the other hand, could not be separated from each other in that way. Both these minerals are easily soluble in diluted hydrochloric acid as well as in strong acetic acid. It was found, however, that the solubility of delhayelite is slightly less in diluted warm acetic acid than that of kalsilite. A treatment of the material with very dilute warm acetic acid dissolved the kalsilite grains and left delhayelite only very slightly attacked. In the analysed material no kalsilite could be detected under the microscope nor by powder pattern. A grain count indicated a contamination of 2 % admixed nepheline that had remained unattacked by the acid treatment. Owing to the small amount of delhayelite available, a pycnometric specific gravity determination could not be made.

Table II. Chemical composition of delhayelite.

SiO_2	52·60	CaO	7·99	F	0·33
TiO_2	0·09	Na_2O	3·20	SO_3	1·31
Al_2O_3	9·22	K_2O	9·27		101·02
Fe_2O_3*	2·72	H_2O+	5·93	Less O for F and Cl	1·01
MnO	0·07	H_2O-	3·35		
MgO	1·03	Cl	3·91	Total	100·01

* Total iron.

Table II presents the result of the chemical analysis, corrected for the nepheline admixture. The purity of the analysed material was rather low. Except for nepheline, the impurities mainly consist of pigment, which for a large part represents alteration products of delhayelite. Owing to the relatively low purity of the material and the fact that it was slightly attacked by the acid, the analysis may give only an approximate idea

of the composition of the mineral. A new analysis of pure and fresh material is highly desirable.

The scarcity of the material did not permit a differential thermal analysis. The high proportion of total water as H_2O- is noteworthy. Because of the relatively low purity of the analysed material, an accurate calculation of the unit-cell content cannot be given. For the super-cell with the dimensions mentioned above, the analysis yields the following provisional approximation: $(Na,K)_4Ca_5Al_6Si_{32}O_{80} \cdot 18H_2O \cdot 3(Na_2,K_2)(Cl_2,F_2,SO_4)$.

If *a*- and *b*-axes are interchanged, the unit-cell dimensions for delhayelite become very similar to those for rhodesite. Both minerals have the same cleavage. In optical properties, however, they differ very distinctly from each other. The chemical composition of delhayelite also differs from that of rhodesite, delhayelite containing Al and, in addition, Cl, F, and SO_4.

The properties of delhayelite given above are not consistent with any previously known species. The mineral is found in a holocrystalline lava for which the crystallization occurred in presence of volcanic gases. This mode of occurrence apparently explains the incorporation of Cl, F, and SO_4 in the structure of the mineral.

Acknowledgements. The authors are indebted to the Government Scientific Council of Finland for funds covering the expenses of the chemical analysis and to Mr. Pentti Ojanperä, of the Geological Survey of Finland, for undertaking the analysis.

References.

Gard (J. A.) and Taylor (H. F. W.), 1957. Min. Mag., vol. 31, p. 611.
Mountain (E. D.), 1957. Ibid., vol. 31, p. 607.
Sahama (Th. G.) and Hytönen (Kai), 1957 *a*. Ibid., vol. 31, p. 503.
—— —— 1957 *b*. Ibid., vol. 31, p. 698.
—— and Meyer (A.), 1958. Exploration du Parc National Albert, Mission d'études vulcanologiques, Fasc. 2.

A hydrated barium-strontium pyrochlore in a biotite rock from Panda Hill, Tanganyika.[1]

By E. Jäger, Ph.D., and E. Niggli, Ph.D.

Min.-Petr. Inst., University of Berne, Switzerland

and A. H. van der Veen, Geol. Drs.

Min. Petr. Dept., Research Laboratory of the Billiton Maatschappij N.V., Hollandsche Metallurgische Bedrijven N.V., Arnhem, Netherlands.

[Read 5 June 1958.]

Summary. A hydrated barium-strontium pyrochlore with only subordinate amounts of Ca and Na has been found in a weathered biotite rock (contact-rock of a carbonatite) from Panda Hill, Tanganyika, as small euhedral yellowish-grey cubic crystals (showing the combination of the octahedron and the cube) in a rock containing euhedral biotite, some orthoclase, and several other minerals. Hydrated Ba-Sr pyrochlore is isotropic, the refractive index varies from 2·07 to 2·10. The reflectivity (vertical illumination) is 13·2 %. H. 4½–5. Poor {111} cleavage. The pyrochlore structure (space-group O_h^7–$Fd3m$) and the unit-cell dimensions (a 10·562 Å.) are derived from X-ray powder and Weissenberg photographs. The calculated specific gravity is 4·01 (observed, 4·00 on dried material). Chemical analysis gives BaO 12·5, SrO 6·4, Na_2O 0·28, K_2O 0·25, CaO 1·35, rare earths (mainly Ce_2O_3) 2, ThO_2 0·6, FeO 0·45, TiO_2 3·9, Nb_2O_5 67·0, Ta_2O_5 0·22, H_2O+ 4·0, other constituents 2·21, total 101·16. After deduction for impurities the following formula resulted:

$(Ba_{0\cdot30}Sr_{0\cdot22}Ca_{0\cdot05}Ce_{0\cdot04}Na_{0\cdot03}Fe_{0\cdot02}K_{0\cdot01}Th_{0\cdot01})(Nb_{1\cdot83}Ta_{0\cdot004}Ti_{0\cdot17})O_{5\cdot61}(H_2O)_{0\cdot80}$.

The ideal formula for pyrochlore is $A_2B_2O_6(F,OH)$. In the mineral described only a third of the A-positions are occupied by Ba, Sr, &c. Infra-red spectrophotometry does not indicate hydroxyl-groups. When the mineral is treated with $TlNO_3$ solution the intensities of the X-ray diffraction lines 333/511, and 444 are changed; hydrated Ba-Sr pyrochlore shows a certain exchange-capacity.

The name *pandaite*, from Panda Hill, is proposed for the new mineral.

In the concession area of the Mbeya Exploration Company[2] (Mbexco) near Mbeya (Tanganyika) (fig. 1*a*) Dr. J. F. Osten, former geologist of the Mbexco, found early in 1956 a strongly weathered biotite-rich rock, in which he observed many very small yellowish-grey crystals resembling

[1] Published by permission of the N.V. Billiton Maatschappij and the Colonial Development Corporation.

[2] The Mbeya Exploration Company Ltd. (Mbexco) is jointly owned by the N.V. Billiton Maatschappij, Netherlands, and the Colonial Development Corporation, Great Britain. The Mbeya carbonatite (also known as the Panda Hill carbonatite is a pyrochlore-bearing carbonatite that is being developed by the Mbexco.

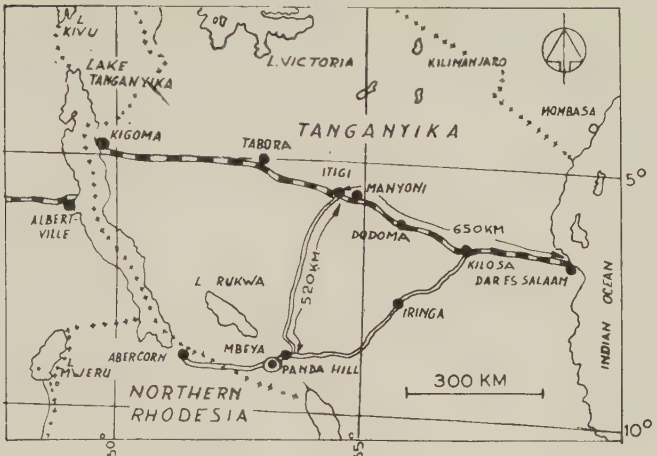

FIG. 1[a] = POSITION OF PANDA HILL IN TANGANYIKA

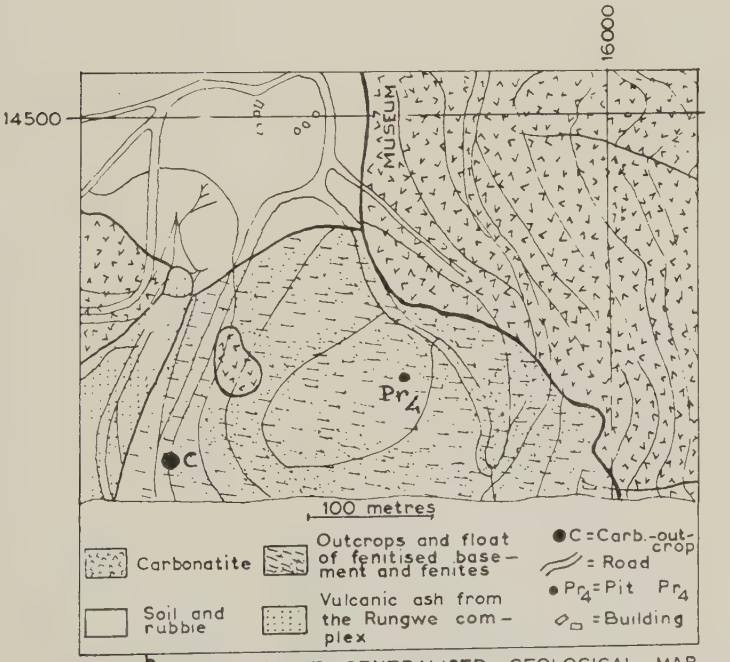

FIG. 1[b] = PART OF THE GENERALISED GEOLOGICAL MAP OF THE MBEYA CARBONATITE (FROM THE PAPER OF FICK AND V.D. HEYDE)

common pyrochlore. He concluded that the relatively high Nb_2O_5 content (1–2 %) of the rock was due to these crystals. Later on, bulk samples of this rock were sent to the laboratories of the N.V. Billiton Maatschappij at Arnhem (Netherlands) for ore-dressing tests. In the Mineralogical and Petrographical Department of these laboratories the yellowish-grey mineral was examined with X-rays, and it was found that it has the pyrochlore structure but that the unit-cell dimension is relatively great. Also the high Ba and Sr content and the lack of Ca were striking. These facts point to a new variety of the pyrochlore family, a barium-strontium pyrochlore. A barium-bearing pyrochlore with nearly the same powder pattern, but with somewhat different intensities of the X-ray reflections, found in Alaska (exact locality unknown), has been reported but not yet described by J. Berman (1955).

The Ba-Sr pyrochlore is found in a strongly weathered biotite-rock. According to L. J. Fick and C. van der Heyde (in press) this rock belongs to a series of fenitized rocks occurring in a roof pendant of the Mbeya carbonatite. The location of the pit where the biotite rock is found can be seen in the small map (fig. 1*b*) and is indicated with Pr_4. The mineral is also found in several other fenitized rocks, in this area for example those of the Kunja zone. For further data concerning the geology of the Mbeya carbonatite, reference is made to the papers of A. P. Fawley and T. C. James (1955) and of L. J. Fick and C. van der Heyde (in press).

The minerals of the biotite rock.

We investigated rock samples and identified in thin sections and polished specimens the following minerals: major components: biotite, orthoclase (nearly always strongly kaolinized), and limonite; minor components: Ba-Sr pyrochlore, fluorite, quartz, apatite, zircon, chlorite, plagioclase (not further determined), rutile, and hematite. During the tests for ore-dressing, concentrates and tailings were investigated. The following minerals were found: In the concentrates, Ba-Sr pyrochlore, hematite, limonite, martite, fluorite, zircon, tourmaline, sphene, red and yellow garnet, magnetite, columbite, rutile, and several tailing components; in the tailings, biotite, apatite, orthoclase, some quartz, and several concentrate components. Cassiterite is also found in the mineral concentrates (perhaps due to mill contamination). Baryte and celestine were never observed, neither microscopically nor in X-ray powder photographs. Biotite and orthoclase were more fully investigated besides the Ba-Sr pyrochlore.

Biotite occurs in the rock in two forms, a euhedral or nearly euhedral and an anhedral shape. The euhedral biotite shows clearly a zonal structure. The kernels of this mica have very dark tints; the border is very light coloured. The measured optical constants and pleochroism are: Border, α light reddish brown, β very light green, γ very light green, n_m (mean index of refraction in the plane of β and γ) approx. 1·583, 2V nearly 0°; kernel, α rather dark reddish brown, β olive-green to dark brownish olive-green, γ olive-green, n_m approx. 1·603, 2V approx. 10°. The anhedral mica has the following optical constants and pleochroism: α light green to reddish brown, β, γ greenish brown to dark olive-green, n_m approx. 1·593, 2V approx. 10°.

A concentrate of mica was prepared from the tailings obtained by ore-dressing tests by treatment with heavy liquids, namely a mixture of alcohol and bromoform, density 2·69, and methylene iodide, density 3·30: this concentrate was analysed, and gave:[1] Na_2O 0·85, K_2O 10·1, Al_2O_3 6·9, SiO_2 36, FeO 3·6, Fe_2O_3 8·5, MgO 15, TiO_2 1·2, Li_2O 0·25 %. An unknown part of the Fe_2O_3 is due to intergrowths of limonite.

According to the tables of W. E. Tröger, pp. 83, 84 (1952), the borders of the euhedral mica-crystals are iron-rich phlogopite. The kernels of these crystals as well as the anhedral mica correspond to varieties of mica between an iron-rich phlogopite and meroxene. The chemical analysis of the concentrate of the biotite is in fair agreement with the measured optical constants.

Orthoclase. In several thin sections 2V was measured in relatively fresh orthoclase, and varied from 36° to 68°. Six measurements were above 53° and only two below this value. An orthoclase concentrate was prepared from the tailings obtained by ore-dressing tests by treatment with a mixture of alcohol and bromoform (sp. gr. 2·69). This concentrate, with about 60 % felspar, was partially analysed. The results are as follows (the alkalis were determined chemically, Ba, Sr, and Al spectrographically): Na_2O 1·3, K_2O 8·8, $BaO < 0·1$, $SrO < 0·1$, Al_2O_3 9·7 %. The orthoclase is mostly anhedral and only rarely subhedral. The rock contains only very few crystals of plagioclase.

Structure and genesis of the biotite rock.

In the fresh fracture plane and in polished surfaces of the biotite rock, greyish-black to dark grey patches with more or less sharply defined contours can be observed. These patches lie in fields of medium grey to

[1] The SiO_2 was spectrographically estimated, the other data chemically determined.

medium dark grey colour (fig. 2). The rock is small to fine grained.

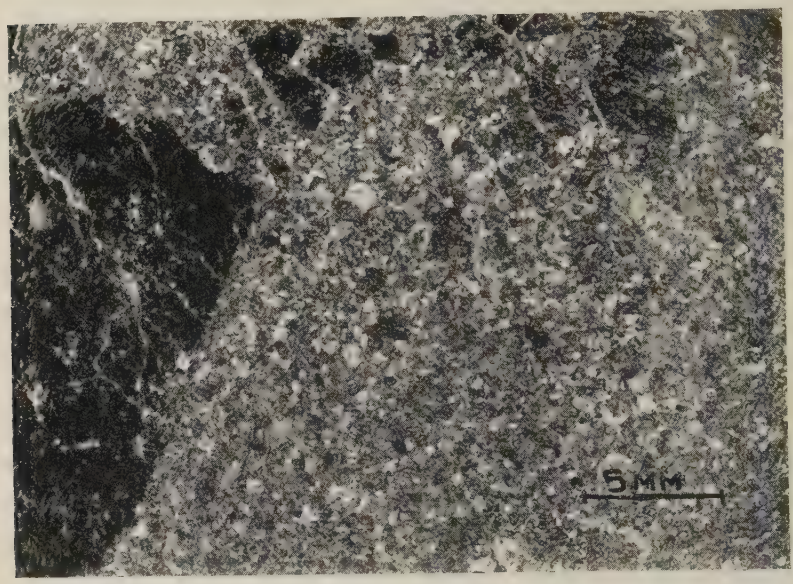

FIG. 2. Photomicrograph of a polished biotite rock (oblique reflected light, 1 mm. on the photo. is *c.* 280 μ). Black patches = biotite aggregates, white spots = Ba-Sr pyrochlore (for more than the half), grey = euhedral biotite (the shape not observable on the photo.).

The dark coloured patches are aggregates of anhedral biotite crystals with reddish-brown to dark olive-green colours in thin sections. Ba-Sr pyrochlore is lacking in the dark parts. Recrystallization zones and veins with euhedral biotite and Ba-Sr pyrochlore are observed in the dark patches, the borders of which are rather irregular, probably due to corrosion by the surrounding greyish areas. In thin section the crystal-size of the biotite in the dark coloured patches was estimated at a mean of 60 to 100 μ, with a range from 10 to 330 μ; in the greyish areas the mean size was about 100 to 300 μ, with a range from 25 to 1900 μ.

The medium grey to medium dark grey parts are mainly composed of euhedral to nearly euhedral biotite with (in thin section) very light coloured borders (fig. 3). The kernels of these mica crystals are dark reddish brown to dark olive-green. Locally they are nearly opaque, owing to abundant very fine inclusions. Other minerals observed in thin

section are rather strongly kaolinized orthoclase (locally concentrated), Ba-Sr pyrochlore, locally much limonite, and rarely some quartz. The composition by volume is roughly estimated at 1 to 25 % orthoclase,

Fig. 3. Photomicrograph of the part of the biotite rock with the euhedral biotite (transmitted ordinary light, 1 mm. on the photo. is *c.* 11·5 μ). P = pyrochlore (here nearly opaque), PL = euhedral biotite, R = light coloured borders of the biotite, L = limonite (photo. made by Prof. Dr. Ir. C. Schouten).

0 to 6 % Ba-Sr pyrochlore, 50 to 100 % biotite, and up to 20 % other minerals in the grey areas, while the dark patches contain 90 to 100 % biotite. The genesis of the rock is not clear. It belongs to the contact zone of the Mbeya carbonatite. The euhedral shape of the biotite in the greyish rock parts points to partial anatexis with supply of material (Ba, Sr, Nb).

Mineral separation.

To obtain a sample of pure Ba-Sr pyrochlore the rock was crushed and the mineral concentrated with a shaking table. This table concentrate had a Nb_2O_5 content of 39 %. 485 g. of this concentrate were centrifuged with methylene iodide (sp. gr. 3·30). About 83 % of the sample had a density more than 3·30, and contained the Ba-Sr pyrochlore.

Since the larger Ba-Sr pyrochlore crystals and fragments contain many inclusions and the smaller ones much less, the dense fraction was sieved on a 200-mesh screen. A Frantz Isodynamic separator was used on the

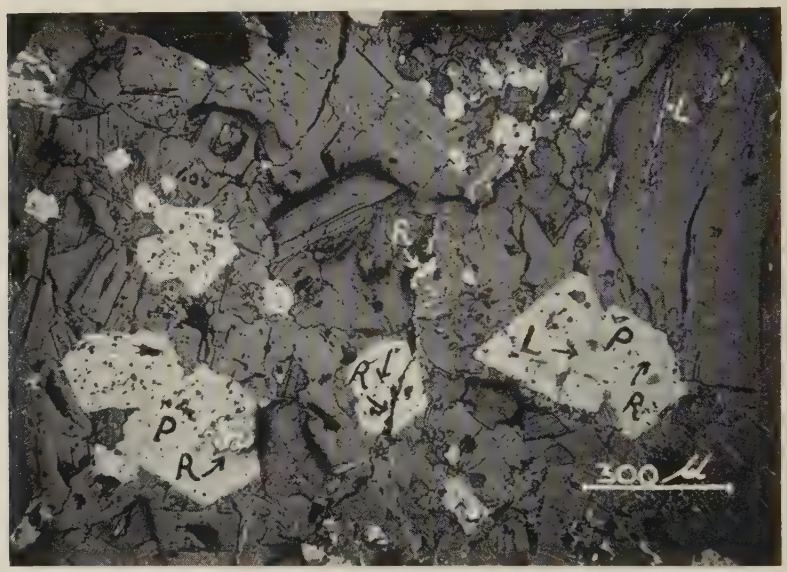

Fig. 4. Photomicrograph of the biotite rock with the Ba-Sr pyrochlore (vertically reflected ordinary light, 1 mm. on the photo. is *c.* 16·2 μ). P = Ba-Sr pyrochlore (light grey), R = rutile (white and light grey), dark grey = gangue material (biotite, &c.), black = pits, cleavages, trenches, &c. (photo. made by Prof. Dr. Ir. C. Schouten).

part of the sample passing 200 mesh, in order to obtain a very high concentrate of Ba-Sr pyrochlore, and this rich product was centrifuged once more with methylene iodide. The dense fraction was treated with Clerici solution (sp. gr. 4·25), and the light fraction of this last separation was treated twice more with methylene iodide, to try to remove the last traces of apatite and zircon. The end-product (19·14 g.) contained only very small amounts of other minerals such as apatite, zircon, rutile, quartz, &c. About 1 g. of the 'pure' Ba-Sr pyrochlore was used to make two polished sections, to study the contamination in the sample; the product was also examined with a binocular microscope and a petrographical microscope. Fifteen grammes of the final product were used for the chemical and spectrographical analysis. In the same manner another Ba-Sr pyrochlore sample was made with a Nb_2O_5 content of

about 70 % (spectrographical estimation); part of this sample was used for the infra-red spectrographic analysis.

Description of the hydrated Ba-Sr pyrochlore.

Physical properties. Ba-Sr pyrochlore occurs as euhedral crystals showing a combination of the octahedron and very small cube faces.

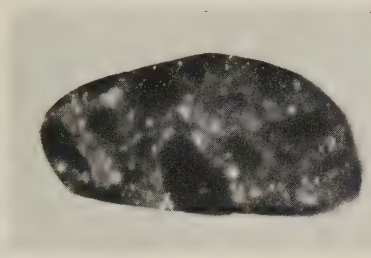

FIG. 5. Positive print of an autoradiograph of biotite rock (real size). Exp. time 28 days, made with Ilford Ilflex X-ray film. Dark grey = biotite aggregates, medium grey = euhedral biotite (weakly radioactive), light grey to white = Ba-Sr pyrochlore.

The small size (down to 10 μ) of the purest crystals and the many inclusions in the larger crystals (the largest measure 800 μ) made measurements of physical properties difficult. The colour of the pure mineral, seen macroscopically, is yellowish-grey (5 Y 7/2) to somewhat light olive-grey (5 Y 5/2) (symbols according to Rock-colour Chart, 1951). With a binocular microscope it is observed that the colour of the crystals is yellowish-grey (5 Y 7/2) to very pale orange (10 YR 8/2). In polished sections a very poor $\{111\}$ cleavage was observed; the fracture is conchoidal. Mr. K. Taylor of the Geological Survey of Great Britain, Atomic Energy Division, measured the micro-hardness of the mineral. He obtained a value of 550 V.H.N. (Vickers Hardness Number); a G.K.N. hardness tester was used with 100 g. load. According to E. W. Taylor (1949) this corresponds with a hardness between $4\frac{1}{2}$ and 5 on Mohs' scale. The mineral is radioactive, due to its U and Th content (see chemical analysis).[1] An autoradiograph (fig. 5) made of a polished rock section shows many radioactive patches. Pure Ba-Sr pyrochlore is non-magnetic. When it has rutile or limonite intergrowths it is weakly magnetic and most of these grains can be removed from the concentrate with a Frantz Isodynamic magnetic separator. In thin section the

[1] After completion of the manuscript, it was found that another Ba-Sr pyrochlore sample with 67 % Nb_2O_5 contained 0·31 % U and 0·72 % Th.

mineral is translucent; when it is weathered or when it contains many fine colourless inclusions it is opaque white. The composition of the products of alteration is unknown.

Ba-Sr pyrochlore is isotropic. The refractive index lies mainly between 2·08 and 2·09, but some crystals have indices between 2·09 and 2·10 and some between 2·07 and 2·08. In vertical reflected light the colour of the mineral is grey. The reflectivity is 13·2 % (determined by Mr. K. Taylor), measured photoelectrically with the apparatus described by S. H. U. Bowie (1957). This was done in air, using white light of colour-temperature 3050° K. With crossed nicols the internal reflection of pure Ba-Sr pyrochlore is colourless to white. Several times a brownish to reddish internal reflection was observed, due to very fine limonite inclusions. These properties agree well with those of the other members of the pyrochlore family.

Density measurements using the pycnometer and immersion methods (in Clerici solution) always gave high values compared with the calculated density from chemical formula, lattice constant, and type of structure (pyrochlore). This is attributed to water adsorbed in the holes of the crystal structure during the weighing of the sample in water and lost when the sample is dried at 110° C. Therefore we changed the pycnometer method as follows: The powder was covered with distilled water, evacuated, and weighed. After this we found a great difference in weight between the sample dried in vacuum at room temperature and the material heated to 110° C. The vacuum-dried sample showed lower density values, but still too high because of the water that remained in the holes of the crystals. The vacuum-dried powder was heated to 130° C. in the thermobalance; the loss in weight gave the correction to dried material. Density values derived from pycnometer method: Normal method, 4·11–4·15; vacuum-dried 4·04; thermobalance correction −1%, so the corrected value for dry material is 4·00. The calculated density value (from X-ray data and chemical composition) is 4·01.

In Clerici solution of density 4·04 the crystals floated in the beginning, but after several days they sank to the bottom while their colour had changed from greyish to orange-yellow.

Chemical composition. Before analysis the sample was dried during several hours at a temperature of 100–110° C. The H_2O^+ content was then established by the Penfield method. During this analysis the sample was heated to a temperature not higher than 500° C. After 5 to 10 minutes no more water was lost. SO_3, F, and rare earths together with ThO_2 were determined by the usual chemical methods. Subtracting

the spectrographically determined value of ThO_2 ($\pm 0{\cdot}6$ %) the total amount of the rare earths could be found. Spectrographically Ce, Yt, and La were found in the proportion of roughly 40:2:1. CO_2 was determined by a gas-evolution method and Na_2O and K_2O by flame-photometry. The other values, including ThO_2, were spectrographically determined. The Nb_2O_5 content was checked spectrophotometrically, using hydrogen peroxide in sulphuric acid; this gave the same value as the spectrographic determination. CaO and FeO were determined both by chemical methods and spectrographically, giving (spectrographic data in parentheses): CaO 1·4 % (1·3 %), FeO 0·45 % (0·45 %).

Mr. J. H. L. Zwiers of the Analytical Institute T.N.O., Rijswijk, did not find any indication of hydroxyl groups by infra-red spectrophotometry. Unfortunately, it was impossible to prepare a completely pure pyrochlore sample. In a polished section a minor quantity of rutile was observed (estimated 0·1–0·2 per cent. by weight). Other impurities are zircon, phlogopite, orthoclase, apatite, cassiterite, and quartz.

Table I gives the spectrographical-chemical analysis of the mineral, from which we derive the formula:

$$(Ba_{0{\cdot}30}Sr_{0{\cdot}22}Ca_{0{\cdot}05}Ce_{0{\cdot}01}Na_{0{\cdot}03}Fe_{0{\cdot}02}K_{0{\cdot}01}Th_{0{\cdot}01})$$

$$(Nb_{1{\cdot}83}Ta_{0{\cdot}004}Ti_{0{\cdot}17})O_{5{\cdot}61}(H_2O)_{0{\cdot}80}.$$

We cannot decide if Fe is, according to this formula, really in *A*-positions; Fe⇌Nb substitution is also possible. The formula, compared with the normal pyrochlore formula $CaNa(Nb_2O_6)F = A_2B_2O_6F$, indicates a lack in Ba, Sr, Ca, Na . . . atoms; only a third of the *A*-positions are occupied. There is also a small deficit in oxygen (5·6 instead of 6) and instead of 1 fluorine we found only 0·8 water molecules. In the *A*-group of elements Ba and Sr dominate over Ca and Na. The pyrochlore-mineral in the biotite rock of Panda Hill is thus a partially hydrated *barium-strontium pyrochlore*, with only one-third of the *A*-positions occupied by cations.

D.T.A. and thermobalance investigations. 0·4 g. of Ba-Sr pyrochlore and of common Ca-Na pyrochlore from Panda Hill were analysed with D.T.A. apparatus (E. Jäger and S. Schilling, 1956), giving the results shown in fig. 6. Ba-Sr pyrochlore shows an endothermic peak at 330° C. and exothermic reactions at 540°, 800°, and 820° C. The endothermic peak is the dehydration-peak; at the first exothermic reaction the pyrochlore structure of the Ba-Sr pyrochlore is totally destroyed, as we found by X-ray analysis. Common Ca-Na pyrochlore shows no dehydration peak;

the broad exothermic peaks at 400° and 600° C. might be due to oxidation or recrystallization. X-ray diagrams of Ca-Na pyrochlore heated to 600° C. indicate recrystallization from a weakly metamict state. The dehydration by means of the thermobalance apparatus (Chevenard type) was carried out with 2·0 g. of Ba-Sr pyrochlore previously dried at 130° C., and gave the curve shown in fig. 7. D.T.A. and thermobalance analyses show that the dehydration process is finished at 350° C. Therefore it is probable that in this structure the water is present as H_2O molecules and not as (OH) groups.

TABLE I. Chemical composition of hydrated barium-strontium pyrochlore from Panda Hill.

	Analysis of the purest material available.	*Analysis corrected for impurities.**	*Molecular ratios*	*Atomic ratios on a basis of* $2(Nb,Ti,Ta)$.
Na_2O	0·28	0·28	4·5	Na 0·031
K_2O	0·25	0·15	1·6	K 0·011
CaO	1·35	0·86	15·3	Ca 0·054
BaO	12·5	12·88	84·0	Ba 0·295
SrO	6·4	6·60	63·7	Sr 0·224
Rare earths† ...	2	2·06	6·3	Ce 0·044
ThO_2	0·6	0·62	2·3	Th 0·008
FeO‡	0·45	0·44	6·1	Fe″ 0·021
TiO_2	3·9	3·87	48·4	Ti 0·170
Nb_2O_5	67	69·06	259·8	Nb 1·826
Ta_2O_5	0·22	0·23	0·5	Ta 0·004
H_2O+	4·0	4·11	228·1	H_2O 0·802
MnO	0·01			O 5·61
MgO	0·07			
ZrO_2	0·28			
SnO_2	0·32			
SiO_2	0·89			
PbO	0·01			
CuO	0·01			
Al_2O_3	0·12			
SO_3	trace			
CO_2	0·1			
F	trace			
P_2O_5	0·4			
Total	101·16	101·16		

* The analysis is corrected for impurities by deduction of 0·42 % zircon, 0·27 % phlogopite (with some Fe″), 0·42 % orthoclase (with some Na), 0·92 % apatite, 0·32 % cassiterite, 0·33 % quartz, 0·15 % rutile (estimated in polished section), and by deduction of 0·01 % CuO, 0·01 % PbO, and 0·1 % CO_2.

† Calculated as Ce_2O_3.

‡ All iron is calculated to FeO.

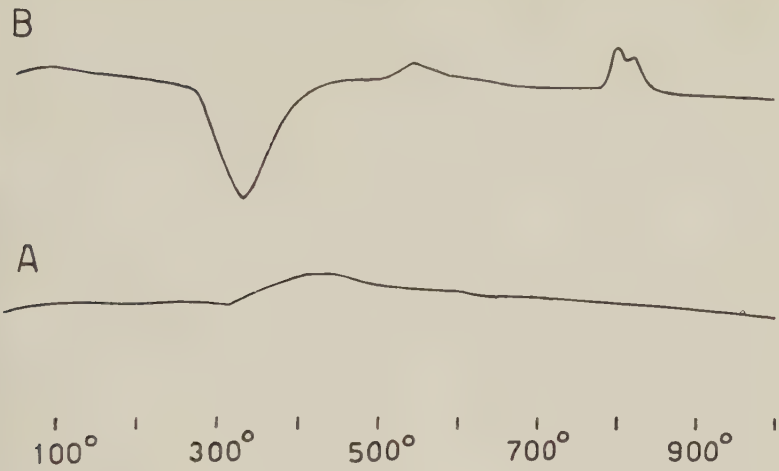

FIG. 6. A: D.T.A. curve of Na-Ca pyrochlore; B: D.T.A. curve of Ba-Sr pyrochlore. Heating-rate 10° C. per minute, inert material corundum.

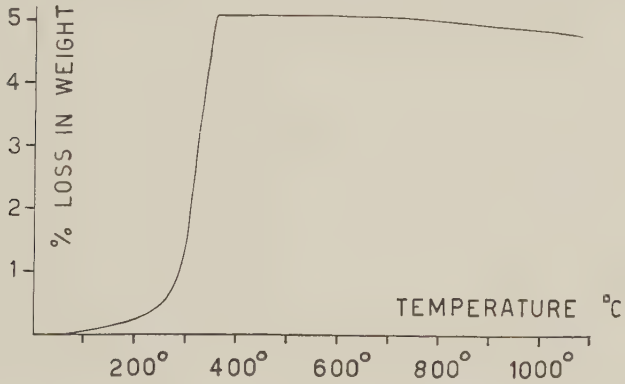

FIG. 7. Dehydration curve of Ba-Sr pyrochlore, heating-rate 2·5° C. per minute.

X-ray data. A small crystal of Ba-Sr pyrochlore 0·08 mm. in diameter was examined by rotating crystal and Weissenberg methods. We looked for forbidden reflections according to R. S. Roth (1956), but only spots with the indices allowed in the pyrochlore structure were found. We conclude that the mineral is a true member of the pyrochlore group. From powder photographs (table II) we calculated the lattice constant a 10·562 ±0·006 Å. This value was found by linear extrapolation to the zero value of the function $\cos^2\theta/\sin\theta+\cos\theta/\theta$.

TABLE II. Powder data (Fe-$K\alpha$ radiation) of two Ba-Sr pyrochlore samples. Intensities estimated.

1488 CB.	*1614 DA.*		
d, Å.	*d*, Å.	*I.*	*hkl.*
6·11	6·09	80	111
3·18	3·18	50	311
3·045	3·044	100	222
2·638	2·636	40	400
2·421	2·424	<1	331
2·156	2·152	5	422
2·033	2·029	20	511/333
1·866	1·864	70	440
1·783	1·781	15	531
1·611	1·609	5	533
1·592	1·590	70	622
1·524	1·521	20	444
1·479	1·477	15	711/551
1·373	1·373	15	731/553
1·320	1·319	15	800
1·243	1·244	5	822/660
—	1·218	2	751/555
1·211	1·210	50	662
1·180	1·180	50	840
1·159	1·158	10	911/753
1·107	1·106	10	931
1·077	1·077	40	844
1·061	1·061	10	933/771/755
1·0164α_1	1·0164α_1	60	10.2.2/666
1·0160α_2	1·0160α_2	10	

In some powder patterns of Ba-Sr pyrochlore we also found reflections with *d*-values of 2·238 and 1·755 Å., which might correspond to the forbidden indices 332 and 600/422. In Weissenberg photographs these spots are always absent; in powder patterns they are caused by small quantities of quartz (d = 2·24 Å.) and perhaps tapiolite (d = 1·75 Å). The stongest quartz line (d = 3·343 Å.) is always present. In addition, the Weissenberg diagrams gave us the allowed reflection 620 (d = 1·670 Å.).

From the gravity measurements we might expect an exchange capacity. Therefore Ba-Sr pyrochlore was treated with a concentrated solution of $TlNO_3$ for 10 days and then an X-ray diffractometer diagram was made. Comparing this with the diagram of untreated Ba-Sr pyrochlore we found a marked change in the intensities of the 333/511, and 444 reflections. Moreover the 222, 400, and 440 reflections of the $TlNO_3$-treated Ba-Sr pyrochlore are accompanied by very weak lines (the intensity of these reflections is less than 5 % of the main reflection) with higher *d*-values (see refl. 440 of curve I in fig. 8). The differences between main reflection and satellite agree with $\Delta a = +0{\cdot}1$ Å. It is not clear why only three reflections show this effect. We tried to remove the Tl-ions from the treated Ba-Sr pyrochlore by digestion with $\frac{1}{4}$ *N* nitric acid for 5 days. A new X-ray diffractometer diagram showed the disappearance of the satellites and the intensities of the 333/511, and 444 reflections approached the mean value between $TlNO_3$-treated and normal Ba-Sr pyrochlore (see fig. 8). Diffractometer curves from Ba-Sr pyrochlore treated with Clerici solution also showed strong changes in the intensities and a

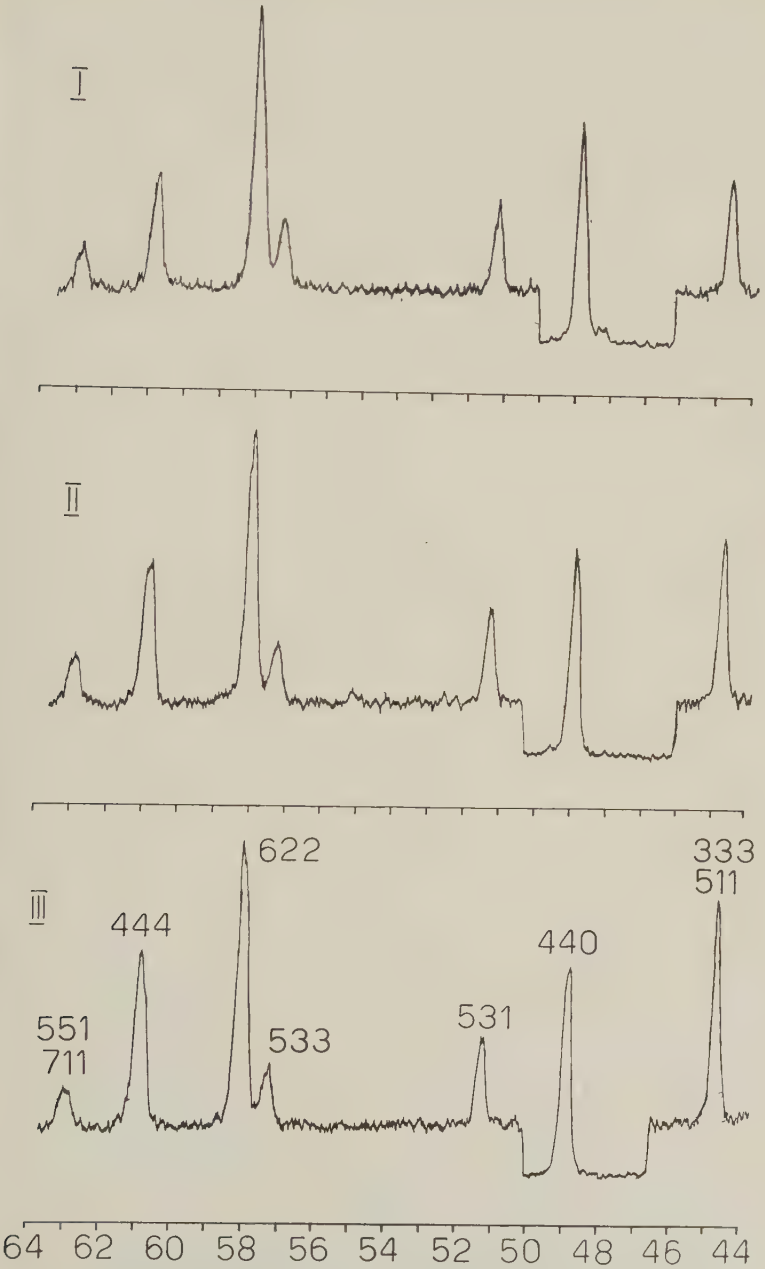

FIG. 8. X-ray diffractometer diagrams of Ba-Sr pyrochlore: I, $TlNO_3$ treated; II, sample I HNO_3-treated; III, untreated. The numbers under the diagram III indicate the diffraction angles, 2θ; reflection 440 is measured with half the sensitivity of the others.

broadening of many reflections to higher d-values. A diffractometer diagram of Ba-Sr pyrochlore heated to 350° C. gives only minor differences in intensities and a small shrinkage of the lattice constant, $\Delta a = 0{\cdot}015$. The following points can be stated from X-ray experiments: the mineral shows pyrochlore structure; the lattice constant is higher than usual in natural pyrochlores (except the Ba-bearing pyrochlore reported by J. Berman, 1955); the holes in the structure can be filled up reversibly by Tl-ions; and heating to 700° C. destroys the pyrochlore structure whereas heating to dehydration (350° C.) does not give essential changes.

Discussion of the experimental results. Infra-red, D.T.A., and thermobalance analyses indicate the presence of water molecules. From chemical analysis a domination of $(Ba,Sr)_{0{\cdot}52}$ over $(Ca,Na,Fe,Ce,Th,K)_{0{\cdot}16}$ was found. Besides this some F and (Ca,Na) positions must be vacant or occupied by water molecules. This leads to the following considerations:

In the normal pyrochlore structure the fluorine ions are surrounded by 4 (Ca,Na) positions and each Ca or Na ion has two F ions as nearest neighbours. The result is a network of Ca F links, branched at every fluorine position. In the Ba-Sr pyrochlore described only half of this network of positions is occupied: $(Ba,Sr,Na...)_{0{\cdot}68} + (H_2O)_{0{\cdot}80} = 1{\cdot}48$ instead of $(Ca,Na)_2 + F = 3$. Thus results a system of irregular channels in the Ba-Sr pyrochlore structure. From this point of view a certain possibility of exchange capacity can be expected, which was confirmed by treatment with concentrated $TlNO_3$ solution. We do not yet understand the results with Clerici solution. These exchange experiments have just been started and are being continued.

The mineral occurs in a weathered rock and it is possible that, connected with a hydration process, the pyrochlore of the biotite-rock of Panda Hill lost a part of the A-position ions.

Nomenclature. It is well known that there is no unanimously accepted rule in the nomenclature of the pyrochlore group. Some authors prefer to include under pyrochlore all the members of the group. Others give distinct names to the various members of this group.

We prefer the latter and therefore propose to give the mineral described above the name of *pandaite* (after Panda Hill). This name shall be used for those minerals of the pyrochlore group in which Ba predominates over other elements in the A positions.

The pandaite of Panda Hill having an important Sr-content can be characterized more exactly as a strontian pandaite.

Acknowledgements. The authors are indebted to the Boards of Directors of the N.V. Billiton Maatschappij, the Colonial Development Corporation, and the N.V. Hollandsche Metallurgische Bedrijven and to their staffs for permission to publish this paper, for the use of their instruments, and for the several analyses so devotedly done. We thank Prof. Dr. Ir. C. Schouten, Prof. Ir. H. J. de Wijs (Technical University, Delft, Mining Department), Prof. Dr. W. P. de Roever (Geological Institute, University of Leiden) and their staffs for helpful comments, several photographs, for the use of instruments in their laboratories, and for special polished sections. Also we are indebted to Mr. K. Taylor of the Geological Survey of Great Britain, Atomic Energy Division, for measuring the micro-hardness and the reflectivity of Ba-Sr pyrochlore, and Mr. J. E. T. Horne of this Survey for kind suggestions; Mr. R. S. Roth, Chemist of the National Bureau of Standards, Washington for the supply of a sample of $Nd_2Sn_2O_7$; to the Analytical Institute T.N.O., Rijswijk for permission to publish the results of the analysis of Ba-Sr pyrochlore for hydroxyl groups, and to Mr. J. H. L. Zwiers of this institute for making the analysis. We are indebted to Prof. Dr. W. Nowacki (Abteilung für Kristallographie und Strukturlehre, Universität Bern), who put at our disposition the diffractometer of his department.

References

Berman (J.), 1955. Amer. Min., vol. 40, p. 824.

Bowie (S. H. U.), 1957. Min. Mag., vol. 31, p. 476.

Fawley (A. P.) and James (T. C.), 1955. Econ. Geol., Chicago, vol. 50, p. 571.

Fick (L. J.) and Heyde (C. van der), 1959. Econ. Geol., Chicago (in press).

Jäger (E.) and Schilling (S.), 1956. Schweiz. Min. Petr. Mitt., vol. 36, p. 595.

Roth (R. S.), 1956. Journ. Res. Nat. Bur. Standards, vol. 56, no. 1, p. 17. Research paper 2643.

Taylor (E. W.), 1949. Min. Mag., vol. 28, p. 718.

Tröger (W. E.), 1952. Tabellen zur optischen Bestimmung der gesteinsbildenden Minerale, Stuttgart.

The formation of a diffusion reaction skarn by pure thermal metamorphism.

(With Plates I and II.)

By W. Q. Kennedy, D.Sc., F.R.S.

Dept. of Geology, University of Leeds.

[Taken as read 6 November 1958.]

Summary. Veins and nodules of cornstone, enclosed in sandstone, have reacted to the thermal influence of a Tertiary dolerite dyke by the development of a wollastonite reaction skarn. This can be shown to have formed as a result of pseudomorphous replacement of the quartz grains by wollastonite, due to outward diffusion of calcium. The process is believed to have taken place at the inversion temperature of quartz (573° C.).

ALTHOUGH metamorphic diffusion is frequently invoked to explain various phenomena of metamorphic rocks, it is normally a matter of considerable difficulty to obtain convincing petrological proof of its action as distinct from that of high-temperature regional or contact metasomatism. The best evidence is perhaps provided by the so-called 'reaction-skarns' (Magnusson, 1936, p. 343) that sometimes develop, under the influence of regional or regional-thermal metamorphism, at the contacts between pre-existing carbonate and silicate rocks by interchange of constituents across the mutual boundaries. Such reaction-skarns have, so far, been described mainly from the Archaean rocks of Fenno-Scandia, where, however, the problem of their origin is rendered somewhat more complex in detail by the possible presence of regionally or locally derived (magmatic) emanations, and by the poly-metamorphic nature of the rocks concerned. It is consequently a matter of interest to record a particularly simple example, from a Scottish locality, in which a diffusion-reaction skarn has formed at a sedimentary contact, under the influence of pure thermal metamorphism induced by the intrusion of a dolerite dyke.

The locality in question is situated on the southern shore of the Firth of Clyde, close to the Renfrewshire–Ayrshire boundary, and immediately to the south of the village of Inverkip (Geological Survey, Scotland, one-inch-to-the-mile map, sheet 29). At this point the rocks exposed on the shore consist of typical red fluviatile sandstones and subordinate

greenish marls of Upper Old Red Sandstone age, which enclose a massive, pale-coloured, concretionary limestone or *cornstone*. The cornstone is nodular in character, with irregular upper and lower surfaces, and shows a tendency to vein and replace the enclosing rocks. It appears to be a relatively pure calcite rock, with scattered quartz grains and a little argillaceous or feldspathic material as the only impurities, and is comparable in nature, structure, and presumably origin, with the surface limestones or calcretes of South Africa.

Immediately to the south of Inverkip village these sediments are intersected by a broad (50-foot), NNW.-trending olivine dolerite dyke (Tertiary), which has converted the siliceous portions of the cornstone into a mass of fine-grained wollastonite for a distance of a foot or more outwards from its contact. The associated sandstones are less strongly affected and although darkened and obviously metamorphosed, have not suffered complete recrystallization, and still retain the original clastic forms of the sand grains.

The most interesting effects, and those to which attention is here particularly directed, concern the metamorphism of individual veins and nodules of cornstone. These have reacted to thermal metamorphism in a characteristic manner and now consist of a central core of relatively pure, recrystallized, bluish calcite-marble separated from the enclosing sandstone by a narrow, sharply defined zone of dense wollastonite from a few millimetres up to a centimetre or so in width (pl. I, figs. 1 and 2). For a further distance of several millimetres beyond the outer margin of the wollastonite zone the sandstone may be darkened owing to the development of tiny granules of grossular and a little wollastonite in the brownish, siliceous cement.

The central core of calcite-marble usually contains some small scattered patches of wollastonite and isolated tiny crystals of grossular, representing original quartz grains and aluminous (feldspathic) impurities, but appears to have suffered no material change in composition apart from the loss of carbon-dioxide due to the formation of the silicate minerals. The wollastonite zone, on the other hand, has no sedimentary chemical counterpart, and represents a true reaction-skarn developed at the expense of the enclosing sandstone by outward diffusion of lime from the adjacent cornstone under the influence of pure thermal metamorphism. This is very clearly indicated in thin section by the essentially monomineralic character of the wollastonite zone, which normally contains, in addition to the main mineral, only a very small amount of grossular, but neither residual quartz nor calcite, and

by the fact that the forms of the original quartz grains, now replaced by aggregates of wollastonite, are still clearly to be discerned (pl. II, figs. 1 and 2). The pseudomorphous replacement of quartz by wollastonite, in this manner, illustrates the operation of Lindgren's 'law of equal volumes' (Lindgren, 1933, p. 93) and could have been effected only by diffusion of lime into the reacting zone and concomitant removal of silica.[1] It can be demonstrated, moreover, that the wollastonite zone has developed *entirely* at the expense of the enclosing sandstone, as the relict quartz grain structure is sometimes seen to extend from the inner to the outer margin.[2] The inner margin consequently marks the original (sedimentary) phase boundary, and the reaction must, therefore, have involved *one-way* (outward) migration of calcium, presumably in the form of the oxide.

This is consistent with the experimental results obtained by Jagitsch, Bengtson, and Perlstroem (Niggli, 1948, p. 391) who showed that when tablets of PbO and $PbSiO_3$ were heated in contact at temperatures between 600° C. and 700° C. the formation of an intermediate reaction zone of Pb_2SiO_4 could best be explained by assuming that PbO (in the form of the oxide) had diffused across the original phase boundary and reacted with the material of the adjacent tablet. The possibilities of diffusion have also been discussed by Adams in connexion with an investigation of two refractory bricks, of different composition, burned in contact at high temperature in a laboratory kiln (Adams, 1930). Subsequent examination showed that calcium had diffused from one brick into and through the substance of the other, where it accumulated with a well-defined 'front' beyond which the proportion of the element dropped abruptly to that characteristic for the second brick. At the same time, silica was displaced from the highly transfused area and accumulated partly in advance of the calcium front. The parallelism with the Renfrewshire occurrence is here very evident despite the fact that the experimental temperatures (*c.* 1400° C.) were far in excess of those ever encountered in rock metamorphism.

[1] The conversion of each cubic centimetre of quartz into an equal *volume* of wollastonite would necessitate the addition of 1·4 g. of CaO, and the simultaneous removal of 1·15 g. of SiO_2. The excess silica appears to have diffused *outwards* into the adjacent sandstone as it has obviously not reacted with calcite to form additional wollastonite at the inner margin of the zone.

[2] Normally, however, the inner part of the zone, adjacent to the calcite-marble core, is more coarsely crystalline than the outer, and the relict structures are there partially or wholly obliterated, possibly owing to an effect of 'Sammelkristallization'.

The nature of the diffusion mechanism was not discussed in these experimental cases, but some evidence is available with regard to the manner of operation of the process in the formation of the Renfrewshire reaction skarn. Two types of diffusion mechanism, involving inter-granular diffusion on the one hand, and solid state or intra-granular diffusion on the other, can be distinguished on the basis of the microscopical evidence as follows:

Inter-granular diffusion is clearly indicated in those instances where, towards the outer margin of the wollastonite zone, isolated cores of unreplaced quartz still persist locally in the centres of the original grains. The replacement has here extended inwards from the margins of the grains towards their centres, and must, therefore, be attributed to the presence of an inter-granular medium.

Elsewhere, however, the diffusion front is very sharply defined and can be seen to cut abruptly across adjacent quartz grains without respect to their boundaries (pl. II, figs. 1 and 2). In such instances the process obviously did not depend primarily or necessarily on the presence of an inter-granular medium, but must have operated, in part at least, as solid state or *intra-granular diffusion* in the form of an evenly advancing front.

Irrespective of the actual nature of the diffusion process, however, it is very evident that the development of the wollastonite reaction skarn represents a sufficiently unusual phenomenon to require some special explanation. Under apparently similar conditions, in other instances, no such reaction has taken place, and the operation of some exceptional factor must, therefore, be postulated to explain the enhanced reactivity. This can scarcely depend on any chemical peculiarity of the materials concerned and must be attributed to a physical cause, such as a unique temperature control. It is suggested, therefore, that the reaction took place under the accelerating influence of crystallographic inversion at the transition point of quartz (573° C.). This view is supported by the following considerations:

It is known from experimental work (Hedvall, quoted by Turner and Verhoogen, 1951, p. 405) that crystallographic inversion has an accelerating influence on the reactivity of quartz, as ferric oxide 'is capable of diffusion into the quartz lattice only when the lattice itself is in process of inversion, namely, in the vicinity of 573° C., and again above 900° C.'. And in the present example temperatures falling within the range of the required order of magnitude are suggested by the presence of wollastonite, by the failure of quartz to recrystallize completely, and by the

stable co-existence of wollastonite and calcite at the inner margin of the wollastonite zone. These features show that while the temperature was sufficiently high to produce wollastonite by the reaction

$$CaCO_3+SiO_2 = CaSiO_3+CO_2 \qquad (I)$$

it was insufficient to cause the formation of spurrite by the reaction of wollastonite and calcite as follows:

$$3CaCO_3+2CaSiO_3 = 2Ca_2SiO_4.CaCO_3+CO_2. \qquad (II)$$

The most recent information (Harker and Tuttle, 1956, p. 252; Tuttle and Harker, 1957, p. 228) indicates that, at atmospheric pressure, reaction I takes place at, or slightly below, 400° C., and reaction II below 700° C. The reaction temperature increases with pressure, but in rock metamorphism, for various reasons, this factor probably has no great influence (Barth, 1952, p. 288). Nevertheless, it is desirable to examine the possible pressure conditions that may have prevailed at the time of the reaction. A very rough estimate can be based on the field evidence, which shows that whereas the wollastonite skarn and the associated dyke are exposed at sea-level, dykes belonging to the same Tertiary (Mull) Swarm are exposed on the high ground to the south-west at altitudes of up to 1600 or 1700 feet. The skarn could therefore have formed below a cover of this order of magnitude, equivalent to a rock pressure of approximately 2000 lb. per square inch. At this pressure, according to the data of Harker and Tuttle (op. cit., 1956 and 1957), reaction I would take place at a temperature of 550° C., and reaction II at a temperature of approximately 870° C. It can be assumed, therefore, that the temperature of formation of the wollastonite reaction skarn lay within the range of 400°–650° C. at atmospheric pressure, or 550° 850° C. at a maximum rock pressure of 2000 lb. per square inch. These ranges both include the significant crystallographic inversion point of quartz (573° C.) at which greatly enhanced reactivity might be expected.

The formation of the reaction skarn is therefore attributed to a fortuitous and exceptional physical control, whereby the rocks attained the inversion temperature of quartz for a sufficient period of time to allow the reaction to take place.

In conclusion, the writer would again emphasize that this represents an exceptional occurrence and mainly serves to demonstrate a principle, the importance of which as a factor in metamorphism still remains to be established.

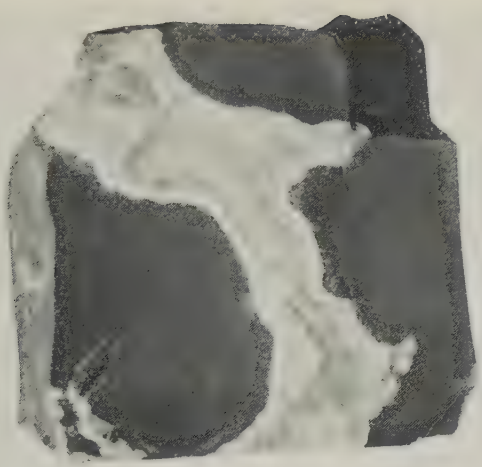

1

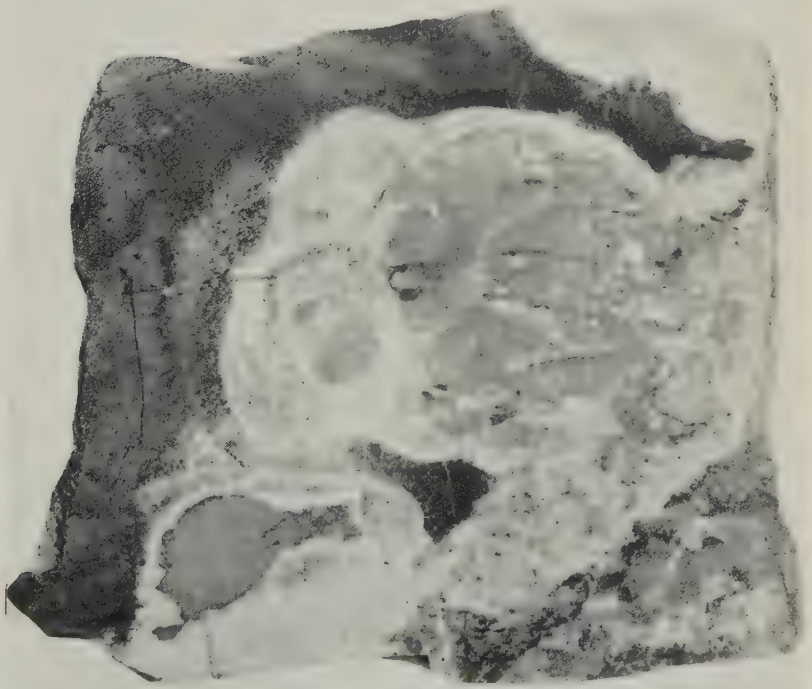

2

W. Q. Kennedy: A diffusion reaction skarn

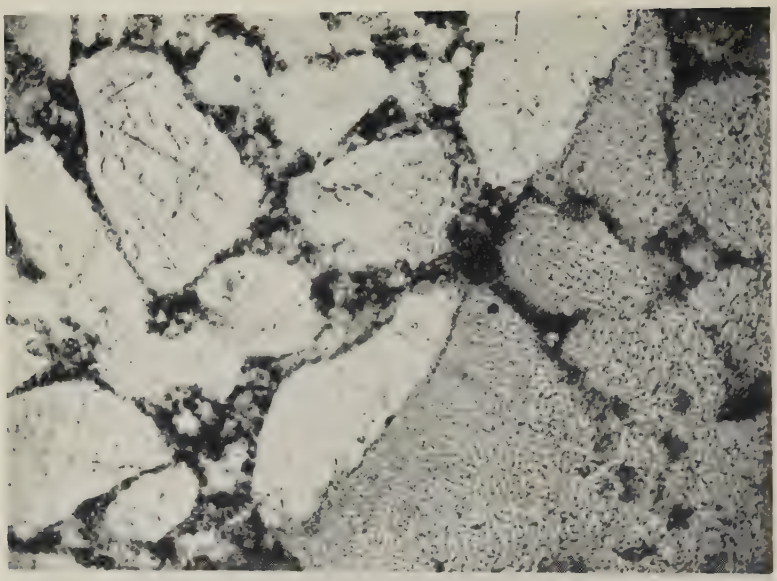

1

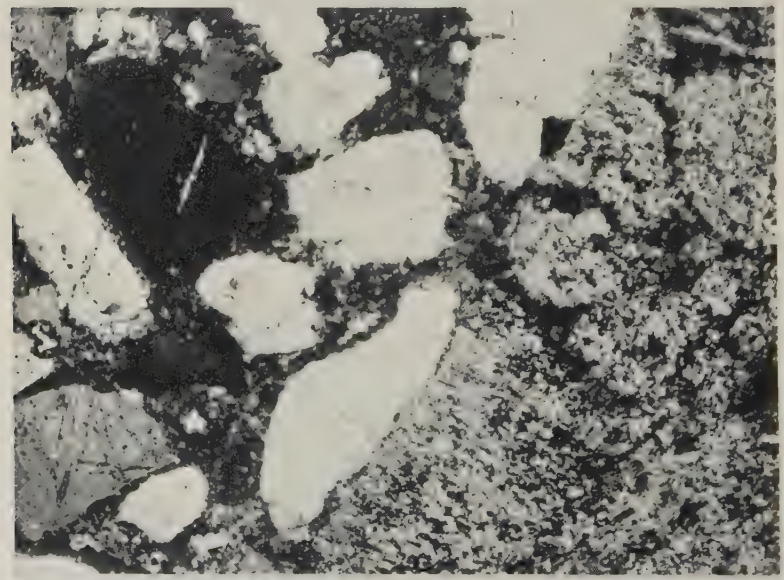

2

W. Q. Kennedy: A diffusion reaction skarn

References.

Adams (F. D.), 1930. Canad. Journ. Research, vol. 2, p. 153.

Barth (Tom. F. W.), 1952. Theoretical petrology, a textbook on the evolution of rocks. New York (John Wiley and Sons) [M.A. **11**–514].

Harker (R. I.) and Tuttle (O. F.), 1956. Amer. Journ. Sci., vol. 254, p. 239 [M.A. **13**–176].

Magnusson (N. H.), 1936. Quart. Journ. Geol. Soc., vol. 92, p. 332.

Niggli (P.), 1948. Gesteine und Minerallagerstätten, Bd. 1. Basel (Birkhäuser) [M.A. **10**–349].

Turner (F. J.) and Verhoogen (J.), 1951. Igneous and metamorphic petrology. New York (McGraw-Hill).

Tuttle (O. F.) and Harker (R. I.), 1957. Amer. Journ. Sci., vol. 255, p. 226.

Explanation of Plates I and II

Plate I. Thermally metamorphosed 'cornstones' from Renfrewshire. Approximately natural size.

Fig. 1. Vein type.

Fig. 2. Nodular type.
Dark areas = enclosing sandstone, white = wollastonite, grey = calcite marble.

Plate II. Photomicrographs of outer margin of wollastonite reaction skarn against enclosing sandstone. ×60 diameters.

Fig. 1. Ordinary light.

Fig. 2. Crossed nicols.

Some further heating experiments on natural titaniferous magnetites.

(With Plate III.)

By J. B. Wright, B.A., B.Sc., F.G.S.

Department of Geology and Mineralogy, University Museum, Oxford.[1]

[Read 6 November 1958.]

Summary. Samples of magnetite containing exsolution bodies of ilmenite, or of ulvöspinel and ilmenite, were heated at 1,250–1,300° C. under oxidizing and under reducing conditions.

In the former case, the product consisted of magnetite, ferri-ilmenite, and pseudobrookite. In the latter, loss of oxygen converted a magnetite–ilmenite intergrowth into a homogeneous Fe_3O_4–Fe_2TiO_4 spinel solid solution, while a magnetite sample originally carrying ulvöspinel in addition to ilmenite yielded a spinel phase with surprisingly low cell dimension, together with some metallic iron.

In a recent paper (Vincent, Wright, Chevallier, and Mathieu, 1947)[2] were described results of heating experiments, at temperatures up to 950° C., on a series of titaniferous magnetites, in which the over-all chemical compositions of the samples were unchanged after heat treatment. In the experiments briefly described here, the titaniferous magnetites were heated to between 1250° and 1300° C. One series of samples, heated in insufficiently degassed platinum sheaths sealed *in vacuo*, became oxidized; samples of another series, heated under continuous evacuation, or in argon at 1 atmosphere pressure, lost oxygen and were reduced. The results of these experiments, although not intentionally produced, are sufficiently interesting to merit brief description.

Two of the titaniferous magnetites investigated by Vincent *et al.* (1957) were used: E.G. 4359 and 4353, respectively magnetite–ilmenite and magnetite–ulvöspinel–ilmenite intergrowths. The changes in these minerals, produced by heating, were followed microscopically, chemically, and by X-rays. Quantitative data for unheated and three representative heated samples are given in table overleaf I, p. 34.

[1] Present address: Mines and Geological Department, P.O. Box 30009, Nairobi, Kenya.

[2] E. A. Vincent, J. B. Wright, R. Chevallier, and S. Mathieu, Min. Mag., 1957, vol. 31, p. 624 [M.A. 13–556].

Series 1. Oxidized samples. Microscopic examination of both samples after heating showed considerable coalescence and growth of the original very small ilmenite lamellae (pl. III, A, B, C), which had also become

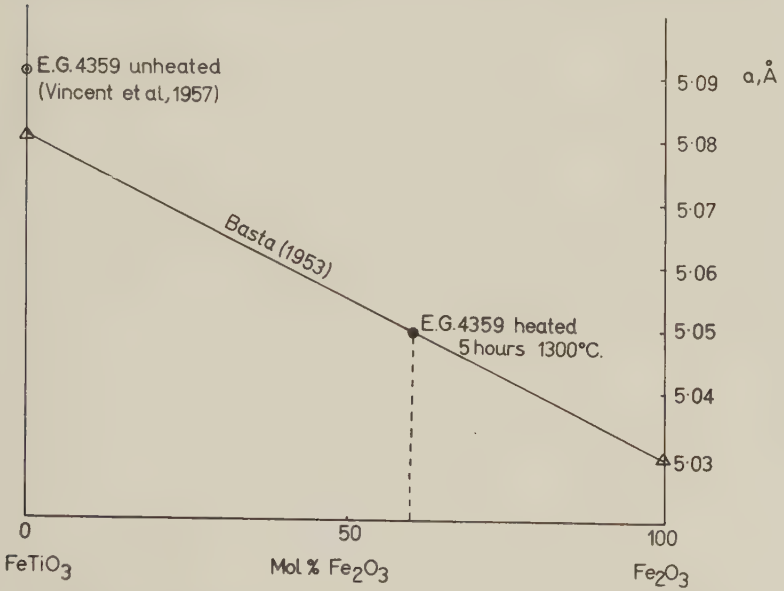

FIG. 1. Diagram showing approximate Fe_2O_3 content of rhombohedral phase in E.G. 4359, heated 5 hours, at 1300° C. under oxidizing conditions, as deduced from the *a* cell dimension (hexagonal axes).

much whiter in reflected light due to the intake of Fe_2O_3 (Vincent *et al.*, 1957): about 60 mol. % of Fe_2O_3 is indicated by the *a* cell dimension of the rhombohedral phase of the heated sample E.G. 4359 (fig. 1). Pseudobrookite is well developed in these oxidized samples (plate III, B and C) and can be identified in the X-ray powder patterns. It is probably developed from the rhombohedral $FeTiO_3$–Fe_2O_3 solid solution produced on heating, by the reaction:

$$FeTiO_3 + 2Fe_2O_3 \rightarrow Fe_2TiO_5 + Fe_3O_4.$$

In the previous series of heating experiments (Vincent *et al.*, 1957) it was shown that Fe_2O_3 can enter the rhombohedral phase of a heated magnetite-ilmenite intergrowth in appreciable amounts without over-all compositional changes occurring in the complex mineral. Heat treatment under oxidizing conditions has encouraged the formation and entry

of considerable amounts of Fe_2O_3 into the rhombohedral ilmenite phase, and also the formation of pseudobrookite.

A homogeneous titaniferous magnetite could probably never be produced by heating under neutral or oxidizing conditions, because Fe_2O_3 in an exsolved rhombohedral phase apparently cannot invert to the cubic γ-Fe_2O_3 form (Mason, 1943;[1] Vincent *et al.*, 1957). Under reducing conditions, however (series 2, below), a completely homogeneous cubic titaniferous magnetite can readily be produced.

Series 2. *Reduced samples.* Microscopic examination of E.G. 4359, after heating under reducing conditions, showed that the original magnetite–ilmenite intergrowth had become a uniform pale yellow in colour in reflected light (plate III, D); while X-ray and chemical data indicate that the sample has been reduced to an almost pure magnetite–ulvöspinel solid solution (table I).

TABLE I.

	E.G. 4359 unheated, Vincent et al., 1957	*E.G. 4359 heated 5 hrs., 1300° C. Series 1. Oxidation*	*E.G. 4359 heated 24 hrs., 1250° C. Series 2. Reduction*	*E.G. 4353 heated 24 hrs., 1250° C. Reduction*	*E.G. 4353 unheated, Vincent et al., 1957*
			Chemical data		
FeO	34·13	31·1 (det.)	43·5 (det.)	58·6 (det.)	39·8
MgO	1·84	assumed unchanged	assumed unchanged	assumed unchanged	0·9
MnO	0·37				0·4
CaO	0·49				0·7
Fe_2O_3	40·70	44·1 (calc.)	30·3 (calc.)	15·9 (calc.)	36·8
Al_2O_3	2·54	assumed unchanged	assumed unchanged	assumed unchanged	3·1
V_2O_3	1·52				2·1
Cr_2O_3	0·03				—
TiO_2	18·55				15·6
SiO_2	0·05				0·1
	100·22	100·6	99·2	97·4	99·5
			Calculated norms Very approximate		
	Approx.				*Approx.*
$MO.Fe_2O_3$ ...	58·2	57	44	22	53·5
$MO.R_2O_3$ ...	6·5	6	7	8	8·3
$2MO.TiO_2$ ...	2·5	—	44	44	26·3
$MO.TiO_2$ ...	32·8	31	5	—	11·8
$R_2O_3.TiO_2$ ...	—	6	—	—	—
Excess MO ...	—	—	—	26	—
	100·0	100	100	100	99·9
			X-ray data Powder films		
	Diffractometer				*Estimated*
Mag: *a*	8·40 Å.	8·40 Å.	8·44 Å.	8·39 Å.	*c.* 8·40 Å.
Ilm: *a*	5·09 Å.	*c.* 5·05 Å.	*c.* 5·08 Å. (weak lines)	no lines	*c.* 5·08/9 Å.

The mineral E.G. 4353, originally in a more reduced state than E.G.

[1] B. H. Mason, Geol. För. Förh., 1943, vol. 65, p. 97 [M.A. 9-32].

4359 (since it contains exsolved ulvöspinel, Pl. III, E), has been further reduced to such an extent that metallic iron has separated and the colour of the remaining spinel phase is dark brown, similar to that of pure ulvöspinel (pl. III, F).

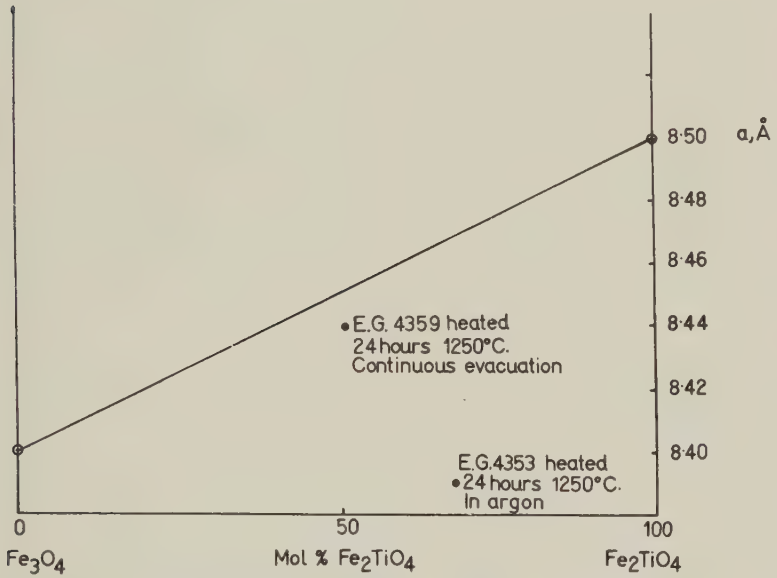

FIG. 2. Diagram illustrating variation in cell-dimension with approximate estimated compositions of spinel phases, in reduced titaniferous magnetite samples. It is very unlikely that E.G. 4353, after heating, is a normal magnetite–ulvöspinel solid solution.

In fig. 2 are plotted values of the spinel cell-dimensions for the reduced samples of E.G. 4359 and 4353, against their approximate normative compositions in terms of ulvöspinel and magnetite. The point representing E.G. 4359 lies close to the Végard line joining the end members, but the point for E.G. 4353 lies well below it; i.e. the cell-dimension of the spinel phase is far too small for a material which both chemical and optical data indicate as being very rich in ulvöspinel.

The spinel phase in this reduced sample of E.G. 4353 thus appears not to be a normal solid solution of magnetite and ulvöspinel. It may be a transitional stage between cubic ulvöspinel and the orthorhombic series Fe_2TiO_5 $FeTi_2O_5$, recently synthesized by Akimoto *et al.* (1957).[1] The

[1] S. Akimoto, T. Nagata, and T. Katsura, Nature, 1957, vol. 179, p. 37.

$FeTi_2O_5$ member of this series might be produced together with metallic iron from ulvöspinel by the reaction:

$$2Fe_2TiO_4 \rightarrow 3FeO + FeTi_2O_5$$
$$\downarrow$$
$$3Fe + 3O\uparrow$$

Mason (1943) showed that a gradual increase in cubic cell-dimension occurred in the solid-solution series Fe_3O_4–Mn_3O_4, before a symmetry change from cubic Fe_3O_4, with a unit-cell volume of 592 Å^3., to tetragonal Mn_3O_4, with a unit-cell volume of 617 Å^3. For the reduced spinel phase of E.G. 4353, therefore, a reduction in cell-dimension might perhaps be expected if it were prior to a symmetry change from cubic ulvöspinel, with a unit-cell volume of 613 Å^3., to orthorhombic $FeTi_2O_5$, with the smaller unit-cell volume of 368 Å^3.

Finally, it is of interest to note that, in contrast to grains of the separated mineral, the magnetite–ilmenite intergrowths in a whole rock chip of E.G. 4359, sealed *in vacuo*, became completely homogeneous after heating to only 940° C., and are very similar, microscopically, to the titaniferous magnetite grains separated from this rock and heated at higher temperatures under reducing conditions.

Previous workers (Ramdohr, 1926;[1] Kamiyama, 1929;[2] Wilson, 1953;[3] Supriya Roy, 1955[4]) have reported homogenization of magnetite–ilmenite intergrowths in heated rock samples. The experiments discussed here strongly suggest that such homogenization can only have occurred because reducing conditions were brought about by volatile substances released from the rock during heating. This process was originally suggested by Ramdohr (1926), as one of the possible explanations for his experimental results; but hitherto there has been no further experimental data to confirm his suggestion.

Explanation of Plate III.

Photomicrographs of titaniferous magnetites before and after heat treatment.

A. E.G. 4359, Middle Gabbro, Skaergaard Intrusion, E. Greenland. Magnetite carrying an exceedingly fine network of ilmenite lamellae arranged parallel to {111} and some much broader ilmenite lamellae with which are associated granules of a transparent spinel (black in photograph). Note the development of larger ilmenite

[1] P. Ramdohr, Neues Jahrb. Min., Abt. A, 1926, Beil.-Bd. 54, p. 320.

[2] M. Kamiyama, Journ. Geol. Soc. Tokyo, 1929, vol. 36, p. 12.

[3] H. D. B. Wilson, Econ. Geol., 1953, vol. 48, p. 370.

[4] S. Roy, Proc. Nat. Inst. Sci. India, 1954, vol. 20, p. 691; ibid. 1955, vol. 21, B, p. 222.

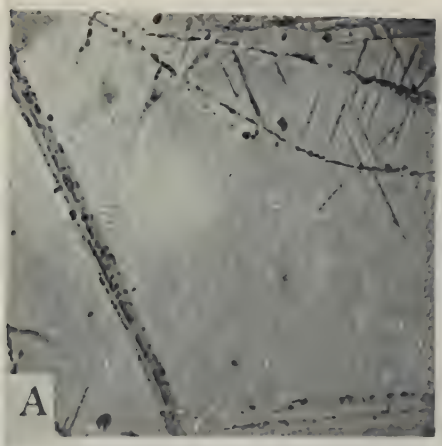
A

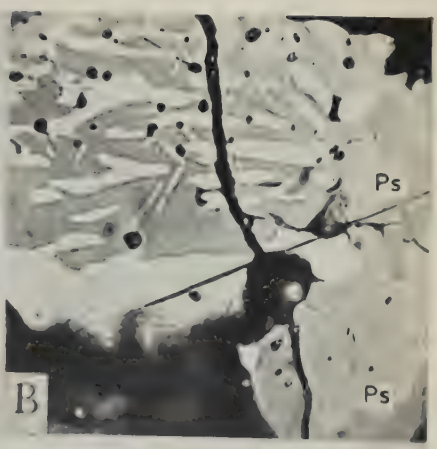
Ps
Ps
B

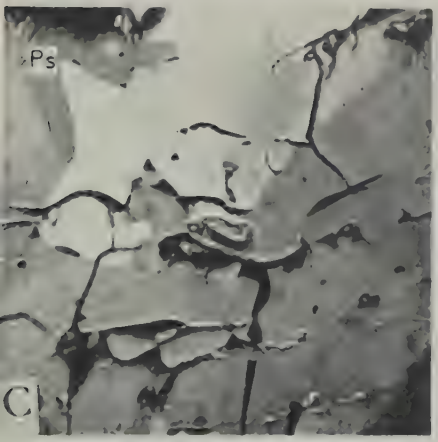
Ps
C

D

E

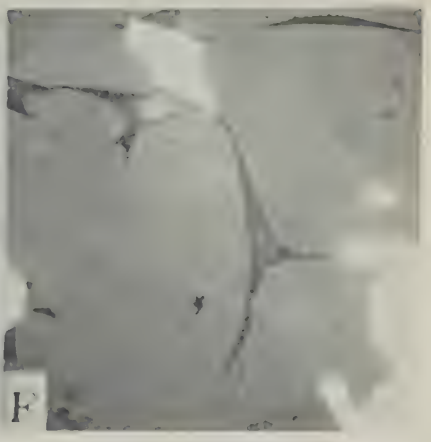
F

lamellae on either side of veinlets at the top of the photograph. Reflected light, oil immersion, ×410.

B. E.G. 4359, Separated titaniferous magnetite grains heated 5 hours at *c.* 1300° C. under oxidizing conditions. The ilmenite has taken Fe_2O_3 into solid solution and has coalesced into large lamellae and irregular masses (white in photograph). Pseudobrookite (Ps) is seen as darker irregular areas in the spinel phase. Reflected light, oil immersion, ×410.

C. E.G. 4359, Separated titaniferous magnetite grains heated at *c.* 1300° C. under oxidizing conditions. The process shown in fig. B has continued further, the ferri-ilmenite (white) now forming large irregular masses covering several sintered grains. (Irregular curved cracks are former grain boundaries; darker grey areas, Ps, are pseudobrookite.) Reflected light, oil immersion, ×410.

D. E.G. 4359, Separated titaniferous magnetite grains heated for 24 hours at 1250° C. under continuous evacuation, causing loss of oxygen. Completely homogenized, rounded and sintered spinel grains bordered by a fine network of (?) titanomagnetite and transparent material. Reflected light, oil immersion, ×410.

E. E.G. 4353, Middle Gabbro, Skaergaard Intrusion, E. Greenland. Magnetite carrying ilmenite lamellae with which are associated (black) granules of transparent spinel. A further set of very much finer exsolution bodies —partly ilmenite, partly ulvöspinel—is seen in the spaces between the larger ilmenite lamellae. Reflected light, oil immersion, ×410.

F. E.G. 4353, Separated titaniferous magnetite grains heated for 24 hours at 1250° C. in argon at 1 atmosphere pressure. Loss of oxygen has reduced the sample to a homogeneous dark brown spinel in sintered grains cemented by a fine-grained lamellar mass of transparent material. Note also the development of metallic iron (white in photograph). Reflected light, oil immersion, ×410.

Residual hydroxyl groups in the metakaolin range.[1]

By V. Stubičan, Ph.D., Dipl.Ing.

Institute for Silicate Chemistry, Zagreb, Yugoslavia.

[Taken as read 29 January 1959.]

Summary. Infra-red absorption spectroscopy has been used to study the retention of hydroxyl groups by kaolinite and halloysite after heat treatment in the range 600° C. to 850° C. Structurally disordered specimens initially lose water more rapidly than do ordered specimens, but retain hydroxyl groups at higher temperatures. Work on the phases obtained above 1100° C. is incomplete, but results for the lower temperatures indicate that the ordered structures tend to retain their atomic arrangement and form metakaolin, whereas disordered structures readily rearrange to yield γ-alumina, to the formation of which water is probably essential.

A NUMBER of investigators have studied the products obtained by the heating of kaolinite and kaolin minerals. In their investigations they have used the samples obtained either by a comparatively quick heating of minerals up to a given temperature followed by air-quenching or by a more prolonged heating at a determined temperature. In the first case data are obtained on phases which may often be intermediate and subject to changes by longer heating, whereas in the second case a picture of more stable phases is brought out. However, to obtain a better insight into the nature of the processes going on in the course of the heating of minerals, the use of both methods is needed in most cases.

In the attempt to explain the nature and the structure of the heating products of kaolinite and kaolin clays, one is faced with two fundamental problems: the problem of the existence of metakaolinite, i.e. the problem of the structure of the products of dehydroxylation in the temperature range from about 600° C. to 850° C., and the problem of the formation of γ-alumina and mullite in the temperature range above 950° C.

Insley and Ewell (1933) dealt with both problems in an extensive form, but the development of new experimental methods has made it possible to obtain a more detailed knowledge of the nature of the phases occurring in the course of heating.

[1] Extracted from a thesis submitted to the University of Zagreb for a title of Assistant Professor.

Recently Brindley and Hunter (1955), investigating X-ray rotation diagrams of samples of heated nacrite, have given direct experimental evidence of the residual structural regularity maintained by the Si–O hexagonal network in the metakaolinite range.

At the same time, but quite independently, Roy, Roy, and Francis (1955) have succeeded in demonstrating by single-crystal electron diffraction data that in the metakaolin range dehydroxylated kaolinite maintains a two-dimensional (a–b) plane structure very similar to that of kaolinite, whereas in halloysite and hydrothermal kaolinite γ-alumina can already be observed at 650° C. after a prolonged heating of primary substances (12 to 200 hours).

In spite of such considerable advances, we thought it worthwhile to supplement these results with a further study of the heating products of kaolin minerals by means of infra-red spectroscopy, on the assumption that this may be a more direct approach to the understanding of the mechanism of dehydroxylation.

Experimental data.

The samples studied were a well-ordered kaolinite (Skočaj, Croatia; different fractions), a poorly crystallized kaolinite showing a random displacement of layers by multiples of $b/3$, and a halloysite (Gradešnica, Macedonia).

The samples of the well-crystallized kaolinite and the halloysite were first purified by sedimentation and then their purity and the degree of crystallinity were determined by X-ray diffraction. The sample of the poorly crystallized kaolinite was prepared hydrothermally, by a method of Saalfeld (1955), from a well-crystallized kaolinite previously heated at 700° C. for an hour. Rehydration was performed in a pressure bomb at 300° C., 100 atm., in 30 hours. The X-ray diagram of the same sample showed fewer reflections than that of a well-crystallized kaolinite; in fact, it was very similar to the X-ray diagram of a fireclay mineral.

To enhance the reliability of the results, parallel experiments were carried out with the purified Zettlitz kaolin and the kaolin from Dry Branch, Georgia, as well as with halloysite from Djebel Debar. The results obtained with these samples were the same as those obtained with the well-crystallized kaolinite from Skočaj and the halloysite from Gradešnica.

It is a well-known fact that on the average the particles of hydrothermal kaolinite and metahalloysite are smaller in size than those of a well-crystallized kaolinite, and in the interpretation of the results the

effect of this factor should be taken into account. In view of this, two fractions were separated from the sample of the well-crystallized kaolinite from Skočaj: one with the platelets larger than *c.* 0·6 μ in the direction of the longer axis, and the other with the platelets smaller than

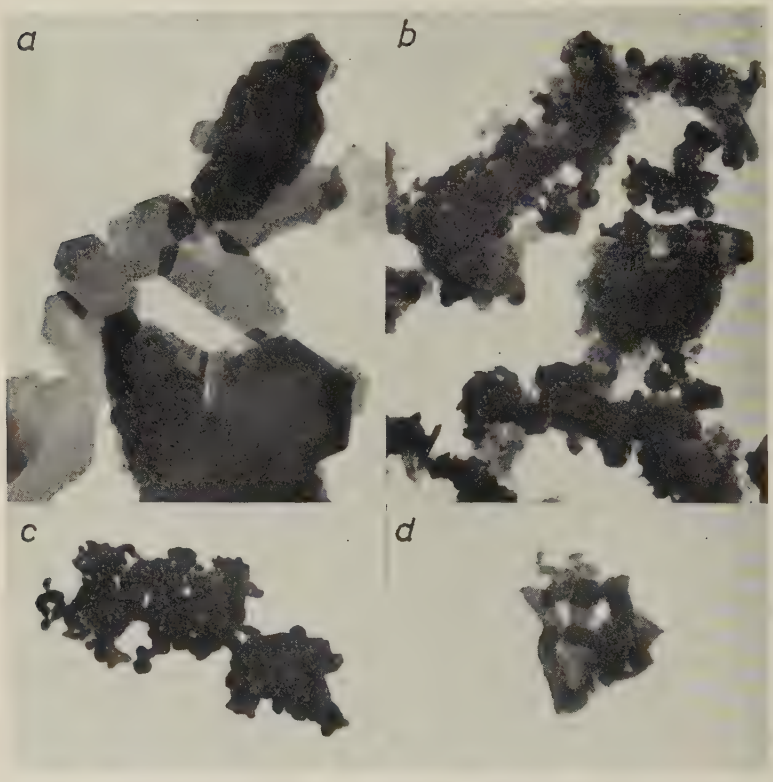

FIG. 1. Electron micrographs: (*a*) a well-crystallized kaolinite, particles larger than 0·6 μ; (*b*) a well-crystallized kaolinite, particles smaller than 0·15 μ; (*c*) a hydrothermal kaolinite; (*d*) a halloysite. All the samples heated at 650° C.

c. 0·15 μ. The platelets of the hydrothermal kaolinite were smaller than *c.* 0·2 μ, while the size of the primary metahalloysite particles was below *c.* 0·3 μ. The electron micrographs are reproduced in fig. 1.

The characteristic temperature ranges of thermal reactions in the minerals examined were determined by differential thermal analysis in a very sensitive apparatus described by Preining and Schedling (1953) (fig. 2).

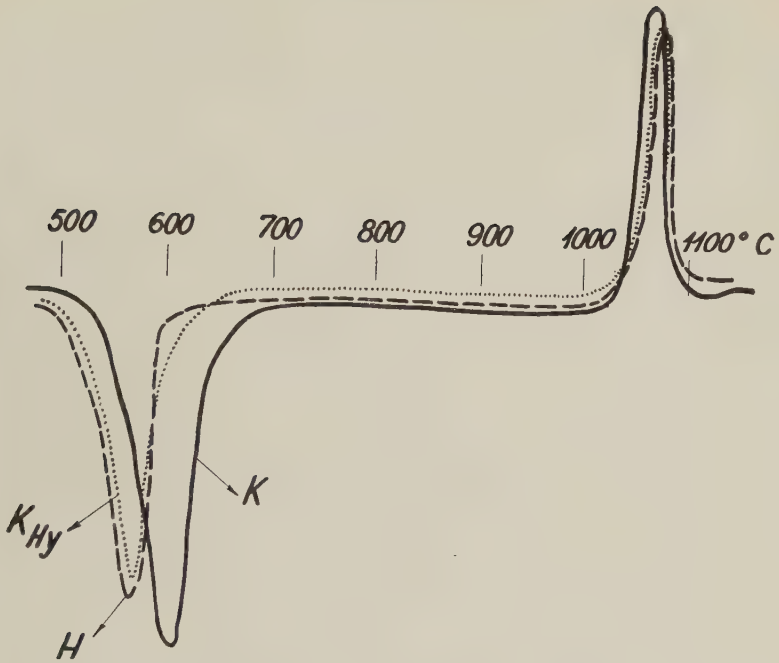

Fig. 2. Differential thermal curves: (K) a well-crystallized kaolinite; (K_{hy}) a hydrothermal kaolinite; (H) a halloysite. Rate of heating 10°/min. Ni-CrNi.

For the preparation of infra-red spectra the samples were for the most part heated in a differential thermal apparatus, air quenched, and mulled after weighing in high-boiling paraffin ('Nujol') or hexachlorbutadiene. Infra-red spectra were obtained on a Perkin-Elmer Model 21 spectrometer.

The infra-red spectrum of the well-ordered kaolinite (fig. 3 A) shows an absorption band at 2·72 μ, which belongs to the hydroxyl groups in the structure; absorption bands between 8 and 10 μ are likely to belong to the Si–O linkage, while the octahedral alumina sheet gives the absorption band between 10 and 11 μ (Adler *et al.*, 1950; Hunt, Wisherd, and Bonham, 1950; Keller and Pickett, 1950). The absorption bands at 3·4, 6·8, and 7·2 μ belong to 'Nujol'. The infra-red spectrum of halloysite (fig. 3 B) differs from that of kaolinite in that it shows an additional absorption band at 2·9 μ suggesting the presence of interlayer water molecules. Other minor differences in the spectra of kaolinite and halloysite in the range of 8 to 14 μ are not very clear.

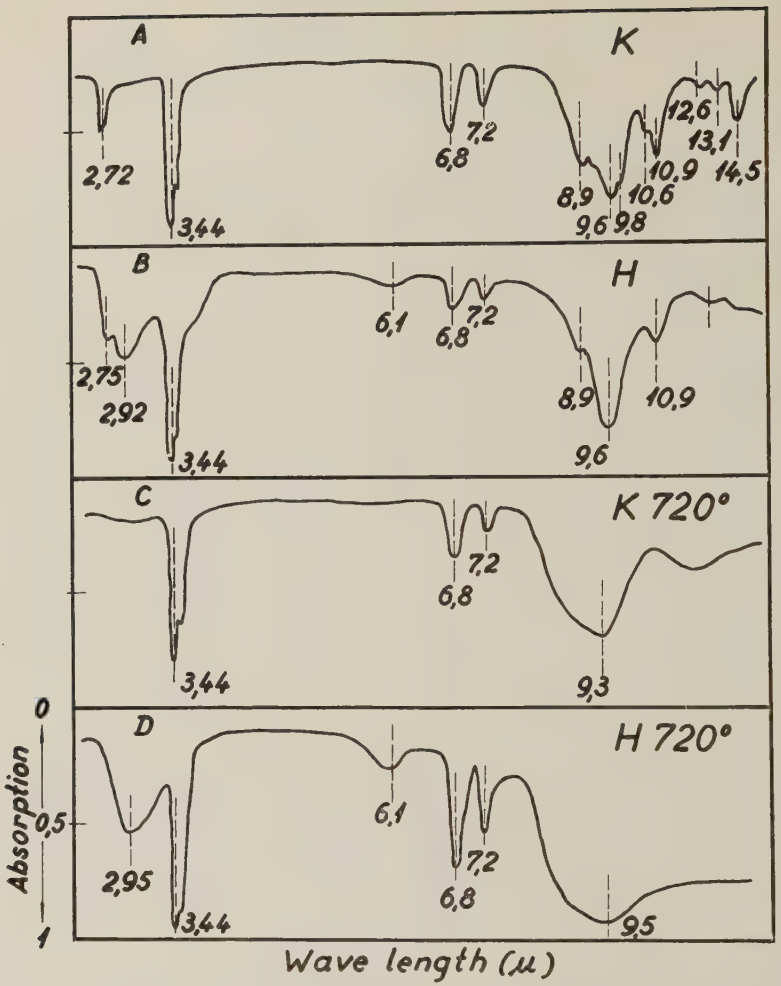

Fig. 3. Infra-red spectra in 'Nujol': (A) a well-crystallized kaolinite; (B) a halloysite; (C) a well-crystallized kaolinite heated up to 720° C.; (D) a halloysite heated up to 720° C.

Heating at 720° C. results in several important changes in the absorption spectra of the well-crystallized kaolinite and halloysite over the spectral range of hydroxyl groups from 2·3 to 4 μ, as well as in the range above 11 μ (fig. 3 C and D). The samples of the well-crystallized kaolinite no longer show the absorption band at 2·72 μ, indicating the

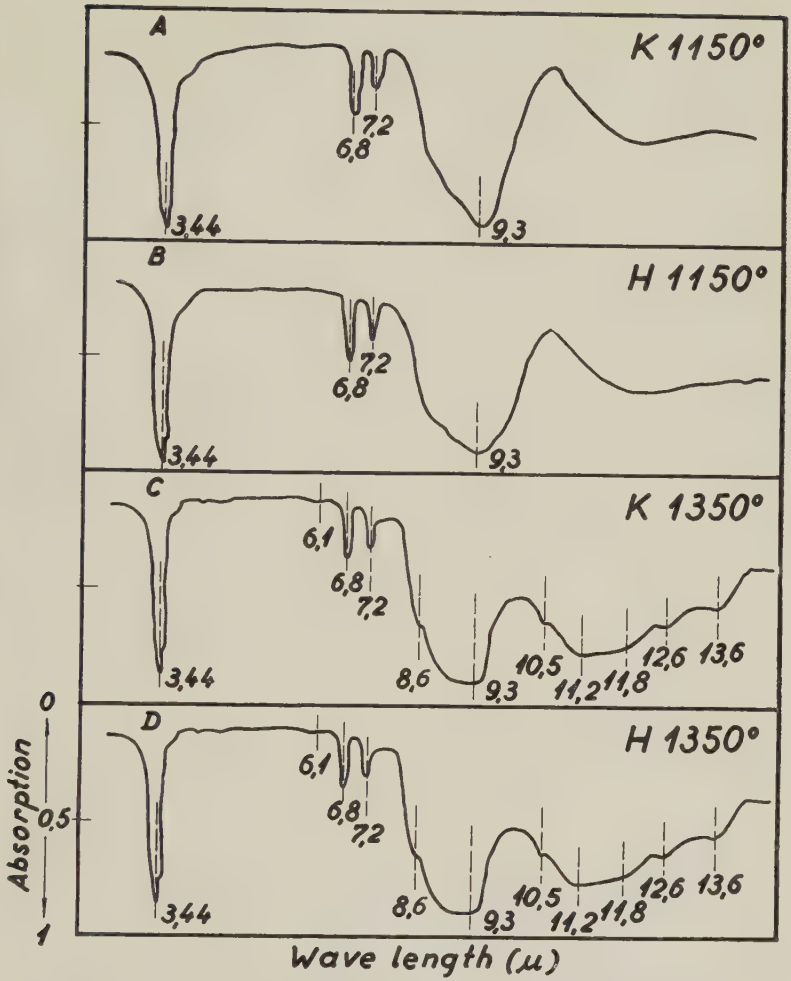

FIG. 4. Infra-red spectra in 'Nujol': (A) a well-crystallized kaolinite heated up to 1150° C.; (B) a halloysite heated up to 1150° C.; (C) a well-crystallized kaolinite heated at 1350° C. for 3 hours; (D) a halloysite heated at 1350° C. for 3 hours.

absence of hydroxyl groups; absorption bands between 8 and 10 μ are replaced by a wider band with a maximum at 9·3 μ, while the absorption band at 10·9 μ has completely disappeared, suggesting a dislocation of the octahedral sheet. By more quantitative work with spectra corrected for background absorption it can be shown that the absorption

band with a maximum at 9·3 μ is of lower intensity and narrower than that produced by a coprecipitated alumina–silica gel of the same composition heated at the same temperature. This suggests a greater order in the Si–O linkage in metakaolinite.

Halloysite heated at 720° C. shows a wide absorption band in the absorption range of hydroxyl groups with a maximum at 2·95 μ, as well as an absorption band at 6·1 μ corresponding to adsorbed molecules of water. The absorption spectrum reveals also a very strong absorption in the range above 11 μ. It might be assumed that this absorption is due to some aggregation of particles brought about by heating. However, if the samples are reground and fractionated after heating, and the secondary particles smaller than 2 μ are photographed, a high absorption in this spectral range is observed again. The samples of kaolinite and halloysite heated at 1150° C. give absorption maxima only at 9·3 μ (fig. 4 A and B). However, if heated at 1350° C. for 3 hours, they show a more complicated spectrum with maxima at 8·6, 9·3, 10·5, 11·2, 11·8, 12·6, and 13·65 μ (fig. 4 C and D).

Further study was concentrated on the explanation of the occurrence of an absorption band between 2·5 and 3·5 μ in the samples of halloysite heated in the temperature range 680°–800° C., and on the investigation of the products obtained by heating in the temperature range above 1150° C.

Fig. 5 shows a wide absorption band in the absorption range of hydroxyl groups of the halloysite samples heated above the endothermic maximum. The intensity of this band depends on the relative humidity of the air. The samples heated at temperatures between 800 and 1000° C. do not show this band any longer.

These preliminary results have shown that the properties of the heating products of a well-crystallized kaolinite and halloysite in the temperature range 650° C.–800° C. are different. This led us to the assumption that the mechanism of dehydration of these minerals might be different as well. Since the primary structures of metahalloysite and kaolinite are similar with regard to the structure of layers, the differences obtained by heating may be understood either as a result of the different degree of crystallinity or as an effect of the particle size of the primary substances.

Further investigations have, therefore, been carried out with the samples whose electron micrographs are shown in fig. 1. Care was taken that the heated samples should be protected from humidity as much as possible. The samples were heated in Pyrex tubes in a very thin

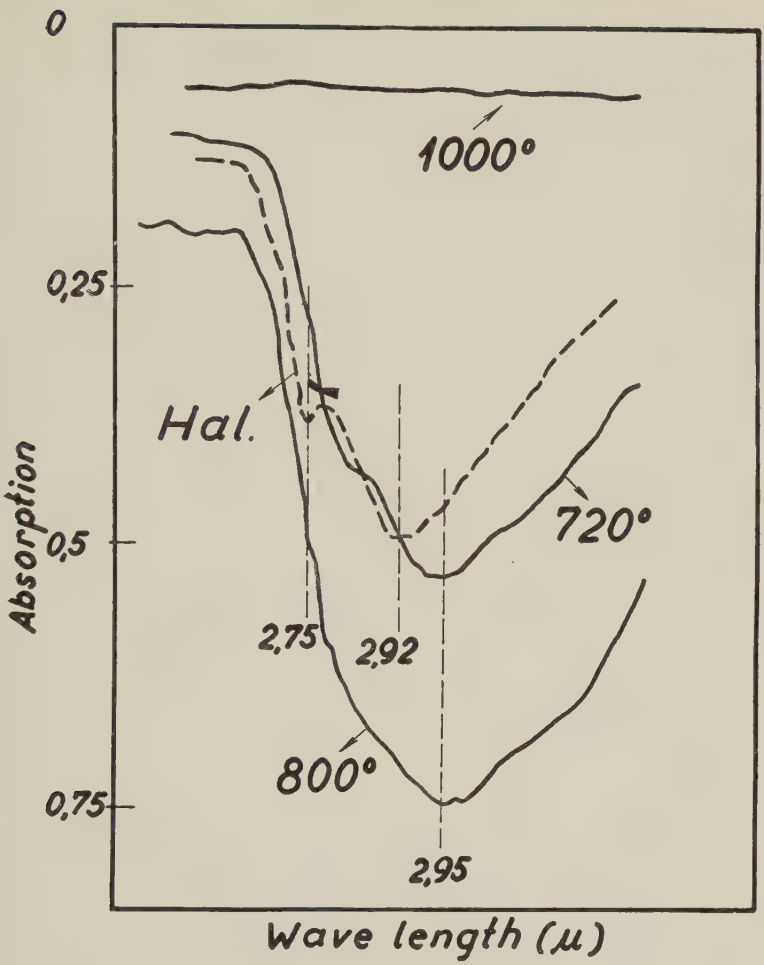

FIG. 5. Absorption of the samples of halloysite heated up to 720°, 800°, and 1000° C. in the range of hydroxyl groups. Rate of heating 10°/min. 'Nujol.'

uncompacted layer. The tubes were sealed as soon as the proper temperature was obtained. After cooling, the tubes were broken and the samples immediately mixed with 'Nujol' or hexachlorbutadiene. In another case, the heated samples were cooled and dried in a vacuum. The best resolution of the absorption bands was obtained when the first procedure was applied.

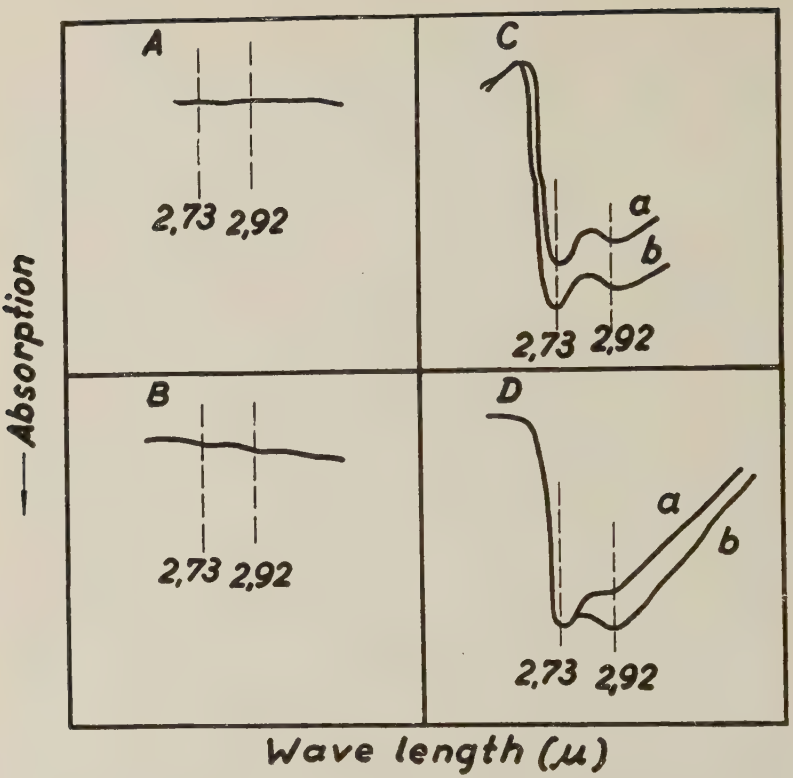

FIG. 6. Absorption in the range of hydroxyl groups: (A) a well-crystallized kaolinite heated up to 680° C., particles larger than 0·6 μ, 'Nujol'; (B) a well-crystallized kaolinite heated up to 680° C., particles smaller than *c.* 0·15 μ, 'Nujol'; (C) a hydrothermal kaolinite heated up to 680° C. (*b*) and 720° C. (*a*), 'Nujol'; (D) a halloysite heated up to 680° C. (*b*) and 720° C. (*a*), hexachlorbutadiene. Rate of heating 10°/min.

The samples of the well-crystallized kaolinite heated at the temperature immediately above the endothermic peak no longer show absorption in the range of hydroxyl groups, the dehydroxylation being complete regardless of the size of platelets (above 0·6 μ or below 0·5 μ) (fig. 6 A and B). But the samples of hydrothermal kaolinite and halloysite heated in the same temperature range and protected from humidity show in the range of hydroxyl groups two absorption bands with maxima at 2·73 μ and 2·92 μ (fig. 6 B and C), one hardly noticeable band at 6·1 μ, and one pronounced absorption band in the range above 11 μ.

It is interesting to note that the presence of hydroxyl groups is

observed in samples of hydrothermal kaolinite heated at 650° C. for an even longer time (3 or 8 hours), while dehydroxylation is complete if heating is performed at 750° C. (heating velocity 10° per minute). With halloysite, dehydroxylation is complete after about a 10-minute heating at 750° C. (fig. 7).

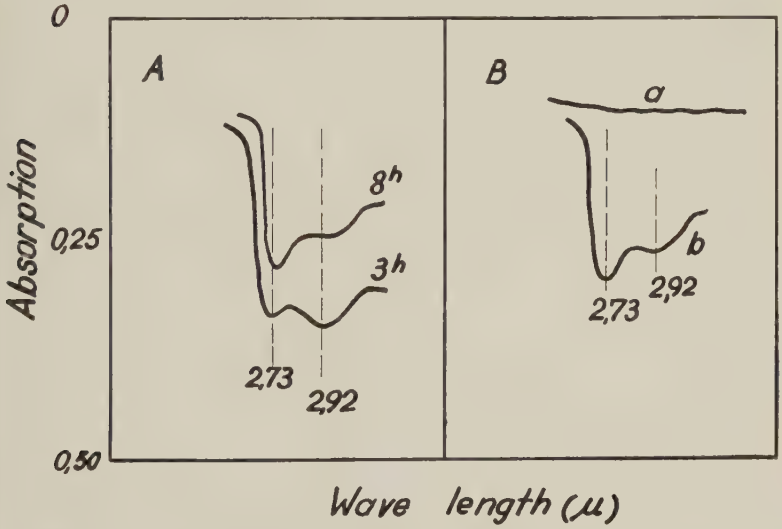

Fig. 7. Absorption in the range of hydroxyl groups: (A) a hydrothermal kaolinite heated at 650° C. for 3 and 8 hours respectively; (B) a hydrothermal kaolinite (*a*) and a halloysite (*b*) heated up to 750° C. Rate of heating 10°/min. 'Nujol.'

No doubt the band at 2·73 μ belongs to free hydroxyl groups most probably present in the structure of the phases occurring in the course of heating. The absorption band at 2·92 μ may be partly but not entirely assigned to adsorbed water. The difficulties in interpreting these bands have already been pointed out by Roy, Roy, and Francis (1957). According to Glemser (1957), in the heating products of hydroxides (aluminium, iron, &c.) the same band can be split into two bands: one supposed to correspond to the free and the other to the bound hydroxyl groups. It is very likely that this band is of a very complex nature.

The further problem relates to the nature of the absorption maxima in the samples heated up to 1350° C. Since in this temperature range a part of the silica remains free, heated samples were treated with 40 % HF

for 4 hours at 0° C. (Konopicky, Hopmann, and Kampa, 1956). Infrared spectra of these samples show maxima at 8·55 μ and 8·66 μ respectively, and at 8·96, 9·25, 10·5, 11·2, and 13·6 μ (fig. 8).

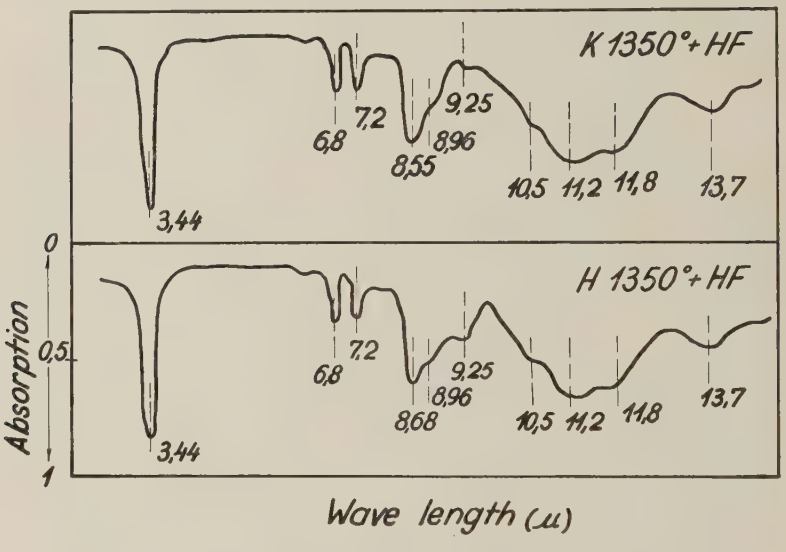

Fig. 8. Absorption spectra of samples of kaolinite and halloysite heated at 1350° C. for 3 hours and treated with hydrofluoric acid. 'Nujol.'

Discussion.

At first sight the results of these experiments may seem incompatible with the fact that structurally disordered kaolin minerals decompose by heating more quickly than well-crystallized kaolinite. This relates to the velocity of dehydroxylation. Kinetic investigations carried out by Murray and White (1955) have given evidence that in some clays of the kaolin type and in halloysite dehydroxylation follows only approximately the first order kinetics, and that there is a certain retardation in the velocity of dehydroxylation after *c.* 90 % of the water produced by the reaction of hydroxyl groups has left the structural network. The same problem has recently been treated by Brindley and Nakahira (1957) when observing isothermally the velocity of dehydroxylation on compact specimens of different thicknesses. The reaction rate constants at various temperatures depend on the size, shape, and compactness of the specimen. If the extrapolation is performed to an infinitely thin disk, the reactions strictly follow the first order kinetics. According to

these authors, the retention of water vapour within the specimen and the retardation of the process of dehydroxylation are considerably influenced by geometrical factors.

The results obtained in the study of infra-red spectra show distinct differences in the mechanism of dehydroxylation of kaolin minerals, which are determined by the crystal order of the primary minerals. The same differences may be observed in the samples heated in a very thin layer of uncompacted powder. A well-crystallized kaolinite heated immediately above the endothermal peak no longer shows the presence of hydroxyl groups, while structurally disordered kaolin minerals show two absorption bands in the range of hydroxyl groups (2·72 μ and 2·92 μ).[1] Pronounced differences can also be observed in the properties of the phases obtained above the endothermal peak. The question arises: what brings about these differences, and how do they relate to the nature of the dehydroxylated products?

Johns (1953) discussed the problem of the occurrence of new phases in the process of heating kaolin minerals in relation to structural disorders. A well-crystallized kaolin heated at 1000° C. shows mullite and γ-alumina interferences, while at that temperature with structurally disordered kaolin only γ-alumina can be observed. However, this only relates to the samples heated at the temperature mentioned for a short time. According to Glass (1954), the crystal order of the primary material and the impurities determine the quantitative relations of the phases near the exothermic maximum. Thus, for instance, the amount of mullite near the exothermic peak decreases as the structure becomes more random, and with halloysite smaller dimensions of layers bring about a poor development of mullite nuclei, so that the X-ray diagrams of the samples heated near the exothermic maximum show γ-alumina as the only crystallized phase. Experimental methods used by these authors were not appropriate to give more decisive evidence with regard to the properties of the phases occurring immediately after the endothermal peak.

The present-day knowledge of the phases in the metakaolinite range has considerably advanced, offering strong evidence that a well-crystallized kaolinite heated in the temperature range 650° to 850° C. retains a certain crystal order, while in halloysite a more pronounced decomposition of the network is observed, as well as the formation of γ-alumina by longer heating (Roy, Roy, and Francis, 1955).

[1] G. Kulbicki and R. E. Grim (this issue, p. 53) have also adduced direct evidence of the retention of water in metakaolin.

The question may now be raised, in what relation these results stand to the properties of the heating products of kaolin minerals heated in the metakaolinite range under non-equilibrium conditions for a short time. Particularly interesting is the retention of hydroxyl groups above the endothermic peak, not being dependent on the size of particles but only on the structural order of primary minerals.

No doubt there is a considerable effect of water vapour pressure on the velocity of dehydroxylation. According to Karšulin (1956), this pressure may be high owing to the presence of water vapour produced in the process of dehydroxylation (hydrothermal conditions). The same author assumes that the mechanisms of dehydroxylation in kaolinite and halloysite are identical, since amorphous silica and a compound of the $5Al_2O_3.H_2O$ type are obtained in the process of dehydroxylation. According to Karšulin, the difference in the behaviour of inner and outer hydroxyls plays an important part in the mechanism of dehydroxylation.

In fact, Houben and de Boer (1952) have shown that the presence of a certain amount of water is probably essential to the existence of γ-alumina. According to this idea, in the spinel structure the aluminium ions should be found in octahedral and tetrahedral configuration, the hydrogen ions only in octahedral configuration. Consequently, the optimum structure of such γ-alumina would correspond to the formula HAl_5O_8. Besides the hydroxyl groups in its structure, such γ-alumina may also, under certain conditions (the effect of water vapour pressure, heating time), contain hydroxyl groups on the surface, and adsorb water molecules.

This interpretation of the phases produced by the thermal decomposition of aluminium hydroxide is supported by the infra-red absorption spectra, i.e. by a wide absorption band in the range of hydroxyl groups and the absence of the absorption band at 6·1 (Glemser and Rieck, 1956). Moreover, the small nuclei of aluminium oxide show an intense absorption in the range above 11 μ. This absorption also seems to be characteristic of very thin aluminium oxide films (250 Å.) obtained by anodizing aluminium foil (Harris, 1955).

It would be difficult to explain the results of our experiments if the properties of the phases occurring in the process of dehydroxylation of kaolin minerals were not taken into account. As has already been said, structurally disordered kaolin minerals obtained in the temperature range 650°–800° C. by even a short heating show some characteristics of mixed phases, i.e. the characteristics of amorphous silica and small crystal nuclei of active γ-alumina.

In a well-crystallized kaolinite dehydroxylation is complete after the endothermic peak, the residual structure of the primary material no longer containing hydroxyl groups. The Al–O groups remain in the monolayer, while the Si–O hexagonal network prevents the nucleation of γ-alumina. So far it has not been possible to determine either the structure of the dehydrated gibbsite sheets or the relation between these sheets and the Si–O hexagonal network, but a strong charge deficiency of the metakaolinite phase has been proved by the adsorption of colloidal gold on the (001) faces of dehydroxylated platelets (Stubičan and Wrischer, 1958).

It seems very likely that in disordered kaolinite minerals the process of dehydroxylation is connected with the more complete destruction of the crystal lattice by even a short heating. The gibbsite sheet produces small nuclei of active γ-alumina, which contain a certain number of hydroxyl groups and can adsorb water molecules on their surface. The properties of these nuclei depend on the duration of heating, on temperature, and on the presence of water vapour. A greater movability of the Si–O complex from the hexagonal network in the structurally disordered kaolin minerals is most probably connected with a weaker bond between successive layers.

Our experiments have offered no evidence in favour of the assumption that the so-called inner and outer hydroxyl groups behave differently in the process of dehydroxylation.

As regards the identification of the heating products above the endothermic peak by their infra-red absorption spectra, the problem is far more complex, and requires further investigation. The heating products of kaolinite and halloysite obtained by short heating in the temperature range 1100°–1350° C. only show a maximum absorption at 9·3 μ, which does not appear to contradict the assumption that mullite is formed in this range. However, the absorption maxima observed in the products obtained by longer heating at 1350° C. (fig. 4) led us to the idea of making spectra of the same samples treated with hydrofluoric acid. The absorption spectra of these samples were not typical of mullite, neither did they show all the maxima of sillimanite (Roy and Francis, 1953).

Acknowledgements. The author thanks Prof. Dr. D. Hadži for his help in the preparation of spectra and for many stimulating discussions. Thanks are also due to Miss M. Wrischer, of the Institute 'Rudjer Bošković', for her work on electron micrographs.

References.

Adler (H.), 1950. Amer. Petroleum Inst. Project, vol. 49, p. 1.
Brindley (G. W.) and Hunter (K.), 1955. Min. Mag., vol. 30, p. 182.

Brindley (G. W.) and Nakahira (M.), 1957. Journ. Amer. Ceram. Soc., vol. 40, p. 346.

Glemser (O.) and Rieck (G.), 1956. Angew. Chem., vol. 68, p. 182.

—— 1957. Trans. XVI Intern. Cong. Pure & Appl. Chem. Paris, vol. I, p. 52 (abstract).

Harris (L.), 1955. Journ. Opt. Soc. Amer., vol. 45, p. 27.

Houben (G. M.) and de Boer (J. H.), 1952. Trans. Intern. Ceram. Congr.: 3rd Congr., Paris, p. 77.

Hunt (M.), Wisherd (M. P.), and Bonham (L. C.), 1950. Anal. Chem., vol. 22, p. 1478.

Insley (H.) and Ewell (R. H.), 1935. Journ. Res. Nat. Bur. Stand., vol. 14, p. 615.

Karšulin (M.), 1956. Dachema Monograph, vol. 27, p. 91.

Keller (D. W.) and Pickett (E. E.), 1950. Amer. Journ. Sci., vol. 248, p. 264.

Konopicky (K.), Hofmann (U.), and Kampa (P.), 1956. Ber. deutsch. keram. Gesell., vol. 33, p. 52.

Murray (P.) and White (J.), 1955. Trans. Brit. Ceram. Soc., vol. 54, p. 137.

Preining (O.), Schedling (J. A.), and Wein (J. B.), 1953. Acta Phys. Austriaca, vol. 8, p. 89.

Roy (Rustum) and Francis (E. E.), 1953. Amer. Min., vol. 38, p. 725.

——, Roy (D. M.), and Francis (E. E.), 1955. Journ. Amer. Ceram. Soc., vol. 30, p. 198.

Roy (D. M.) and Roy (Rustum), 1957. Geochimica Acta, vol. 11, p. 72.

Saalfeld (H.), 1955. Ber. deutsch. keram. Gesell., vol. 52, p. 150.

Stubičan (V.) and Wrischer (M.), 1958. Kolloid Zeits., in press.

A new method for thermal dehydration studies of clay minerals.

By Georges Kulbicki,[1] D.Sc., and Ralph E. Grim, Ph.D.

Department of Geology, University of Illinois, Urbana, Illinois.

[Taken as read 29 January 1959.]

Summary. The water vapour released upon heating the specimen is driven through a water absorber. The intensity of the exothermic reaction produced by absorption of the water is recorded against the temperature of the specimen. A series of curves obtained with various clay minerals are presented to illustrate the method. The significance of results in the identification of the clay minerals and the determination of their structure is considered.

THE present equipment originated in a search for a sensitive procedure able to detect the possible release of small amounts of water by clay minerals above 800° C. For example, it was desired to verify whether any water-loss is connected with the endothermic reaction of montmorillonites around 900° C., and whether the slight endothermic feature sometimes preceding the exothermic reaction of kaolinites at about 950° C. is accompanied by any dehydration. The curves obtained by thermogravimetric and differential-thermal methods do not provide completely convincing information on these matters, and it was thought that a more sensitive procedure might be helpful. Also it was desired to study the rate of evolution of water vapour versus temperature.

Apparatus and method. The principle of the new method is as follows: The water vapour evolved from the specimen is carried by a flow of nitrogen, previously dried, through a water absorber; the absorption of water causes an exothermic reaction, which causes a slight increase in the temperature of the carrying gas, which is detected by means of a differential thermocouple and recorded as a function of the temperature of the specimen.

Details of the apparatus are shown in fig. 1. The furnace is made of a tube of Vycor glass, 40 cm. long and 12 mm. inside diameter. Five feet of Nichrome wire, of 0·02 in. diameter, is wound in a double layer around the central part of the tube with a sheet of asbestos for insulation. The ends of the tube remain cool so that rubber stoppers can be used. The

[1] On leave from the University of Toulouse, Toulouse, France.

applied voltage is automatically raised by a 'Variac' transformer driven by an electric motor through a speed reducer; the temperature of 1100° C. was reached with 40 volts and 5 amps. An approximate heating rate of 15° C. per minute was chosen for the curves reported herein. A platinum, platinum-rhodium thermocouple indicates the temperature of the specimen, which is placed in a small flat porcelain crucible.

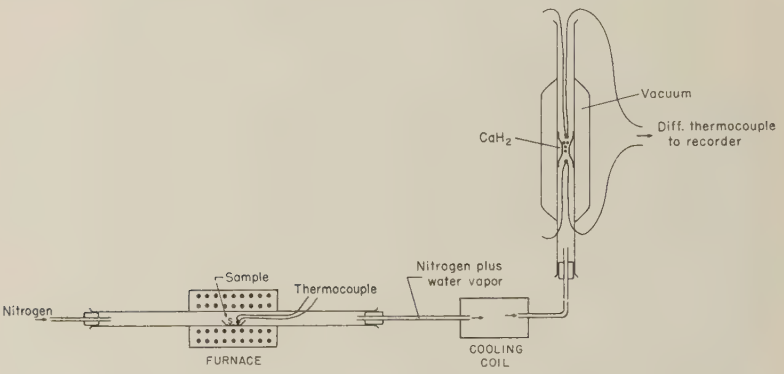

FIG. 1. Sketch of apparatus used in obtaining vapour-absorption curves.

Dried nitrogen gas is directed through the furnace at a constant rate of 25 ml. per minute to sweep out any water vapour. The nitrogen with any water vapour is cooled to room temperature in a small coil and then directed through the absorber.

The absorber is a vertical glass tube with a silvered vacuum jacket for thermal protection. A grid holds some pellets of a dehydrating agent and a differential thermocouple records the changes in temperature of the gas before and after absorption of water. In the first series of experiments, the thermal sensitivity of crystal diodes was used for detecting the temperature variations of the gas flow. Two germanium diodes mounted on a Wheatstone bridge were utilized as differential thermal gauges; however, the extreme sensitivity of the device created many experimental difficulties. For example, the weight of the specimen had to be kept at a fraction of a milligram and very complete thermal insulation was necessary. Finally, differential thermocouples of chromel and alumel wires were adopted.

Several water absorber compounds were tried. Calcium hydride gave the best results, but silica gel was also used successfully. The curves were recorded on a Brown electronic potentiometer. Operating under

the above conditions, the dehydration of 40 mg. of kaolinite produced a deflection of about 15 cm.

Analytical results. The curves in fig. 2, for halloysite with gibbsite, for kaolinite, and for dickite, show peaks for loss of water of a size and shape that would be anticipated from D.T.A. (differential thermal analysis) curves (Grim, 1953). It is not expected that the vapour curves should be precisely the same as the D.T.A. curves since any structural changes accompanying dehydration are not reflected in the vapour curves.

Each of the vapour curves, fig. 2, shows a faint depression at about 950°–1000° C. D.T.A. curves for these minerals frequently show a slight endothermic reaction at this temperature which has been interpreted (Grim, 1953) as being caused by the destruction of the dehydrated kaolinite structures. The present data suggest that, at least during very rapid heating, a small amount of water is present in the so-called metakaolin structure and is expelled when this structure is destroyed. In this conclusion we agree with V. Stubičan (this issue, p. 38), who presents infra-red absorption spectrum evidence for the presence of hydroxyl groups in metakaolin.

The fireclay sample, fig. 3, which has a clay mineral composition of about 75 % kaolinite and 25 % illite, produces the vapour-loss curve expected from its mineral composition and D.T.A. curve.

The illite samples, fig. 3, show the expulsion of adsorbed water at low temperatures. The curves show that the hydroxyl water is driven off gradually over a considerable temperature interval, at least at the rapid heating rates of the experiments. There is no suggestion of any water loss at high temperatures corresponding to the third endothermic reaction shown on D.T.A. curves (Grim, 1953) of these minerals.

The nontronite sample shows a vapour-loss curve that corresponds closely to the D.T.A. curve of the mineral (Grim, 1953). The hectorite sample shows the loss of adsorbed water at low temperatures, and the expulsion of hydroxyl water between about 650° and 950° C. The dioctahedral montmorillonites studied, fig. 4, show the expulsion of the hydroxyl water at a somewhat lower temperature and often more abruptly than this trioctahedral montmorillonite. The talc sample, fig. 3, shows only the loss of hydroxyl water over a wide temperature interval extending from about 700° C. to above 1000° C.

The curves for the three montmorillonite samples, fig. 4, show peaks for the loss of adsorbed water corresponding to those on the D.T.A. curves, fig. 5. The peaks for the expulsion of hydroxyl water also

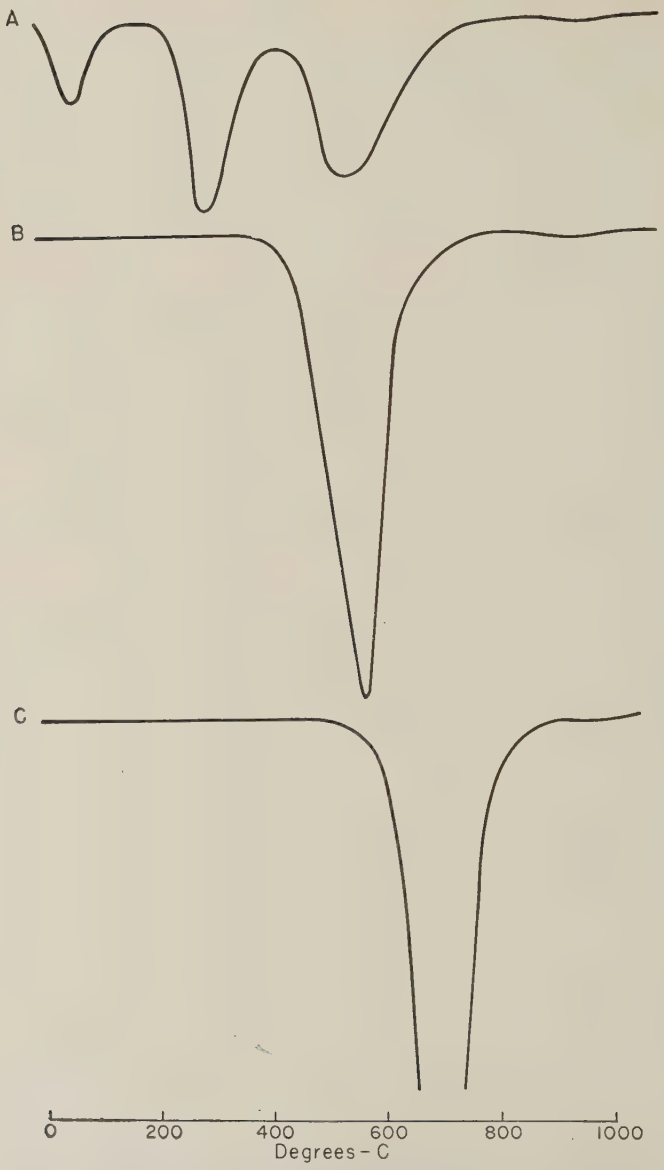

FIG. 2. Vapour-absorption curves: A, Halloysite (with gibbsite), Bedford, Indiana; B, Kaolinite, McIntyre, Georgia; C, Dickite, Baraboo, Wisconsin.

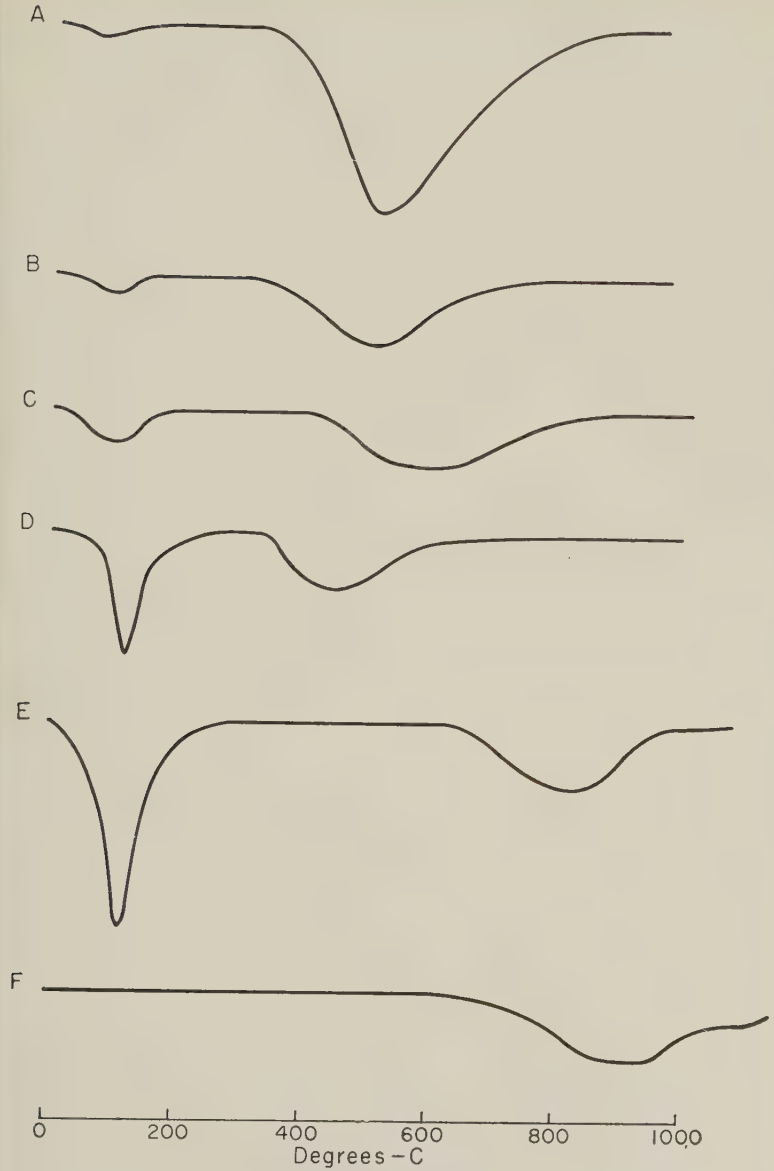

FIG. 3. Vapour-absorption curves: A, 75% kaolinite, 25% illite (fireclay), Grundy County, Illinois; B, Illite, Vermilion County, Illinois; C, Illite, Grundy County, Illinois; D, Nontronite, Manito, Washington; E, Hectorite, Hector, California; F, Talc, New York.

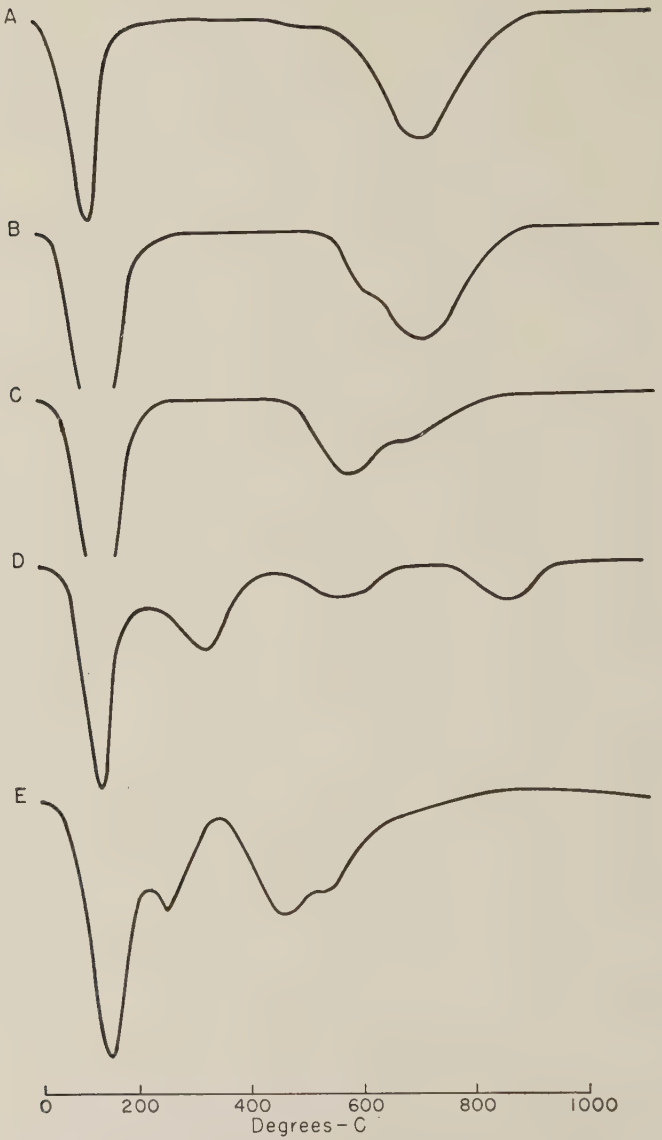

FIG. 4. Vapour-absorption curves: A, Montmorillonite, Colony, Wyoming; B, Montmorillonite, Amory, Mississippi; C, Montmorillonite. Mendoza, Argentina; D, Sepiolite, Vallecas, Spain; E, Palygorskite, Attapulgus, Georgia.

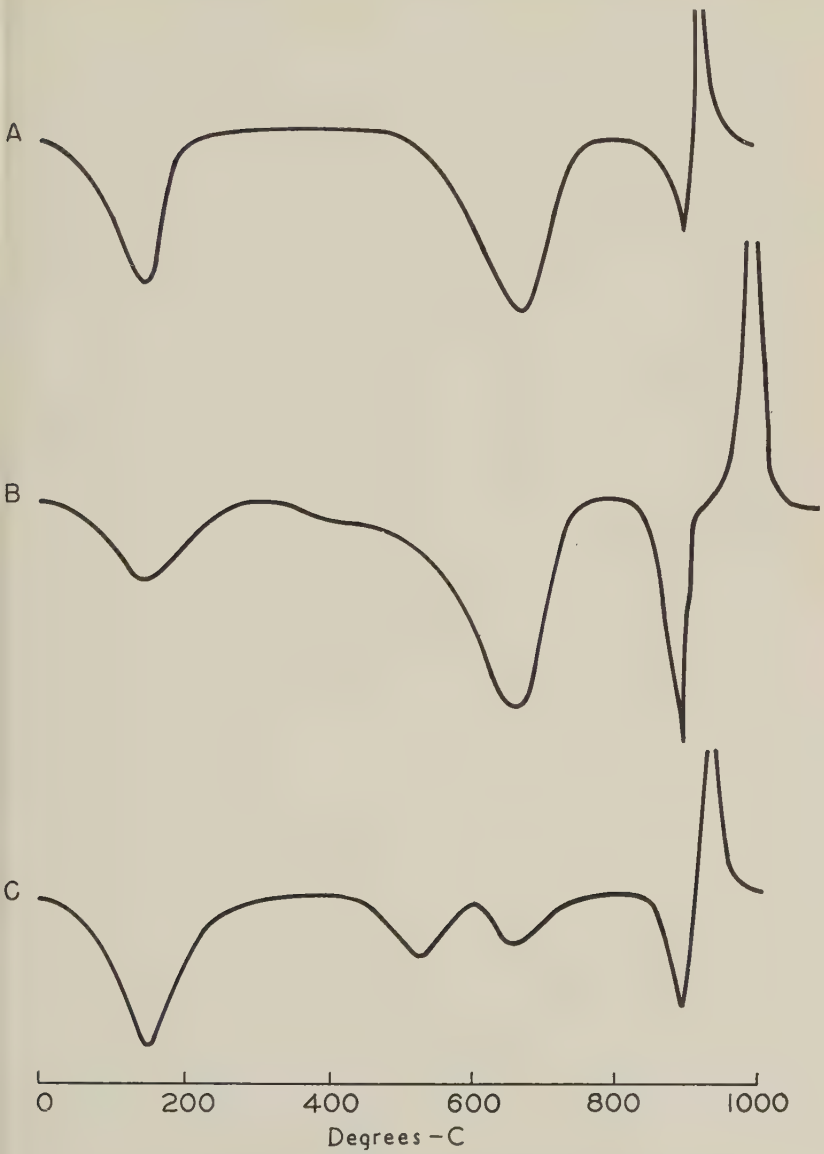

FIG. 5. Differential thermal analysis curves: A, Montmorillonite, Colony, Wyoming; B, Montmorillonite, Amory, Mississippi; C, Montmorillonite, Mendoza, Argentina.

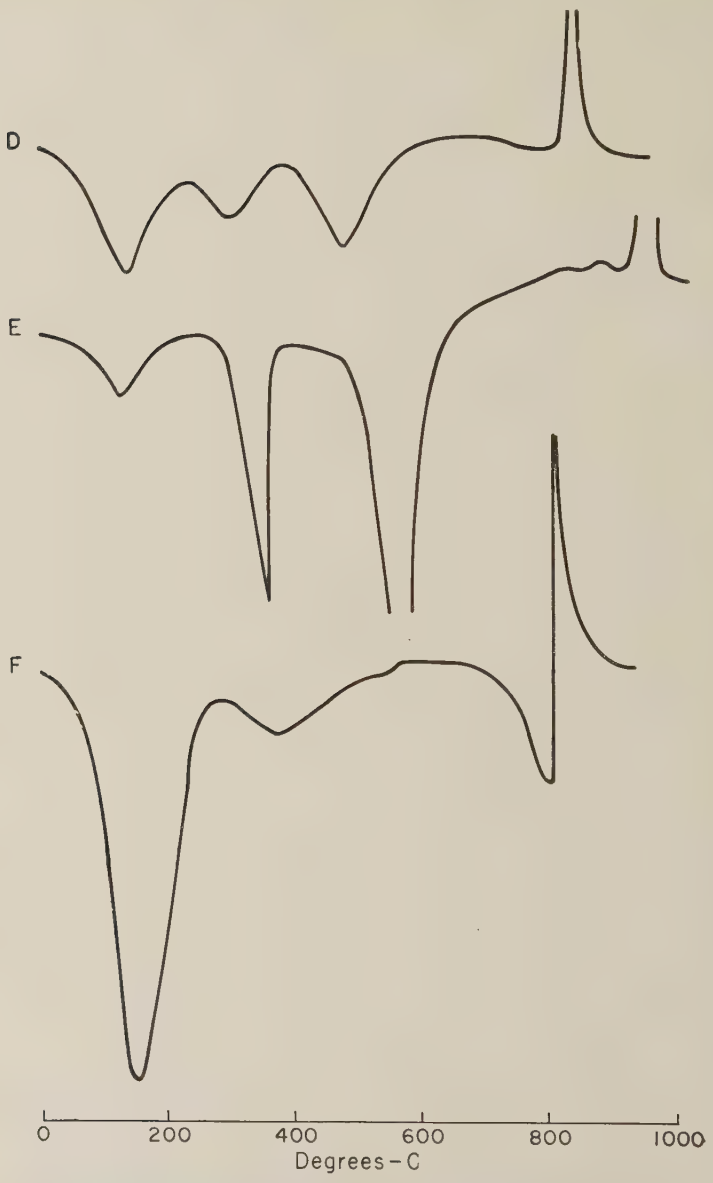

FIG. 6. Differential thermal analysis curves: D, Palygorskite, Attapulgus, Georgia; E, Halloysite (with gibbsite), Bedford, Indiana; F, Sepiolite, Vallecas, Spain.

correlate in the two types of curves. When the hydroxyl dehydration peak is a doublet on the D.T.A. curve, it is also a dual peak on the vapour-loss curve indicating that both parts of the doublet are related to water loss. The vapour-loss curves are at least as sensitive in detecting such doublets as are the D.T.A. curves. The vapour-loss curves do not indicate any expulsion of water corresponding to the high-temperature endothermic peaks of the montmorillonites on the D.T.A. curves, fig. 5.

The vapour-loss curve for the palygorskite (attapulgite) sample, fig. 4, corresponds to the D.T.A. curve, fig. 6, except that the vapour-loss curve resolves the higher-temperature endothermic peak into a doublet.

The low temperature portion of the vapour-loss curve for the sepiolite sample, fig. 4, corresponds to endothermic reactions on the D.T.A. curve for the same sample, fig. 6. The vapour-loss curve shows a definite vapour expulsion at 500°–600° C. which is only suggested on the D.T.A. curve. Also the vapour-loss curve shows that for the sepiolite the endothermic reaction at about 800° C. is accompanied by a loss of water. Martin-Vivaldi and Cano-Ruiz (1956) have recently published a detailed study of the dehydration of the same palygorskite (attapulgite) and sepiolite. Their data correlate exactly with the vapour-absorption curves. In fact the correlation is far superior to that with the D.T.A. curves.

Discussion of results. It is believed that the analytical method presented herein provides a simple means of obtaining additional definitive characteristics of hydrous minerals. Using other absorbents, similar curves could undoubtedly be obtained to record the expulsion of other gaseous materials produced on heating minerals, for example, carbon dioxide from carbonates.

The new method can contribute to structural studies by showing whether or not loss of water accompanies a thermal reaction. In the temperature range for the loss of hydroxyl water, the vapour-loss method appears to be extremely sensitive. In this interval the vapour-loss curves may indicate reactions shown only very slightly on the D.T.A. curve (e.g. montmorillonite from Mississippi), or not at all (e.g. palygorskite).

In the temperature interval of the loss of the adsorbed water the vapour-loss curve appears to be less sensitive than the D.T.A. curve. Thus the double peak of the Mississippi montmorillonite is shown as a single peak in the vapour-loss curve. It should be pointed out that this apparent difference in sensitivity between the vapour-loss and D.T.A. curves may have another explanation, namely, that these thermal reactions shown on D.T.A. curves are a consequence of structural changes to a greater degree than has heretofore been considered. Thus the double

nature of the peak for loss of adsorbed water from calcium montmorillonites as shown on D.T.A. curves may be due to a change in water structure after a certain amount of moisture is lost rather than to any periodicity in the water loss. Further work is necessary to resolve this matter.

It must be remembered that some variations in the vapour-loss curves would result from different heating rates, different particle size of the sample, &c.

References.

Grim (Ralph E.), 1953. Clay Mineralogy, McGraw-Hill Co., New York.

Martin-Vivaldi (J. L.) and Cano-Ruiz (J.), 1956. Clay and Clay Minerals, Pub. 456, U.S. Nat. Acad. Sci., p. 177.

The morphology of the baryte group.[1]

By A. F. Seager, B.Sc., Ph.D., A.K.C., F.G.S.

Department of Geology, Birkbeck College, University of London.

[Read 6 November 1952.]

Summary. The observed order of importance of the forms of baryte, anglesite, and celestine is first determined by a modification of the methods used by Donnay and Harker. Their hypothesis is applied to determine the space-groups of these minerals by morphological means, and a comparison is made of the observed and theoretical orders of importance of forms in these minerals. It is concluded that agreement is poor between the observed and predicted frequencies of forms in the baryte group. The rank distribution of some of the more important forms is presented graphically.

A NEW method of calculating the reticular area of lattice planes which allows for the operation of screw axes and glide planes has been introduced by J. D. H. Donnay and D. Harker.[2] This, in conjunction with Donnay's work on zonal development,[3] makes it possible to extend the Bravais hypothesis to cover the 230 space-groups.[4] They call their work a 'Law of Observation', and say that it only takes into account the geometry of space-groups and does not claim to embrace all the factors governing the morphological development of crystals. They add, however, that the effects of the lattice and *motif* on the habit of a crystal are very rarely masked by other factors.

Donnay has published many morphological analyses of minerals, and one of an artificial compound, some of which are based on relatively scanty data. Three further papers have been published by his research students, E. D. Taylor and J. A. Tremblay.[5] The author believes it is better to use as examples minerals for which more data are available.

In some papers Donnay uses different methods to determine the relative importance of forms. It seems desirable to find one method which

[1] 'The morphology of baryte' forms part of a thesis approved for the degree of Ph.D. by the University of London, 1953.

[2] J. D. H. Donnay and D. Harker, Amer. Min., 1937, vol. 22, p. 446 [M.A. **7**–241].

[3] J. D. H. Donnay, Ann. Soc. géol. Belgique, 1938, vol. 61, p. B 260 [M.A. **7**–242].

[4] J. D. H. Donnay and D. Harker, Naturaliste Canadien, 1940, vol. 67, p. 33 [M.A. **8**–4].

[5] J. D. H. Donnay, Bull. Soc. franç. Min., 1946, vol. 69, p. 152. A bibliography of papers by Donnay and others (1937–46) on the morphology of crystals.

can be applied consistently to all minerals. In this paper a new method of determining the observed morphological aspect is suggested, which consists, in part, of a synthesis of several of Donnay's methods.

Method of determining the observed morphological aspect.

The 'observed morphological aspect' is a list of forms observed on crystals of a substance in order of decreasing importance. There is no simple criterion by which the importance of a form can be assessed or calculated. The information from which the observed morphological aspect has to be derived is usually a number of drawings of crystals from various localities. Donnay regards the 'locality frequency', or number of localities at which the form has been found, as the most important factor. He separates forms that have equal, or nearly equal, locality frequencies by their 'mean rank', which indicates the degree of development of a form relative to other forms on the crystal. Sometimes Donnay uses the 'mean rank of the locality' and at other times the 'mean rank of the figures'.

In morphological studies the best index of form importance would probably be the mean velocity of growth, and the observed morphological aspect would then consist of a sequence of forms in order of increasing growth velocity. Great labour would be involved in making accurate determinations of growth velocities from several hundred drawings, and it appears that sufficiently accurate results can be obtained for the morphological analysis by much simpler means. The size of a face is closely related to its growth velocity, but is also affected by the disposition of surrounding faces. The mean rank of the locality gives a rough measure of growth velocities, and is included in the formula for calculating the observed morphological aspect.

It would be possible to base the observed morphological aspect only on the locality frequency or frequency of occurrence of forms (form frequency). The chief disadvantage of the latter lies in the possibility of giving undue importance to less common forms when, as sometimes happens, a large number of crystals of unusual habit are described from one locality.

For the baryte group it is found that the locality frequency, form frequency, and mean rank when used alone each give a similar, but slightly different, order for the observed morphological aspect.

When preparing observed morphological aspects it seems advisable to make use of all information that is numerically assessable and to combine it into a single figure which may be called the *form rank index*. This information comprises the relative development of the form at each

locality, its frequency of occurrence at each locality, and the number of localities at which it occurs. In this paper these factors have been assessed in the following manner.

Let the number of crystals recorded from any locality be n, and let the number of crystals from any locality showing a particular form x be n_x; let the number of localities from which the mineral has been studied be N, and let the locality frequency or number of localities at which it shows the form x be N_x; and let the general symbol for the rank of a form x on a particular crystal be r.

The rank of forms is found in the manner suggested by Donnay. On each crystal all the forms present are listed in order of decreasing size, the largest, the second largest, ..., rth largest are given the corresponding ranks, 1, 2, ..., r. The mean rank of a form at any locality is then $\Sigma r/n_x$. The mean rank of a form is given by $\bar{R} = \Sigma(\Sigma r/n_x)/N_x$. The actual frequency of a form x is Σn_x and the percentage frequency is $F\,\% = 100\Sigma n_x/\Sigma n$. The relative frequency of a form x at a particular locality is n_x/n. The locality form rank index ρ_l, which assesses the importance of a form at any locality, takes into account the relative development of the form and its frequency of occurrence at the locality; it is obtained by multiplying the reciprocal of the mean rank at the locality by the relative frequency, $\rho_l = n_x^2/n\Sigma r$. The final assessment of the importance of a form is made by the form rank index ρ, which is obtained by summing all the locality form rank indices and dividing by the number of localities from which the mineral has been studied, $\rho = \Sigma\rho_l/N$. Its range is from zero to unity. The locality frequency, of which so much use is made by Donnay, receives indirect expression in the formula; the greater the locality frequency the larger will be the numerator in the expression for the form rank index. This index effectively reduces the importance of rare forms which, owing to unusual conditions of growth, may be common at one or a few localities. The form rank index may be used to compare directly the importance of forms on different minerals as, for example, in isomorphous series. While not suggesting that the form rank index is necessarily the best index of form importance that can be devised, it does appear to be an improvement, as it incorporates all the values which are numerically assessable in one index figure.

Morphology of the baryte group.

The chief source of morphological data is the 'Atlas der Krystallformen' compiled by V. Goldschmidt. Some of the drawings in the

Atlas represent incomplete crystals, some contain errors, while others are illegible. All drawings of crystals the locality of which is unknown were also rejected.

The 'Handbuch der Mineralogie' by C. Hintze was used as an auxiliary source of information to check the relative form frequencies found from the Atlas. The Handbuch gives the habit of crystals from various localities or a list of forms found at a locality. Each list of forms has been counted as one crystal. Some of the longer lists, over about eighteen forms, were omitted from the calculations, as they would give undue importance to the rarer forms. The form frequencies derived from the Handbuch substantially corroborated those derived from the Atlas and gave useful additional information on the occurrence of rarer forms.[1] Since little information is given about the rank of forms quoted in the Handbuch, form rank indices cannot be calculated from these data.

It is not possible to quote very precisely the number of localities at which a common mineral occurs showing a given form. For example, one author may describe a crystal from a particular district, while another quotes a mine in that district, when it is impossible to say whether the mineral is being reported from one or two localities. In this paper each mine in a region is counted as one locality.

Table I gives summaries of form frequency and rank data for baryte, anglesite, and celestine, for forms with frequencies of occurrence of 5 % or more in the Atlas. In each section of the table columns two to five give the form rank index (ρ), locality frequency (N_x), mean rank ($\bar{R}$), and percentage frequency of occurrence (F %) calculated from data in the Atlas, and the last column gives the percentage frequency of occurrence calculated from the Handbuch (F' %). In each section of the table the forms are arranged in the order of decreasing importance of rank. Table II gives rank and frequency data for the rarer forms of baryte, anglesite, and celestine. There is little point in calculating the mean rank or form rank index of forms with low frequencies of occurrence, as they are not likely to be very reliable. In order to obtain more data for the assessment of the relative importance of the rarer forms the information from the Atlas and the Handbuch has been combined. In

[1] For baryte the Atlas yielded the required data for 486 crystals with an aggregate of 3373 forms from 153 localities and the Handbuch gave 505 crystals with 3527 forms from 423 localities. For anglesite the Atlas gave 359 crystals showing 2204 forms from 63 localities and the Handbuch gave 167 crystals with 1173 forms from 108 localities. For celestine the Atlas gave details of 201 crystals with 941 forms from 48 localities and the Handbuch of 159 crystals with 935 forms from 123 localities.

many cases the same crystal is recorded in both sources, but all such cases of duplication have been eliminated. The rarer forms have been listed in order of decreasing locality frequency (N_x), and when this is equal, in order of decreasing frequency of occurrence (Σn_x). This is taken as the order of decreasing rank, the observed morphological aspect. It would be unwise to place too much reliance on the order of the rarer forms, as the discovery of a few more examples of these forms could alter the order. This table does, however, serve a useful purpose in giving at least an approximate order of importance for the rarer forms. There is insufficient data to justify arranging the still rarer forms in order of rank.

Morphological analysis of the baryte group.

It has been shown by X-ray analysis of the minerals of the baryte group that the a-axis of the unit-cell[1] has twice the value indicated by the axial ratios assigned on morphological grounds. In the morphological analysis the latter values must be used unless the analysis indicates that they are incorrect. The axial ratios used are shown in table I, and the symbols of forms in this paper are always referred to these axes, unless otherwise stated.

TABLE I. Morphological analysis of the baryte group. Summary of form rank and frequency data.

Baryte. *Axial ratios** $a:b:c = 0{\cdot}8152:1:1{\cdot}3136$						*Anglesite.* *Axial ratios*† $a:b:c = 0{\cdot}78516:1:1{\cdot}28939$						*Celestine.* *Axial ratios*‡ $a:b:c = 0{\cdot}77895:1:1{\cdot}28005$					
Form	ρ	N_x	$\bar{R}$	F%	F'%	Form	ρ	N_x	$\bar{R}$	F%	F'%	Form	ρ	N_x	$\bar{R}$	F%	F'%
001	0·708	149	1·77	91	96	110	0·333	56	2·91	82	86	011	0·601	47	1·95	87	89
110	0·341	145	3·25	89	87	001	0·326	51	2·85	69	72	001	0·405	37	2·05	71	80
011	0·298	137	3·70	77	74	102	0·300	51	3·31	75	77	102	0·276	41	3·36	76	88
102	0·293	137	3·82	82	82	011	0·225	51	3·88	68	61	110	0·251	40	3·20	71	80
111	0·126	114	5·70	54	47	100	0·162	37	3·41	31	45	100	0·067	19	3·96	25	26
010	0·123	106	4·81	47	45	111	0·155	51	4·85	64	66	104	0·067	17	4·17	26	32
100	0·104	95	5·65	42	40	104	0·130	29	3·91	24	31	133	0·067	8	2·48	10	8
210	0·062	54	6·49	26	18	122	0·128	39	4·90	52	50	111	0·058	20	4·83	30	35
101	0·061	67	6·37	26	32	120	0·043	25	5·36	20	26	144	0·038	8	3·25	6	10
104	0·047	64	5·92	23	30	010	0·042	30	5·31	26	35	122	0·019	11	5·16	8	15
122	0·033	57	7·59	20	21	324	0·040	22	6·47	19	29	120	0·008	6	5·57	7	6
320	0·029	38	6·46	14	10	112	0·031	22	7·04	19	25	010	0·007	4	5·30	6	15
130	0·022	37	7·31	13	12	221	0·008	11	6·54	8	10						
113	0·020	44	9·40	15	13	124	0·008	10	8·50	5	9						
112	0·017	33	9·28	8	9												
120	0·016	24	7·28	6	8												
114	0·011	27	9·71	9	6												
115	0·009	25	9·49	7	5												

* R. Helmhacker, Denkschr. Akad. Wiss. Wien, 1872, vol. 32, Abt. II, p. 1.

† N. von Koksharov, Min. Russlands, 1853, vol. 1, p. 34.

‡ A. von Auerbach, Sitzungsber. Akad. Wiss. Wien, Math.-naturwiss. Cl., Abt. I, 1869, vol. 59, p. 549.

[1] R. W. James and W. A. Wood, Proc. Roy. Soc., 1925, ser. A, vol. 109, p. 598 [M.A. 3-345].

TABLE II. Rank and frequency data for the rarer forms.

*Baryte.**			*Anglesite.**			*Celestine.**		
Form.	$N_{x^\cdot}$	$\Sigma n_{x^\cdot}$	*Form.*	$N_{x^\cdot}$	$\Sigma n_{x^\cdot}$	*Form.*	$N_{x^\cdot}$	$\Sigma n_{x^\cdot}$
106	25	33	130	17	32	124	10	11
124	23	28	012	12	22	113	9	9
012	23	26	132	10	21	221	8	8
103	20	25	144	8	15	101	8	8
132	15	23	210	8	12	324	6	9
230	15	17	121	7	19	012	5	8
223	14	17	142	7	15	132	5	7
116	12	14	113	6	9	1.10.10	5	7
302	11	14	114	5	8	103	5	5
142	9	13	018	5	8	015	4	8
312	9	11	212	5	7	0.1.12	4	6
021	8	11	133	4	9	210	4	5
140	8	10	021	4	7			
212	7	12						
121	6	9						

* Axial ratios as in table I.

TABLE III. Development of the central zones in the baryte group. Actual form frequencies derived from the Atlas (A) and Handbuch (H).

*Baryte.**

{*hhl*}.	*A.*	*H.*	{*hkk*}.	*A.*	*H.*	{*hkh*}.	*A.*	*H.*
1.1.26	—	1	1.22.22	1	1	616	1	1
1.1.20	—	1	1.18.18	—	1	414	2	4
1.1.17	—	1	188	1	—	313	4	2
118	3	3	177	1	3	212	8	4
117	—	3	166	—	1	111	263	235
116	6	8	155	1	2	121	8	1
115	36	25	144	1	3	131	3	1
114	42	28	133	3	4	141	3	—
4.4.15	—	1	255	—	1	151	1	—
113	73	64	122	95	108			
337	—	1	355	—	1			
7.7.16	—	1	344	—	1			
6.6.13	1	1	111	263	235			
112	38	47	322	—	1			
223	10	7	211	—	1			
111	263	235	522	—	1			
887	1	1	311	—	1			
776	—	1	411	—	1			
441	—	1						

*Anglesite.**

{*hhl*}.	*A.*	*H.*	{*hkk*}.	*A.*	*H.*	{*hkh*}.	*A.*	*H.*
116	3	2	1.12.12	3	1	212	4	3
114	4	4	166	2	2	111	231	110
113	4	5	155	5	3	121	14	5
112	68	42	144	8	7			
111	231	110	133	5	4			
221	27	16	122	186	83			
331	1	—	233	1	2			
441	—	1	344	—	1			
			111	231	110			

*Celestine.**

{*hhl*}.	*A.*	*H.*	{*hkk*}.	*A.*	*H.*	{*hkh*}.	*A.*	*H.*
119	—	1	1.19.19	—	1	959	—	1
117	—	1	1.10.10	6	3	111	60	55
115	1	2	177	—	4	121	2	2
114	2	—	166	—	1			
113	2	9	155	1	2			
112	1	3	144	12	16			
111	60	55	277	1	1			
332	—	1	133	20	12			
221	2	7	122	17	24			
			111	60	55			
			322	1	2			

* Axial ratios as in table I.

Determination of the lattice type.

The lattice type is determined from the three zones $[1\bar{1}0]$, $[0\bar{1}1]$, and $[\bar{1}01]$, of forms {*hhl*}, {*hkk*}, and {*hkh*}. These are called 'central zones' by Donnay, as they all intersect in {111}. Form rank indices and other frequency data for the commoner forms in these zones are given in

table I. Frequency data for the rarer forms appear in table II. In both these tables the forms are listed in the order of decreasing importance. Table III contains the actual frequency of all the forms in these three zones derived from the Atlas and the Handbuch.

Baryte. The zone [1$\bar{1}$0] of forms {*hhl*}. The observed morphological aspect already obtained for forms with frequencies over 1 % is {111}, {113}, {112}, {114}, {115}, {223}, and {116}. There is little point in discussing the remaining rarer forms. The form {111} is clearly predominant. In the harmonic segment of the zone[1] there is a complete sequence of the primary series[2] from {111} to {118}. The only secondary form[2] is {223} which, as might be expected, is the simplest possible. The arithmetic segment[1] is virtually undeveloped, no form in it even attaining a frequency of 1 %.

The predominance of {113} over {112} suggests the presence of an *F*-lattice, but this is definitely ruled out by the relative importance of the other forms in the zone. The zonal series is of the simple type with the unit form dominant. This conclusion is confirmed by a study of the two remaining central zones.

The zone [0$\bar{1}$1] of forms {*hkk*}. The observed morphological aspect for forms with frequencies over 1 % is {111} and {122}. These are followed in importance by {133}. The primary series extends from the dominant form {111} to {188} in the harmonic segment and to {411} in the arithmetic segment of the zone, although most of the forms are very rare. Three forms of the secondary series and two of the tertiary series are each recorded once. The primary series is of the simple type with the unit form dominant.

The zone [$\bar{1}$01] of forms {*hkh*}. The observed morphological aspect for forms with frequencies over 1 % is {111}, {212} $\simeq$ {121}. A complete zonal series extends from {414} through {111} to {151}. It is clear that {111} is the dominant form of the zone, the adjacent forms {212} and {121} are approximately equal and very much less important than {111}, while the next pair of forms, {313} and {131}, are less important still. This establishes the zone to be of the simple type with the unit form dominant.

In the zone of forms {*hhl*} the superiority of {113} over {112} left a slight doubt as to the character of that zone, although the distribution of the other forms indicated that it was of the simple type with the unit form dominant. This conclusion is completely confirmed by the study

[1] M. A. Peacock, Amer. Min., 1937, vol. 22, p. 210.

[2] J. D. H. Donnay, Ann. Soc. géol. Belgique, 1938, vol. 61, p. B 260.

of the two other central zones; since they are both of the simple type with the unit form dominant the third central zone must also have this character. It can thus be concluded that baryte has a primitive lattice and that Helmhacker's choice of axial ratios is fully justified on morphological grounds.

Anglesite. The zone $[1\bar{1}0]$ of forms $\{hhl\}$. For this zone the observed morphological aspect is {111}, {112}, {221}, {113}, and {114}. The unit form is clearly dominant. In the harmonic segment of the zone only forms of the primary series occur, and these decrease in importance from {111} to {114}. The only important form in the arithmetic segment of the zone is {221}. These features indicate that the zone is of the simple type with the unit form dominant.

The zone $[0\bar{1}1]$ of forms $\{hkk\}$. In this zone the observed morphological aspect is {111}, {122}, {144}, and {133}. {155} is less important. In this zone, in which the unit form is dominant, the harmonic segment alone is developed, and in it only forms of the primary series are of importance. Apart from the reversal of {133} and {144}, which are not forms with high frequencies, there is a continual decrease in importance from {111} to {166}, indicating the presence of a zone of the simple type with the unit form dominant.

The zone $[\bar{1}01]$ of forms $\{hkh\}$. This zone is poorly developed. The observed morphological aspect is {111}, {121}, and {212}. This is a zone of the simple type with the unit form dominant.

The three central zones thus prove to be of the simple type with the unit form dominant. This indicates that the lattice is primitive, and gives complete support on morphological grounds to Koksharov's choice of axial ratios.

Celestine. The zone $[1\bar{1}0]$ of forms $\{hhl\}$. This zone is poorly developed. The observed morphological aspect is {111}, {113}, and {221}. In the harmonic segment of the zone only forms of the primary series occur, and there is a complete sequence from {115} to {111}. {113} is more important than {112}, as is the case with baryte. Although little information is available to indicate the nature of the zone, the presence of {221} as the only primary form in the arithmetic segment of the zone and the series from {115} to {111} in the harmonic segment suggests that the zone is of the simple type with the unit form dominant.

The zone $[0\bar{1}1]$ of forms $\{hkk\}$. The observed morphological aspect in this zone is {133}, {111}, {144}, {122}, and {1.10.10}. Of the pyramidal zones this is quite the best developed. There is a primary series in the harmonic segment extending from {177} to {111}. Only the first four

forms listed are of any importance. It is rather surprising that {133} ranks above {111}. From table I it may be seen that the latter has a much higher frequency of occurrence and locality frequency. In the fewer localities where it occurs {133} is often well developed, as indicated by its mean rank, and this raises it above {111} in the final assessment. The unusual frequency and mean rank of {133} together suggest that, where it does occur, local conditions of growth, such as the presence of particular impurities, may favour its development at the expense of other forms. Although the relative development of forms in this zone is far from ideal, the fact that the four most important forms are the first four of a primary series does suggest that this zone is of the simple type. The unit form is dominant in respect of locality frequency and frequency of occurrence, but comes after {133} in the list of form rank indices.

The zone [$\bar{1}01$] of forms {*hkh*}. The unit form is dominant, and there are no others of importance. The presence of {121} may suggest that the zone is of the simple type.

The evidence for the lattice type is rather unsatisfactory. Since the zones [$1\bar{1}0$] and [$\bar{1}01$] clearly have the unit form dominant, and the zones [$1\bar{1}0$] and [$0\bar{1}1$] show some evidence of a primary series it may be concluded that the lattice is primitive and the choice of axial ratios is justified.

Determination of the space-group.

The space-group is determined from the development of the zones [100], [010], and [001], termed 'axial zones' by Donnay. Since it is known on morphological grounds that the point group of baryte, anglesite, and celestine is *mmm*, it is necessary to determine whether a mirror plane or a glide-plane exists parallel to each pinacoid, and in the latter case the nature of the glide-plane present.

The observed morphological aspect for the commoner and rarer forms in these three zones, with the data on which it is based, will be found in tables I and II. The actual frequency of all the forms occurring in these zones is given in table IV.

Baryte. The zone [100] of forms {0*kl*}. The observed morphological aspect for forms with frequencies over 1 % is {011}, {012}, and {021}. This zone is difficult to interpret. Although a complete series of forms extends from {014} through {011} to {051} most of the forms are very rare, only three having a frequency over 1 %. The unit form is completely dominant and followed, in order, by {012} and {021}, while {031} and {013} are still more rare. In view of their rarity and approximately

equal frequency no useful purpose can be served by discussing the relative importance of {014}, {013}, {031}, {041}, and {051}.

TABLE IV. Development of the axial zones in the baryte group. Actual form frequencies derived from the Atlas (A) and Handbuch (H).

*Baryte.**

{0kl}.	A.	H.	{h0l}.	A.	H.	{hk0}.	A.	H.
0.1.12	—	1	1.0.80	—	1	1.10.0	—	1
018	—	1	1.0.30	—	1	170	—	1
014	1	1	1.0.10	1	—	150	—	1
027	—	1	109	—	1	140	7	3
013	1	1	108	1	2	3.10.0	1	1
025	1	1	106	9	24	130	64	61
012	9	19	105	3	4	120	31	39
047	1	1	8.0.33	—	1	350	—	1
035	4	3	104	113	152	230	10	8
023	3	4	103	9	17	450	1	—
034	—	3	7.0.20	—	1	110	431	438
079	1	2	308	1	5	540	—	1
089	1	—	5.0.13	—	1	430	—	1
011	376	372	205	3	3	320	68	53
065	—	1	102	400	415	530	2	1
032	1	1	407	1	1	740	1	1
085	—	1	508	1	2	210	126	90
053	—	1	203	2	4	310	2	4
021	6	6	304	3	2	410	—	6
083	1	1	405	1	2	910	—	1
031	—	4	23.0.24	1	—			
041	1	1	101	124	161			
051	—	1	403	1	—			
			302	6	8			
			905	—	1			
			201	1	2			

*Anglesite.**

{0kl}.	A.	H.	{h0l}.	A.	H.	{hk0}.	A.	H.
0.1.10	—	1	1.0.24	1	1	270	1	1
018	7	4	1.0.22	—	1	130	17	18
016	—	1	1.0.14	—	1	120	72	44
0.2.11	1	1	108	1	—	230	2	3
013	4	1	106	1	1	340	4	3
012	17	7	105	1	1	110	294	143
035	1	1	104	87	51	320	—	1
045	1	—	103	1	2	740	1	1
011	245	102	102	270	128	210	7	5
021	4	3	101	—	4	520	—	2
031	1	2	21.0.2	—	1	310	1	1
041	—	1				410	2	2

*Celestine.**

0.1.20	1	1	1.0.17	—	2	140	—	1
0.1.16	—	1	1.0.14	—	1	130	—	1
0.1.14	—	1	1.0.12	—	2	120	14	9
0.1.12	3	4	1.0.10	—	1	350	—	1
0.1.10	1	2	108	1	2	580	—	1
019	1	3	107	—	1	110	142	127
018	1	1	106	1	1	650	2	1
017	—	2	2.0.11	1	1	750	5	2
015	7	2	105	—	3	320	4	2
0.3.10	—	2	104	53	51	530	2	2
013	2	2	207	1	1	210	—	5
012	7	3	103	3	3	520	—	1
035	—	1	7.0.15	—	1	10.3.0	—	1
023	—	2	11.0.23	—	2	410	—	1
067	—	1	102	153	140			
011	175	141	304	—	1			
021	1	2	101	1	8			
0.15.2	—	1	908	2	1			
			705	—	1			

Pinacoids.

Baryte.			*Anglesite.*			*Celestine.*		
	A.	H.		A.	H.		A.	H.
100	204	201	100	113	75	100	51	41
010	227	228	010	94	58	010	12	24
001	444	486	001	247	121	001	142	127

* Axial ratios as in table I.

Since the lattice is primitive the planes of symmetry parallel to (100) could be *m*-planes, *b*-glide planes, *c*-glide planes, or *n*-glide planes. The dominance of the unit form rules out the possibility of *b*- or *c*-glide planes. The relative order of importance

$$\{011\} > \{012\} > \{021\} > \{031\} \doteq \{013\}$$

is consistent with the existence of *m*-planes, but the very low frequency of all the forms in the zone, except {011}, is hardly reconcilable with such

an assumption. The high frequency of {011} and low frequency of the other forms is much more in accord with the existence of *n*-glide planes parallel to (100), but in that case it would be expected that {013} and {031} would predominate over {012} and {021}, but this is not so. In this case the matter must be left open, and it can only be stated that *m*-planes or *n*-glide planes exist parallel to (100).

The zone [010] of forms {*h*0*l*}. The observed morphological aspect is {102}, {101}, {104}, {106}, {103}, and {302} for forms with frequencies over 1 %. The dominant form is not the unit form {101}, but the form with the last index even, {102}. In the harmonic segment of the zone forms with the last index even predominate over those in which it is uneven. {104} is completely predominant over {103}, and {106} is more important than {105}.

Parallel to (010) there could be *m*-planes, or *a*-, *c*-, or *n*-glide planes. This type of zonal development could be accounted for quite satisfactorily by the existence of *c*-glide planes parallel to (010).

The zone [001] of forms {*hk*0}. The observed morphological aspect for forms with frequencies over 1 % is {110}, {210}, {320}, {130}, {120}, {230}, and {140}. This zone is also difficult to interpret. The dominant form is indisputably {110}, which is followed by {210}. {320} and {130} are almost equal, and both these forms are clearly more important than {120}, the last prism with a frequency over 5 %. {230} and {140} have frequencies between 1 % and 5 % and {310} has a frequency below 1 %.

In this zone the unit form {110} is clearly dominant. This rules out the possibility of *a*- or *b*-glide planes parallel to (001), leaving *m*-planes and *n*-glide planes for consideration. Turning attention first to the arithmetic segment of the zone the forms {110}, {210}, and {310} form a series of decreasing importance. These have the appearance of a primary series, and this is established by the appearance of the first form of the secondary series, {320}, with an importance less than that of its adjacent primary forms, {110} and {210}. From a study of the arithmetic segment alone the zone appears to be of the simple type with the unit form dominant.

The harmonic segment of the zone does not seem, at first sight, to support this conclusion. The undoubted superiority of {130} over {120} suggests the presence of a double zone. In a zone of the double type {110} and {130} would belong to the primary series and {120} would belong to the secondary series, and be denoted by doubled indices {240}. The form {350} of the tertiary series would come between {240} and

{110}, and {460} of the quaternary series would come between {350} and {110}. If the zone is of the simple type, {110} and {120} belong to the primary series, and {230} comes between them as a member of the secondary series, while {350} comes between {230} and {120} as a member of the tertiary series. Since {230} is decidedly more important than {350} it suggests that the zone is of the simple type. This conclusion is strengthened by the fact that {140} is more important than {150}; if the zone was of the double type the reverse should be the case. Thus the evidence of the arithmetic segment and the majority of the evidence from the harmonic segment points to the zone being of the simple type with the unit form dominant, and hence to the existence of *m*-planes parallel to (001).

The pinacoids. In the observed morphological aspect {001} is easily predominant, as it is the most important of all forms in baryte, and {010} has a slight superiority over {100}. This is the order to be expected from the axial ratio $a:b:c = 0{\cdot}8152:1:1{\cdot}3136$.

The analysis now gives two possible morphological aspects[1] *P*c** or *Pnc**. Since the point group is known these may be converted into symbols of actual space-groups, *Pmcm* or *Pncm*.

Anglesite. The zone [100] of forms {0*kl*}. The unit form completely dominates all other forms in the zone; the only other forms to appear in the first 27 places of the observed morphological aspect are {012}, {018}, and {021}, and these are succeeded by {013}. The distribution of forms in this zone is very similar to that in baryte, and is also difficult to interpret. The outstanding importance of the unit form and the relative insignificance of all others suggests the presence of *n*-glide planes, but this is not consistent with the superiority of {012} and {021} over {013} and {031}. The only other possibility is the existence of *m*-planes parallel to (100), but in that case it would be expected that some of the other forms in the zone would have a higher frequency of occurrence. In view of this uncertainty it can only be stated that *n*-glide planes or *m*-planes may exist parallel to (100).

The zone [010] of forms {*h*0*l*}. Only two forms, {102} and {104}, appear in the first 27 places of the observed morphological aspect, and of these {102} is dominant. The fact that {102} and not {101} is the dominant form suggests that there are *c*-glide planes parallel to (010), and this conclusion is strengthened by the fact that {104} and not {103} is the second most important form in the harmonic segment of the zone.

The zone [001] of forms {*hk*0}. In the observed morphological aspect

[1] J. D. H. Donnay and D. Harker, Naturaliste Canadien, 1940, loc. cit.

the prisms are, in order of decreasing importance, {110}, {120}, {130}, and {210}, and no others need be considered in the study of this zone. The unit form is dominant, and there is a steady decrease in importance from {110} to {130} in the harmonic segment of this zone. The only form of any importance in the arithmetic segment of the zone is {210}. This zone shows the type of development to be expected when *m*-planes are parallel to (001).

The pinacoids. In the observed morphological aspect the pinacoids are placed in the order of decreasing importance {001}, {100}, and {010}. This does not agree with the order of the theoretical morphological aspect, which is {001}, {010}, and {100} for the axial ratios $a:b:c = 0{\cdot}78516:1:1{\cdot}28939$ found by morphological means. The analysis thus indicates two possible space groups, *Pmcm* or *Pncm*.

Celestine. The zone [100] of forms {0*kl*}. The only major form in this zone is {011}, which is the most important form on celestine. The other forms of this zone in the observed morphological aspect are {012}, {015}, and {0.1.12}, in order of decreasing importance. The last three forms are of nearly equal importance and are moderately rare. The dominance of the unit form suggests that there are no *b*- or *c*-glide planes parallel to (100), leaving *m*-planes and *n*-glide planes for consideration. With respect to the choice between the last two planes the remarks made when discussing this zone in baryte also apply here.

The zone [010] of forms {*h*0*l*}. The observed morphological aspect in this zone is {102}, {104}, {101}, and {103}. The first two of these forms are important and the last two are rare. Since the dominant form is {102} and the next most important is {104}, and both of these are very much more common than {101} and {103}, the presence of *c*-glide planes is clearly indicated.

The zone [001] of forms {*hk*0}. For this zone the observed morphological aspect is {110}, {120}, and {210} and the first of these forms is clearly dominant. This distribution would be consistent with the presence of *m*-planes parallel to (001).

The pinacoids. The observed morphological aspect is {001}, {100}, and {010}. The order to be expected from the axial ratios

$$a:b:c = 0{\cdot}77895:1:1{\cdot}28005$$

is {001}, {010}, and {100}.

The morphological analysis thus indicates two possible space-groups, *Pncm* or *Pmcm*, the weight of evidence being slightly in favour of the former.

Review of the morphological analysis.

X-ray analysis has shown that members of the baryte group, in the usual orientation, have the space-group *Pnma*, and that the *a*-axis of the unit-cell has twice the value indicated by the axial ratios used in the morphological analysis.[1] It seems very remarkable that the wealth of detail in the zonal development of the three central zones should point unambiguously to the wrong axial ratios. In the cases of the orthorhombic minerals brookite,[2] topaz,[2] and danburite[3] morphological studies led to correct determinations of the structural parametral form.

Since the determination of the lattice type did not indicate that the *a*-axis should be doubled an attempt had to be made to determine the space-group while using incorrect axial ratios. It is now necessary to repeat the analysis briefly, using the doubled value of the *a*-axis. When the indices are modified a form $\{hkl\}$ becomes $\{2h.k.l\}$. In the following section of this paper such modified indices will be used, and it will be stated when their use is discontinued.

In the ensuing discussion it is not practicable to use the same frequency limits for the three minerals. For baryte only forms with a frequency of 1 % or over from either the Atlas or the Handbuch will be considered. For anglesite only forms with actual frequencies of occurrence over three from the Atlas or Handbuch will be used. In the case of celestine some of the zones are so poorly developed that it will be necessary to use lower frequencies to illustrate the argument. For all three minerals the actual frequencies from the Atlas are given after the form, and those from the Handbuch follow in brackets.

Determination of the lattice type.

Baryte. The zone $[1\bar{1}0]$. This zone is greatly reduced in importance when the correct indices are used. The dominant form is {111} 95 (108), followed by {112} 7 (21) and {221} 8 (1). This zone is of the simple type with the unit form dominant.

The zone $[\bar{1}01]$. The dominant form is {111} 95 (108), and the remaining forms are {212} 38 (47), {232} 14 (10), and {121} 6 (7). This zone is also of the simple type with the unit form dominant, containing the three most simple primary forms and one secondary form.

The zone $[0\bar{1}1]$. The dominant form is {211} 263 (235). followed by

[1] R. W. James and W. A. Wood, loc. cit.

[2] F. C. Phillips, An introduction to crystallography, 1946, pp. 287–8 [M.A. **10**–97].

[3] J. D. H. Donnay, Trans. Roy. Soc. Canada, 1940, ser. 3, sect. IV, vol. 34, p. 33 [M.A. **8**–306].

{111} 95 (108). This zone is anomalous, but since two of the three central zones are of the simple type with the unit form dominant the lattice must be primitive, and the analysis of this zone is of no importance for the present purpose.

Anglesite. The zone [1$\bar{1}$0]. The dominant form is {111} 186 (83), followed by {112} 19 (15) and {221} 14 (5). This zone is reduced in importance but is still of the simple type with the unit form dominant.

The zone [$\bar{1}$01]. The dominant form is {111} 186 (83), which is followed by {212} 68 (42), {232} 13 (8), and {121} 11 (4). In the primary series the forms {212} and {121} succeed the dominant form in importance, and the only secondary form has the simplest indices, {232}. This zone is thus of the simple type with the unit form dominant.

The zone [0$\bar{1}$1]. The dominant form is now {211} 231 (110), and is succeeded by {111} 186 (83), {122} 8 (7), {233} 5 (4), and {255} 5 (3). This zone is anomalous, as it is in baryte, the remarks on which also apply in this case. It may be concluded that the lattice of anglesite is primitive.

Celestine. The zone [1$\bar{1}$0]. Only three forms appear in this zone, {111} 17 (24), {112} 0 (11), and {221} 2 (2). Since the unit form is dominant and the other two forms which appear belong to the primary series and are adjacent to the dominant form this zone belongs to the simple type with the unit form dominant.

The zone [$\bar{1}$01]. The observed frequencies of forms germane to the discussion are {111} 17 (24), {232} 7 (0), {121}, {212}, and {414} all 1 (3), and {313} 0 (1). There is a tenuous but complete primary series of forms from {121} to {414}, in which the unit form is dominant. The only secondary form is {232}. This zone is of the simple type with the unit form dominant.

The zone [0$\bar{1}$1]. This zone is more fully developed, and only forms with a minimum frequency of four from one of the sources will be quoted. {211} 60 (55), {111} 17 (24), {233} 20 (12), {122} 12 (16), {277} 0 (4) and {155} 6 (3). The same problem occurs in this zone as was found in baryte and anglesite, in which {211} and not the unit form is dominant. The comments made on the re-analysis of this zone in baryte also apply to celestine. It may be concluded that the lattice is primitive.

Determination of the space-group.

The required frequency data can be obtained from table IV, in which the symbols of forms are referred to morphological and not structural axial ratios. Symbols of forms in the zone [100] are unaffected, and the table may be used without any modification. For the zones [010] and

[001] it is necessary to read the form symbols in table IV with the first index doubled, to allow for the doubled value of the a-axis used in this section of the paper.

Since the symbols of forms in the zone [100] are unaffected by the change of axial ratios it is unnecessary to reinterpret this zone. It was concluded above that n-glide planes or m-planes exist parallel to (100) in all three minerals. The other two zones will be discussed below.

Baryte. The zone [010]. The observed morphological aspect is {101}, {201}, {102}, {103}, {203}, and {301}. In this zone the unit form is now dominant. There is a complete primary series from {301} through {101} to {103}, and the importance of the forms falls off steadily on either side of {101}. There is only one secondary form, {203}. This distribution suggests the presence of m-planes parallel to (010).

The zone [001]. The observed morphological aspect is now {210}, {410}, {310}, {230}, {110}, {430}, and {120}. The dominant form is {210}, and forms with the first index even tend to predominate, indicating the presence of a-glide planes parallel to (001).

The pinacoids. The observed order of decreasing importance, {001}, {010}, and {100}, does not agree with the order calculated from the unit-cell axes, which is {100}, {001}, and {010}.

The space-group can now be read as *Pmma* or *Pnma*.

Anglesite. The zone [010]. The dominant form becomes {101}, and the only other form of importance is {102}, which suggests the presence of m-planes parallel to (010).

The zone [001]. The dominant form is {210}, followed in order of decreasing importance by {110}, {230}, and {410}. Since {210} is dominant and forms with the first index even are common, a-glide planes are probably present parallel to (001).

The pinacoids. The observed morphological aspect is {001}, {100}, and {010}, while the theoretical order for the doubled a-axis is {100}, {001}, and {010}.

The probable space-group is therefore *Pnma* or *Pmma*.

Celestine. The zone [010]. The observed morphological aspect in this zone is now {101}, {102}, {201}, and {203}. The first two forms are important, the last two are rare, and {101} is clearly the dominant form. The first three forms represent a simple primary series in which the unit form is dominant. {203} is the only secondary form, and it comes between the two most important primary forms. This distribution suggests the presence of m-planes parallel to (010).

The zone [001]. The observed morphological aspect of this zone is

{210}, {110}, and {410}. This distribution would be consistent with the presence of *a*-glide planes parallel to (001).

The pinacoids. The observed morphological aspect is {001}, {100}, and {010}, but the expected theoretical order is that given under baryte.

The space-group derived for celestine from the morphology is thus *Pnma* or *Pnma*.

It has now been shown by morphological means that the space-group of baryte, anglesite, and celestine can be reduced to a choice between *Pnma* and *Pmma*, of which the former is correct. It is interesting that, once the correct axial ratios are known, the axial zones lead to the deduction of only two possible space-groups, of which one is correct, while a study of the central zones did not lead to correct determinations of the axial ratios. It may be noted here that Taylor,[1] in his morphological analysis of columbite crystals, obtained the space-group *Pman*, whereas X-ray determination gave it as *Pcan*.

In the succeeding part of this paper the symbols of forms will be referred to the axial ratios given at the head of table I, in conformity with the earlier part.

Predictions of the Donnay-Harker hypothesis.

This hypothesis predicts that the morphological importance of a form will be proportional to its reticular density or inversely proportional to its reticular area, S. If this statement represents an exact law the determination of space-groups by morphological means should be as accurate as those found by X-ray analysis, provided sufficient data are available.

An examination of the above statement has been made by calculating the theoretical order of importance (theoretical morphological aspect) for the minerals of the baryte group, and comparing it with the observed morphological aspect. The theoretical morphological aspect is calculated using the axial ratios with the doubled value of the *a*-axis, corresponding to the structural unit-cell. The symbols of faces referred to these axial ratios will be called 'structural symbols', while those referred to the axial ratios in which the *a*-axis is not doubled will be called 'morphological symbols'.

For the orthorhombic system the value of S^2 is given by the formula $S_{hkl}^2 = h^2b^2c^2 + k^2c^2a^2 + l^2a^2b^2$. Structural symbols are used throughout in the calculation of S^2, modified where necessary by the requirements of the lattice or space-group.

[1] E. D. Taylor, Amer. Min., 1940, vol. 25, p. 123 [M.A. 8–95].

For the space-group *Pnma* no condition is imposed on (*hkl*) planes, the symbols of which are unmodified. The *n*-glide planes parallel to (100) impose the restriction '$k + l$ even' on all forms {0*kl*}, so that the symbols of forms which do not obey this criterion are doubled. In the zone [010] the *m*-planes impose no restriction, and the symbols are unmodified. In the zone [001] the *a*-glide planes impose the restriction '*h* even', and all symbols which do not conform to this criterion are doubled. The 2_1 axes normal to the pinacoids require their symbols to be doubled.

The first thirty forms of the theoretical morphological aspect, based on the values of S^2, are shown in table V, in which the forms are referred to by their more familiar morphological symbols. The data for baryte are given in the left-hand section of the table. The first column indicates the theoretical rank of the forms (R_t), which is the order of the theoretical morphological aspect. The last four columns in this section of the table give the value of S^2, the observed rank of the form (R_0) as shown in tables I and II, and the actual frequencies of the forms from known localities, derived from the Atlas (A) out of 486 crystals, and the Handbuch (H) out of 505 crystals. The theoretical order of importance is the same for the first thirty forms of anglesite and celestine, but it differs appreciably from the order for baryte. The theoretical rank of the forms of anglesite and celestine is given in the second section of the table and the values of S^2, the observed rank and the frequencies of occurrence from known localities, derived from the Atlas and the Handbuch, are shown in the third and fourth sections of the table for anglesite and celestine respectively. In the case of anglesite the number of crystals derived from the Atlas was 359 and from the Handbuch it was 167; for celestine the corresponding numbers of crystals were 201 and 159 respectively.

Table V shows that the agreement between theoretical and observed ranks is very poor. The two most important forms in baryte occupy the 6th and 7th places in the theoretical list. The forms that are 7th and 11th in the observed list should be 2nd and 4th according to the theory. In the case of anglesite the agreement is little better. The two most important forms occupy the 7th and 6th places in the theoretical list and a form which is not placed among the first 27 observed forms should, in theory, occupy the 5th rank. The two most important forms in celestine occupy the 2nd and 6th ranks of the theoretical order, while forms placed 10th and 15th (equal) in the observed list should theoretically occupy the 4th and 5th ranks. Many other such anomalies may be seen for each of the three minerals in table V. It suffices to say that, in the case of the baryte group, the strict statement of the Donnay-Harker

F

Baryte.

R_t.	Pinacoids.	{hk0}.	{h0l}.	{0kl}.	{hkl}.	S^2.	R_0.	A.	H.
1			102			4·39	4	400	415
2	100					6·90	7	204	201
3				011		7·25	3	376	372
4					122	8·98	11	95	108
5			101			9·56	9	124	161
6	001					10·63	1	444	486
7		110				11·49	2	431	438
8			104			12·36	10	113	152
9					111	14·15	5	263	235
10					124	16·95	20	7	21
11			302			18·19	27	6	8
12	010					18·35	6	227	228
13					112	22·12	15	38	47
14					142	22·74	28	6	7
15					322	22·78		—	1
16		120				25·25	16	31	39
17			106			25·65	19	9	24
18			304			26·16		3	2
19					121	27·91	33	8	1
20				013		28·51		1	1
21					126	30·24		—	1
22			201			30·27		1	2
23					144	30·71		1	3
24					324	30·75		1	—
25			103			30·82	22	9	17
26		210				32·20	8	126	90
27					211	34·86		—	1
28					113	35·41	14	73	64
29					342	36·54		1	—
30					212	42·83	32	8	4

Theoretical rank of forms of anglesite and celestine.

R_t.	Pinacoids.	{hk0}.	{h0l}.	{0kl}.	{hkl}.
1			102		
2				011	
3	100				
4					122
5			101		
6	001				
7		110			
8			104		
9					111
10					124
11	010				
12			302		
13					112
14					142
15					322
16		120			
17			106		
18			304		
19					121
20				013	
21					126
22					
23					144
24					324
25					
26			201		
27					211
28					113
29					342
30					212

S^2 and observed rank and frequency of forms of

anglesite.				celestite.			
{hk0}.	{h0l}.	{0kl}.	{hkl}.	S^2.	R_0.	A.	H.
	102			4·13	3	270	128
		011		6·57	4	245	102
				6·65	5	113	75
			122	8·23	8	186	83
	101			9·12		—	4
				9·86	2	247	121
110				10·75	1	294	143
	104			11·52	7	87	51
			111	13·22	6	231	110
			124	15·62	13	19	15
				16·40	10	94	58
	302			17·43		—	—
			142	20·53	21	11	4
			112	20·61	12	68	42
			322	21·53		—	—
120				23·05	9	72	44
	106			23·85		1	1
	304			24·82		—	—
			121	25·52	20	14	5
		013		26.29		4	1
			144	27·92	18	8	7
			126	27·95		—	—
				28·84		1	2
	103		324	28·92	11	70	48
				29·07		—	—
	201			30·70	19	7	5
210				32·94	22	4	5
				33·17		—	—
				33·83		1	—
		031		39·37		1	2

				4·07	3	153	140
				6·41	1	175	141
				6·55	5 =	51	41
				8·05	10	17	24
				8·98	15 =	1	8
				9·71	2	142	127
				10·53	4	142	127
				11·35	5	53	51
				12·96	8	60	55
				15·33	13	—	11
				15·91	12	12	24
				17·18		—	—
				19·98		1	3
				20·24		1	3
				21·16		1	2
				22·46	11	14	9
				23·48		1	1
				24·46		—	1
				24·89		2	2
				25·82		2	2
				27·26	9	12	16
				27·46		—	—
				28·39	21	3	3
				28·44	17	8	4
				28·65		—	—
				30·20	24	—	5
				32·37	14	2	9
				32·63		—	—
				33·09		—	—
				38·22		—	—

hypothesis is not justified; morphological importance or rank is not inversely proportional to reticular area.

Form development in the baryte group.

Some interesting comparisons may be made between the form developments of baryte, anglesite, and celestine. Bipyramids {*hhl*} show a strong development in baryte, but they decrease in anglesite and again in celestine. In baryte forms are common in the primary series from {111} to {115}, but in anglesite the range is not only less, but its centre has moved towards {111}, the commoner forms being from {221} to {112}. In baryte {113} was developed to a greater extent than {112}, but this anomaly disappears in anglesite. Of the bipyramids {*hkk*} only two are well developed in baryte, there is a slightly better development in anglesite and a good series in celestine. It will be observed that some of these changes are of a serial nature, following the order of the ionic radii. The bipyramid {324} has an interesting development; it is quite important in anglesite, scarce in celestine, and almost unknown in baryte. Of the forms {*h*0*l*}, {102}, {101}, and {104} are very important in baryte, but {101} suffers almost total eclipse in the other two minerals. There is a very marked serial change in the development of forms {*hk*0}; in baryte there are five prisms of frequent or fairly frequent occurrence, in anglesite there are two, while in celestine there is only one. A progressive change also takes place in the relative importance of the pinacoids {100} and {010} from baryte to celestine.

Rank distribution of forms.

Finally, as a matter of interest, it seems worth while to record the rank distribution of some of the more important forms. For the crystals from known localities recorded in Goldschmidt's Atlas the frequency of occurrence of a form in each rank has been plotted against the rank, as shown in figs. 1, 2, and 3. Frequencies below 10 have been omitted in figs. 1 and 2, and below 5 in fig. 3, to avoid the straggling 'tails' of the distribution curves, which are of little significance.

It can be seen in fig. 1 that the dominant form on baryte, {001}, has a frequency which is very high in the first rank and falls away rapidly in the later ranks, while the second most important form, {110}, has its highest frequency in the second rank. {011} has a broad maximum in the second and third ranks and {102} has a peak in the third rank. In general, as the importance of forms decreases their peaks become lower and broader and are usually displaced farther to the right.

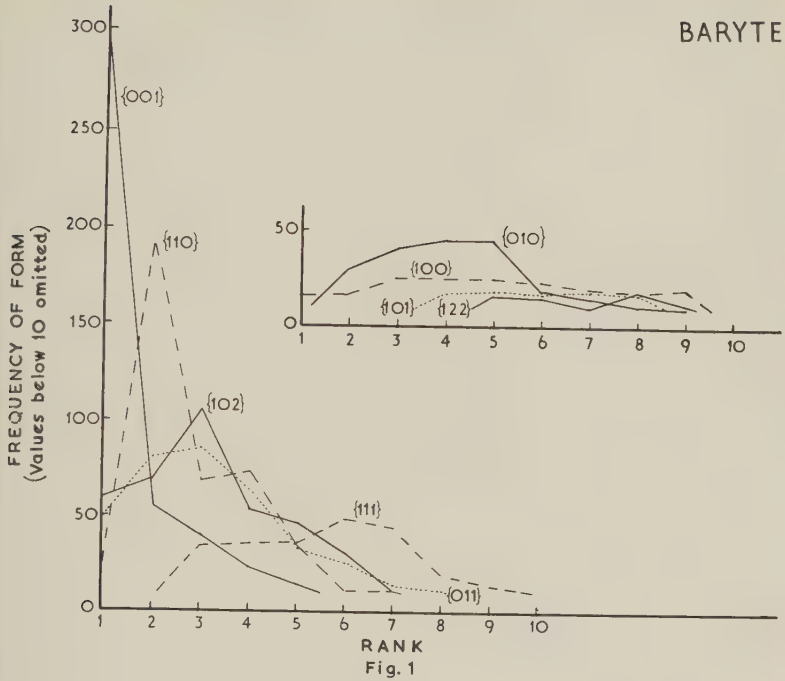
BARYTE
FREQUENCY OF FORM
(Values below 10 omitted)
300
250
200
150
100
50
0
{001}
{110}
{102}
{111}
{011}
50
0
{010}
{100}
{101}
{122}
1 2 3 4 5 6 7 8 9 10
RANK
Fig. 1

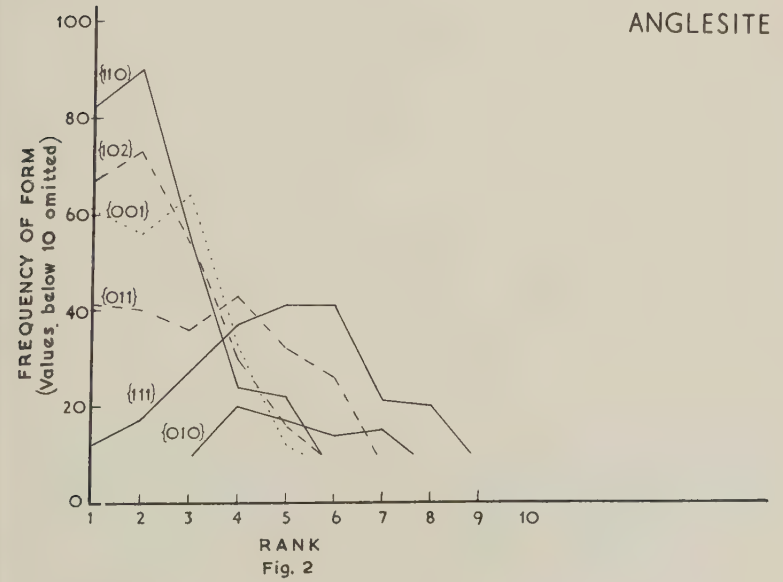
ANGLESITE
FREQUENCY OF FORM
(Values below 10 omitted)
100
80
60
40
20
0
{110}
{102}
{001}
{011}
{111}
{010}
1 2 3 4 5 6 7 8 9 10
RANK
Fig. 2

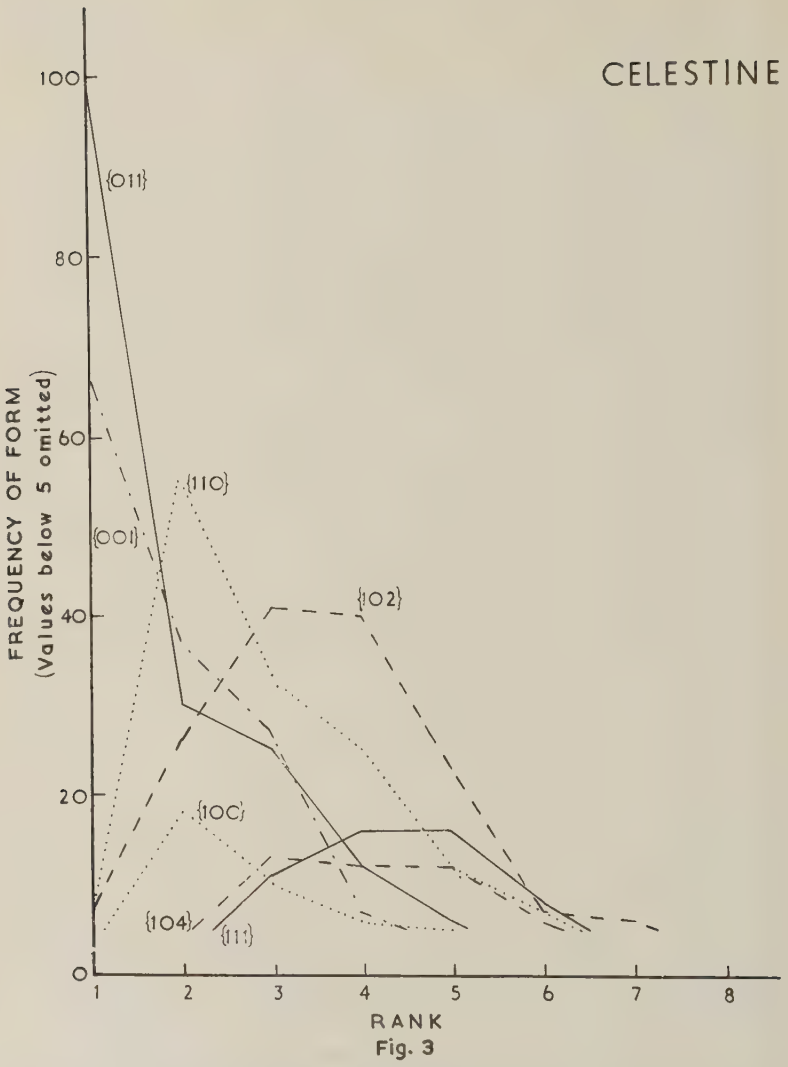

Fig. 3

In the case of anglesite fig. 2 illustrates that {110} is somewhat more important than {001}, while for celestine (fig. 3) it shows the clear superiority of {011} over {001}.

A study of figs. 1 to 3 and table I illustrates some interesting features of the development of bipyramids relative to other forms and to each other in the minerals of the baryte group. In table I it will be seen that

there is an approximate proportionality between the rank of a form and its mean rank, locality frequency, or frequency of occurrence. There are a number of exceptions to this broad generalization, nearly all of which concern bipyramids. In baryte {111} and {122} have high mean ranks compared with the forms adjacent to them in the table, and the bipyramids {113}, {112}, {114}, and {115} have much higher mean ranks than the prism in their midst, {120}. In anglesite the bipyramids {111} and {122} have a relatively low rank for forms with such high values of locality frequency and frequency of occurrence. The same two forms in celestine also appear to be placed low in the table, if only their locality frequency or frequency of occurrence are considered. The apparently anomalous position of these two forms in anglesite and celestine is accounted for by the relatively large value of the mean rank which they possess. It thus appears that most of the common bipyramids in minerals of the baryte group have relatively high values of the mean rank. The probable explanation of this fact may be found by considering the common habits of this group of minerals. In all three minerals there are four dominant forms, {001}, {110}, {011}, and {102}. These determine the common habits, in which crystals are elongated on the *a*- or *b*-axes or tabular on the basal pinacoid and bounded by either {110} or by {011} and a form {*h*0*l*}. Most of the bipyramids which are developed replace coigns or short edges between faces of the dominant forms, and so the faces are relatively small. Because of their geometrical position the pyramids would need a considerably reduced growth velocity to make an appreciable increase in the size of their faces, sufficient to affect their mean ranks and positions in table I.

The bipyramids {133} and {144} in celestine appear to be in a different category to all the others discussed. These forms have rather low frequencies of occurrence and locality frequencies but they are higher in the table than might be expected because of the small value of their mean ranks. The fact that these forms only occur at a few localities yet at these localities the forms are well developed suggests that some aspect of the environment encouraged their growth. The factor most likely to cause the preferential development of a form at a few localities is the presence of a specific impurity.

Postscript. The work described in this paper was completed in 1952, and a paper on the morphology of baryte was read before the Mineralogical Society in November of that year. In the interval before publication a series of papers has appeared by Hartman[1] and by Hartman and

[1] P. Hartman. Thesis, 1953. Groningen [M.A. 12–314].

Perdok,[1] on crystal morphology, some of which make special reference to the minerals of the baryte group. The particular aim of the present paper was to examine the validity of the Donnay–Harker hypothesis with respect to the baryte group. It will have been seen that this hypothesis does not give a very satisfactory prediction of the morphology of this group of minerals. In their work Hartman and Perdok estimate the importance of a form by the study of bond energies. In order to make the calculations the structure of the crystal must be known, which is not the case with the simpler method of Donnay and Harker. Hartman and Perdok are able to give a more accurate prediction of the relative importance of the commoner forms than is provided by the Donnay–Harker hypothesis.

[1] P. Hartman and W. G. Perdok, Acta Cryst., 1955, vol. 8. A paper in three parts, I, p. 49; II, p. 521; III, p. 525 [M.A. **13**–279]. P. Hartman and W. G. Perdok, Amer. Min., 1956, vol. 41, p. 449 [M.A. **13**–280].

Helvine from a lithium pegmatite near Salisbury, Southern Rhodesia.

By O. von Knorring, M.Sc., Ph.D.

Research Institute of African Geology, Department of Geology, The University, Leeds.

[Taken as read 6 November 1958.]

Summary. A new occurrence of helvine, the rare manganese end-member of the helvine group, is described. The mineral is found in a granite pegmatite associated with microcline-perthite, petalite, spodumene, muscovite, and spessartine. A chemical analysis of the mineral is given.

During the summer of 1957 the writer had an opportunity of examining the Casa Ventura lithium pegmatite, situated in Pre-Cambrian rocks some 16 miles to the east of Salisbury, in Southern Rhodesia. During the examination tiny crystals of a sulphur-yellow mineral, considered possibly to be microlite, were observed, but, on subsequent chemical and X-ray examination, they have been identified as the rare manganese–beryllium silicate helvine.

The area in question forms part of the Pre-Cambrian Basement Complex of the Bulawayan System (Macgregor, 1951) and consists of a belt of metamorphosed basic volcanics and igneous rocks referred to as greenstones and greenschists. These are interbedded with various crystalline schists and ironstones of sedimentary origin and enveloped by intrusive granitic rocks.

Apart from important gold occurrences, numerous pegmatites generally rich in a suite of lithium minerals are found within this region. The present pegmatite has the shape of an inclined lenticular sheet surrounded by greenstone. The main body of the pegmatite consists of grey coarse microcline perthite associated with a large amount of dark grey, resinous petalite, forming veins and isolated pods, which intersect and in part replace the feldspar. Abundant quartz with a yellowish muscovite and, in places, containing large amounts of spessartine garnet, constitutes a later phase of mineralization. To this late sequence belong also isolated veins and irregular bodies composed of fine-grained fibrous spodumene, quartz with some muscovite, and albite. Due to its fineness and in part to the striking resemblance to the albite variant cleavelandite,

the spodumene is not always recognized. The helvine is almost invariably associated with the spodumene and forms regular tetrahedral crystals with an edge length of about 1–2 mm. Some larger aggregates of helvine have been observed, together with lepidolite, but also in this case the mineral is confined to the spodumene veinlets.

Small amounts of columbite and a blue manganiferous apatite have also been noted. Large-scale hydrothermal alteration of petalite into rose-pink montmorillonite has taken place, especially along contacts with spodumene veins. Similar alteration of petalite has been recorded from Okehampton, Devon, by McLintock (1923) and from the Varuträsk pegmatite in northern Sweden by Quensel (1937). It is interesting to note that in the present case neither the spodumene nor the microcline show any alteration of this kind.

TABLE I. Chemical analyses of helvines.

	1.	*2.*	*3.*
SiO_2	33·62	31·42	31·54
TiO_2	n.d.	—	—
Al_2O_3	1·21	0·36*	0·37
BeO	12·88	10·97	13·60
FeO	2·24	2·99	18·02
MnO	45·46	51·64	26·51
ZnO	1·20	—	5·61
MgO	tr.	—	none
CaO	0·30	—	1·62†
Na_2O	0·03	—	—
K_2O	0·08	—	—
Li_2O	0·15	—	—
H_2O-	0·02	—	0·06
S	5·64	4·90	5·34
	102·83	102·28	102·68
Less O ≡ S ...	2·81	2·45	2·67
	100·02	99·83	100·01
Sp. gr.	3·22±0·01 (Berman balance)		3·334
n	1·732±0·002		1·746

1. Helvine from Casa Ventura pegmatite, near Salisbury, S. Rhodesia. Analyst: O. von Knorring.

2. Helvine from a pegmatite, Amelia County, Virginia. Analyst: B. E. Sloan (Glass *et al.*, 1944, p. 180).

3. Helvine from a tactite, Iron Mountain, New Mexico. Analyst: R. E. Stevens (Glass *et al.*, 1944, p. 170).

* TiO_2, Al_2O_3, CaO, Na_2O, K_2O, H_2O.

† Partly due to the presence of fluorite.

Observations in the field show that the helvine was formed during the hydrothermal stage of pegmatite consolidation and is connected with the other manganiferous minerals, spessartine, manganapatite, and columbite.

Helvine has been recorded principally in the following types of mineral deposits (Glass *et al.*, 1944; Neumann, 1950): granite pegmatites, nepheline syenite pegmatites, contact metasomatic deposits, hydrothermal veins, and as a cavity mineral in syenite. The mineral is found most frequently and often in large amounts within contact metasomatic deposits, e.g. skarns and tactites, and is of comparatively rare occurrence in granite pegmatites. Helvine with a chemical composition and a mineral association close to the present one has been reported from a granite pegmatite in Amelia County, Virginia, where it occurs with spessartine as the last mineral to crystallize (Holser, 1953, p. 608). Table I shows the composition of the present helvine compared with analyses of helvines from Amelia County, and Iron Mountain in New Mexico. The material used for analysis had some finely intergrown quartz, feldspar, and spodumene impurities.

References.

Glass (J. J.), Jahns (R. H.), and Stevens (R. E.), 1944. Amer. Min., vol. 29, p. 163.
Holser (W. T.), 1953. Ibid., vol. 38, p. 599.
Macgregor (A. M.), 1951. Trans. Geol. Soc. S. Africa, vol. 54, p. 22.
McLintock (W. F. P.), 1923. Min. Mag., vol. 20, p. 140.
Neumann (H.), 1950. Norsk. Geol. Tidsskr., vol. 28, p. 234.
Quensel (P.), 1937. Geol. Fören. Förh., vol. 59, p. 150.

SHORT COMMUNICATIONS

Suitability of polarising film for photometers.

K. D. Mielenz (Fuess, Berlin) and R. Clark Jones (Polaroid Corporation) have discussed the errors expected from path-difference in polarizing film (Optik, 1958, vol. 15, p. 656): '$\cos \delta_2$ . . . ist . . . eine Große die . . . durchaus verschieden sein wird, . . . eine Große also, die auch bei bekanntem R von vornherein die zu erwartende Meß-charakteristik und Meßgenauigkeit des $\cos^4$-Photometers ganz ungewiß läßt. Von dieser Unbestimmtheit ist das $\cos^2$-Photometer frei, und hierin liegt ein weiterer wesentlicher Vorteil dieser einfacherer Anordnung.' A variety of 'polaroid' is described in which the pleochroic layer is overlaid with a parallel birefringent plastic.

Such a parallel sheet will not disturb the Law of Malus if the polarization is perfect. It would appear that the errors feared by these authors could only arise for an imperfect polarizing film. For a good film the ratio $I_{\perp}/I_{\parallel}$ is less than, say, 0·0001, for which the maximum rotation (due to a half-wave coating) would be 0·01 degree. This is negligible, and it seems unlikely that any manufacturer will employ inferior film. The Cooke $\cos^4$ microphotometer (Manual of the polarizing microscope, 2nd edn, York, 1953, p. 131 [M.A. **12**–233]) has been subjected to a wide range of tests (A. F. Hallimond, Min. Mag., 1957, vol. 31, p. 487, in which details of manipulation are given); no trouble of this kind was encountered. There are quite different considerations which determine the preference for photometers of the $\cos^4$ type; these have even been constructed with birefringent calcite prisms (L. Capdecomme and J. Orcel, Rev. Optique, 1941, vol. 20, p. 88; cf. J. H. Dowell, Journ. Sci. Instr., 1931, vol. 8, p. 382).

A. F. Hallimond

75 Corringham Rd.,
London, N.W. 11

BOOK REVIEWS

Fisher (J. C.), Johnston (W. G.), Thomson (R.), and Vreeland (T., Jr.), editors. *Dislocations and Mechanical Properties of Crystals.* New York (John Wiley & Sons) and London (Chapman & Hall), 1957. xiv+634 pp., 9 tables, 348 text-figs. Price (bound) 120*s*.

This book consists of forty-two papers (with discussion) presented at a small International Conference on Dislocations and Mechanical Properties held at Lake Placid, New York, on 6–8 September 1956. There were forty-one members of the conference, each prominent in this field. From the record of this book, it would appear that a small conference of this kind provides the best method for the interchange of information and ideas between leading workers in a particular field. The value of such a conference is immeasurably increased by recording the proceedings so that they are available to all other workers; the editors of this book must be congratulated on producing with great care and promptness a work which will be of great value to those interested in the mechanical aspects of dislocations.

The report is divided into eight parts: I, Direct Observations of Dislocations; II, Deformation of Pure Single Crystals; III, Work Hardening and Recovery; IV, Alloy Crystals, Impurities, Yield Point Phenomena; V, Dislocation Damping and Fatigue; VI, Theory of Dislocations; VII, Whiskers and Thin Crystals; VIII, Radiation Damage. The text is well printed and relatively free from minor errors; it is copiously illustrated by clear and useful figures. The reader is made aware that the subject of dislocation properties has undergone, at least partially, the transition from an entirely theoretical concept to one in which the experimentalists can directly observe the dislocation systems and their relationship to mechanical properties. In this way, the stimulus is provided for a new development of the theoretical approach, particularly in the study of the properties of assemblies of dislocations and in the relatively new field of radiation damage. P. Gay

Lipson (H.) and Taylor (C. A.). *Fourier Transforms and X-ray Diffraction.* London (G. Bell & Sons Ltd.), 1958. vii+76 pp. Price 18*s*. 6*d*.

The application of Fourier-transform theory to the study of X-ray diffraction by crystals is a very important feature of the development

of structure-analysis in recent years. The authors stress the physical principles involved, in preference to the formal rigidity of purely mathematical treatments.

The monograph achieves its aim, which is to serve as a basic introduction for students working in this field; but only those mineralogists with a direct interest in structure analysis, or in rather abstruse aspects of physical-optical principles, will need to master its contents.

W. H. TAYLOR

TWENEY (C. F.) and HUGHES (L. E. C.). *Chambers's Technical Dictionary*. Edinburgh (W. & R. Chambers Ltd.), 3rd edn, 1958. viii + 1028 pp. Price 35*s*.

A useful collection of definitions of technical terms in a wide range of pure and applied sciences. Of the pure sciences, the zoological and botanical branches appear to contribute most terms. To the mineralogist, the main value of a dictionary of this kind is to elucidate terms in other branches of science, and the present volume should prove very useful in this way.

M. H. H.